



Fatigue of hydrogels

Ruobing Bai, Jiawei Yang, Zhigang Suo*

John A. Paulson School of Engineering and Applied Sciences, Kavli Institute for Bionano Science and Technology, Harvard University, Cambridge, MA, 02138, USA

ARTICLE INFO

Earlier and much shorter versions of this review were presented by R.B. as part of a PhD thesis titled “Fatigue of Hydrogels” at Harvard University on 12 April 2018, and by Z.S. as a plenary lecture titled “Chemistry of Fatigue” at the European Solid Mechanics Conference on 4 July 2018. To appear in European Journal of Mechanics - A/Solids, the Special Issue for the plenary lectures at the 2018 European Solid Mechanics Conference.

Keywords:

Hydrogel
Fatigue
Fracture
Damage
Crack growth

ABSTRACT

Hydrogels have been developed since the 1960s for applications in personal care, medicine, and engineering. Evidence has accumulated that hydrogels under prolonged loads suffer fatigue. Symptoms include change in properties, as well as nucleation and growth of cracks. This article is the first review on the fatigue of hydrogels. Emphasis is placed on the chemistry of fatigue—concepts and experiments that link symptoms of fatigue to processes of molecules. Symptoms of fatigue are characterized by testing samples with and without pre-cut cracks, subject to prolonged static and cyclic loads. We describe the use of energy release rate for samples with pre-cut cracks, under the conditions of large-scale inelasticity, for hydrogels of complex rheology. Highlighted are three experimental setups: pure shear, tear, and peel, where energy release rate is readily obtained for materials of arbitrary rheology. We describe chemistries of bonds and topologies of networks. Noncovalent bonds and some covalent bonds are reversible: they reform after breaking under relevant conditions. Most covalent bonds are irreversible. Each topology of networks is a way to connect reversible and irreversible bonds. We review experimental data of hydrogels of five representative topologies of networks. We compare the Lake-Thomas threshold, the cyclic-fatigue threshold, and the static-fatigue threshold. Fatigue is a molecular disease. All symptoms of fatigue originate from one fundamental cause: molecular units of a hydrogel change neighbors under prolonged loads. Fatigue correlates with rheology, according to which we distinguish poroelastic fatigue, viscoelastic fatigue, and elastic-plastic fatigue. Many hydrogels have sacrificial bonds that act as tougheners. We distinguish tougheners of two types according to their stress-relaxation behavior under a prolonged static stretch. A liquid-like toughener relaxes to zero stress, and increases neither static-fatigue threshold nor cyclic-fatigue threshold. A solid-like toughener relaxes to a nonzero stress, increases static-fatigue threshold, but does not increase cyclic-fatigue threshold. We outline a strategy to create hydrogels of high endurance. Because of the molecular diversity among hydrogels, the chemistry of fatigue holds the key to the discovery of hydrogels of properties previously unimagined. It is hoped that this review helps to connect chemists and mechanicians.

1. Introduction

A hydrogel is an aggregate of water and polymers, and usually contains more water than polymers. This review focuses on hydrogels in which polymers form three-dimensional networks. The widespread use of hydrogels is appealing for many reasons. In a hydrogel, the polymer network is sparse, and the spacing between polymer chains is much larger than the size of a water molecule. Water retains its molecular properties, dissolving many other molecules and transporting them. Many polymers can form hydrogels and carry various functional groups. This diversity in chemistry enables hydrogels of a broad range of properties. Most tissues of plants and animals are hydrogels. Synthetic hydrogels can mimic living tissues to high degree of fidelity. Many hydrogels derive from environmentally friendly sources and are biodegradable. For example, alginates are extracted from seaweeds,

which are abundant in the oceans throughout the world (Draget, 2009).

Synthetic hydrogels have been developed since the 1960s (Buwalda et al., 2014). As the property space spans and applications proliferate, hydrogels—like all materials—will be used under conditions that push their limits. In particular, many applications require hydrogels to sustain prolonged static and cyclic loads. For example, hydrogels are required to sustain prolonged deformation in artificial tissues, move repeatedly in robotic arms, stretch repeatedly in artificial skins, and oscillate in loudspeakers. Evidence has accumulated that prolonged loads cause hydrogels to fatigue. Symptoms include change in properties, as well as nucleation and growth of cracks.

Fatigue is a molecular disease. All symptoms of fatigue originate from one fundamental cause: molecular units of a hydrogel change neighbors under prolonged loads. Symptoms of fatigue vary with chemistries of bonds and topologies of networks. Some bonds are strong

* Corresponding author.

E-mail address: suo@seas.harvard.edu (Z. Suo).

<https://doi.org/10.1016/j.euromechsol.2018.12.001>

Received 1 December 2018; Received in revised form 10 December 2018; Accepted 11 December 2018

Available online 14 December 2018

0997-7538/ © 2018 Elsevier Masson SAS. All rights reserved.

(e.g., 3×10^{-19} J for a C-C bond), but others are weak (e.g., 3×10^{-21} J for a specific ionic bond). By a topology of networks we mean an arrangement of various bonds to link monomer units into polymer chains, and to crosslink polymer chains into polymer networks. A common topology is a single network of covalent bonds. Another topology is a primary network of covalent bonds interpenetrating with a secondary network of sacrificial bonds. Whereas a hydrogel of a single polymer network formed by C-C bonds exhibits near-perfect elasticity, a hydrogel having sacrificial bonds exhibits pronounced hysteresis. Under a monotonic load, a double-network hydrogel resists the growth of a crack by dissipating energy through two mechanisms: scission of primary polymer networks on the plane of the crack, and breaking of sacrificial bonds in the bulk of the hydrogel. The sacrificial bonds act as a *toughener*. The sacrificial bonds amplify toughness, but make tough hydrogels susceptible to fatigue. The fatigue of hydrogels is a new lens to view molecular processes.

After fatigue, some hydrogels can heal under certain conditions, but others cannot (Taylor and in het Panhuis, 2016; Wei et al., 2014). Heal is also a molecular process. When a hydrogel is subject to a load or a condition for heal, some broken bonds can reform, but others cannot. The former are called *reversible* or *dynamic bonds*, and the latter *irreversible* or *static bonds*. Most noncovalent bonds and some covalent bonds are reversible. Most covalent bonds are irreversible. Reversible bonds are prerequisite for a hydrogel to heal after distributed damage or growth of a crack. Notably, reversible bonds may prevent fatigue damage in a sample without pre-cut cracks, but do not prevent fatigue crack growth in a sample with pre-cut crack (Bai et al., 2018c).

Fatigue has been studied exhaustively in all established load-bearing materials, including metals, ceramics, plastics, elastomers, and composites (Evans and Wiederhorn, 1974; Fleck et al., 1994; Mars and Fatemi, 2004; Ritchie, 1988; Suresh, 1998). By comparison, the study of the fatigue of hydrogels is recent and scanty. The first report on crack growth in a hydrogel under static load was reported by Tanaka et al. (2000). The first report on crack growth in a hydrogel under cyclic loads has only appeared recently (Tang et al., 2017). The lack of interest may be interesting in materials sociology in the past, but is inexcusable now, given the intense development of tough hydrogels (Tang et al., 2017). It is urgent to span the scope of the study to enable new applications of hydrogels, as well as discovery of fatigue-resistant (i.e., *endurant*) hydrogels. Here we review the fatigue of hydrogels. The mechanical behavior of hydrogels resembles that of elastomers in many ways. We recommend a collateral reading of two reviews on the fatigue of elastomers (Mars and Fatemi, 2002, 2004). Fracture of elastomers and gels under monotonic loads is a vibrant field of study; recent reviews include Lake (2003), Gong (2010), Zhao (2014), Creton and Ciccotti (2016), Long and Hui (2015, 2016), and Creton (2017).

This article is the first review on the fatigue of hydrogels. Emphasis is placed on the chemistry of fatigue—experiments and concepts that link symptoms of fatigue to processes of molecules. Because the subject is young, we view the literature in its entirety, of hydrogels of various chemistries of bonds and topologies of networks, tested using samples with and without pre-cut cracks, subject to prolonged static and cyclic loads. Section 2 sets the stage by briefly describing hydrogels and their applications. We then describe the symptoms of fatigue under prolonged static and cyclic loads, as well as the efficacy of heal (Section 3), characterized by testing samples without pre-cut cracks (Section 4) and with pre-cut cracks (Section 5). We discuss the use of energy release rate in the presence of inelasticity. For materials of any type of rheology, energy release rate can be readily obtained for pure shear, tear, and peel. Tear and peel have additional advantage because active deformation is localized in a zone scaled by the thickness of the sample. We then describe two aspects of chemistry of profound significance to fatigue: chemistries of bonds (Section 6), and topologies of networks (Section 7). Section 8 reviews experimental data of hydrogels of five representative topologies of networks. We then recall and extend the Lake-Thomas model (Section 9), and compare the model to the

experimentally measured cyclic-fatigue threshold (Section 10) and static-fatigue threshold (Section 11). Sacrificial bonds can be either reversible or irreversible. We find another useful way to classify tougheners. Under a constant stretch for a long time, a toughener that relaxes to zero stress is called liquid-like, whereas a toughener that relaxes to a nonzero stress is called solid-like. All irreversible bonds and most reversible bonds are solid-like. Liquid-like tougheners increase neither cyclic-fatigue threshold nor static-fatigue threshold. Solid-like tougheners do not increase cyclic-fatigue threshold, but increase static-fatigue threshold. Fatigue correlates with rheology, according to which we distinguish poroelastic fatigue (Section 12), viscoelastic fatigue (Section 13), and elastic-plastic fatigue (Section 14). Viscoelastic fatigue and elastic-plastic fatigue have been widely studied in metals, plastics, and elastomers, and they need be adapted to gels. Poroelastic fatigue is specific to gels, and its study is nascent. Near the static-fatigue threshold, the crack speed approaches a material-specific value, which we call relaxation speed. We propose theoretical estimates of the relaxation speed, and compare them to experimental measurements. We outline a strategy to create *endurant* hydrogels of high toughness and low hysteresis (Section 15). The study of the chemistry of fatigue is urgent: it holds a key to applications previously unimagined through the discovery of tough and *endurant* hydrogels (Section 16).

2. Hydrogels and their applications

Compared to metals, ceramics, elastomers, and plastics, synthetic hydrogels are relatively new materials, first developed systematically by Wichterle and Lim (1960, 1961). In each synthetic hydrogel described in the initial invention, covalent bonds link monomer units into polymer chains, and crosslink the polymer chains into a single sparse network. Weak bonds between the network and water molecules, as well as the entropy of mixing, aggregate the network and water molecules into a condensed phase. The mixture of covalent bonds and weak bonds enables the hydrogel to exhibit hybrid behavior of solid and liquid. The polymer network acts as an entropic spring, whereas water molecules and monomer units of the network change neighbors constantly, transmit force negligibly, and act like a liquid. Because water has low viscosity, the hydrogel exhibits near-perfect elasticity, with low hysteresis.

Such a single-network hydrogel is highly stretchable, but has low toughness. Toughness is also called fracture energy or tear energy, and is defined as the energy dissipated when a crack extends a unit area. The toughness is about 1–10 J/m² for tofu and Jell-O, about 100 J/m² for polyacrylamide hydrogels, about 1000 J/m² for cartilage, and above 10,000 J/m² for natural rubber. The toughness as defined by the critical stress intensity factor is rarely used in hydrogels and elastomers, because the concept of stress intensity factor is limited to small deformation and linear elasticity. In this review, we will use toughness in the unit of energy per unit area exclusively.

Gong et al. (2003) discovered a tough hydrogel of two interpenetrating networks, one being more stretchable than the other. At a crack front, the more stretchable network bridges the crack, transmits stress to the bulk of the hydrogel, and breaks the less stretchable network in many sites. The hydrogel achieves high toughness by dissipating energy through the synergy of two mechanisms: the scission of the more stretchable network on the crack plane, and the breaking of the less stretchable network in the bulk of the hydrogel. The less stretchable network is a carrier of sacrificial bonds, and acts as a toughener. This discovery has instigated the worldwide search for tougheners. Examples include a network of less stretchable networks crosslinked by covalent bonds (Gong et al., 2003), by hydrogen bonds (Tang et al., 2010), by hydrophobic interaction (Haque et al., 2011), by dipole-dipole interaction (Bai et al., 2011), by ionic bonds (Sun et al., 2012), and by host-guest interaction (Li et al., 2015). The development has led to hydrogels as tough as natural rubber; see reviews (Chen et al., 2016a; Creton, 2017; Gong, 2010; Peak et al., 2013; Zhang and

Khademhosseini, 2017; Zhao, 2014).

Synthetic hydrogels have found diverse applications. Familiar consumer products include contact lenses (Caló and Khutoryanskiy, 2015) and superabsorbent diapers (Masuda, 1994). Hydrogels have transformed many areas of medicine (Caló and Khutoryanskiy, 2015; Hoffman, 2012; Peppas et al., 2006; Slaughter et al., 2009). Examples include drug delivery (Hoare and Kohane, 2008; Li and Mooney, 2016), wound dressing (Li et al., 2017a), tissue repair and replacement (Haque et al., 2012b; Lee and Mooney, 2001). A nascent field of applications, called hydrogel bioelectronics or hydrogel neural interfaces, uses hydrogels to link neurons and computers (Sheng et al., 2019; Yuk et al., 2019).

Potential non-medical applications of hydrogels have also emerged recently. Calvert (2009) has envisioned strong hydrogels for soft machines. Many hydrogels are stretchable, transparent, ionic conductors (Keplinger et al., 2013). They enable ionotronics, devices that function on the basis of both mobile ions and mobile electrons (Yang and Suo, 2018). This family of devices is also called stretchable ionics (Lee et al., 2018). Examples include transparent loudspeakers (Keplinger et al., 2013), transparent membranes for active noise cancellation (Rothenmund et al., 2018), artificial muscles (Acome et al., 2018; Kellaris et al., 2018), artificial skins (Lei et al., 2017; Sarwar et al., 2017; Sun et al., 2014), artificial axons (Le Floch et al., 2017; Yang et al., 2015), artificial eels (Schroeder et al., 2017), artificial fish (Li et al., 2017b), touchpads (Kim et al., 2016), triboelectric generators (Parida et al., 2017; Pu et al., 2017; Xu et al., 2017), liquid crystal devices (Yang et al., 2017), and ionotronic luminescent devices (Larson et al., 2016; Yang et al., 2016a). Other applications include optical fibers (Choi et al., 2015; Guo et al., 2016) and chemical sensors (Qin et al., 2018; Sun et al., 2018). Large scale uses of hydrogels have been proposed, such as pipeline maintenance in food and beverage manufacturing and retardants for wildland fire (Yu et al., 2016).

Tough hydrogels have been explored in applications such as antifouling coating for ships (Murosaki et al., 2009), tissue replacement (Haque et al., 2012b), vibration isolation (Yang et al., 2013), fire-retarding blankets (Illeperuma et al., 2016), wound dressing (Li et al., 2017a), drug delivery (Liu et al., 2017a), coating of medical devices (Parada et al., 2017), soft robots (Coyle et al., 2018; Yuk et al., 2017), stretchable living responsive devices (Liu et al., 2017b, 2017c), and adhesives and sealants for living tissues (Li et al., 2017a).

Many applications require that hydrogels be integrated with other materials through attaching (Keplinger et al., 2013; Liao et al., 2017), casting (Hu et al., 2017; Liu et al., 2018a; Tian et al., 2018; Yuk et al., 2016b), coating (Le Floch et al., 2017; Parada et al., 2017; Qin et al., 2018; Sun et al., 2018), and printing (Gladman et al., 2016; Haghshastiani et al., 2018; Hong et al., 2015; Robinson et al., 2015; Tian et al., 2017). The abundance of water in hydrogels causes a particular challenge: water molecules in the hydrogels transmit negligible loads, so that hydrogels usually adhere poorly with other materials (Rose et al., 2013; Tang et al., 2016). Commercial glues based on cyanoacrylate have long been used to glue hydrogels and tissues (García Cerdá et al., 2015). Cyanoacrylate monomers polymerize in situ and form a glass phase, in topological entanglement with the polymer networks of hydrogels (Chen et al., 2018). The glass phase may constrain the deformation of the hydrogels. Furthermore, cyanoacrylate is cytotoxic, and in situ polymerization limits methods of integration of hydrogel and other materials. Developing new methods of adhesion between hydrogels and other materials is urgent.

Yuk et al. (2016a, 2016b) discovered that a hydrogel strongly adhere to another material if the polymer network in the hydrogel forms strong bonds with the other material, and that the adhesion is further amplified if sacrificial bonds in the bulk of the hydrogel break before the scission of the primary polymer network. Methods have been developed to adhere hydrogels to stiff solids (Wirthl et al., 2017; Yuk et al., 2016a), elastomers (Liu et al., 2018b; Wirthl et al., 2017; Yang et al., 2018b; Yuk et al., 2016a), and living tissues (Li et al., 2017a).

Many of these new methods achieve both strong and stretchable adhesion. The adhesion energy is comparable to the toughness of the hydrogel, and the adhesion does not limit stretchability. The new development of hydrogel adhesion may adhere chemistry and mechanics in new ways; see online discussion (Liu, 2018).

Yang et al. (2018b) have initiated the study of the molecular topology of adhesion. Two polymer networks can be stitched together through topological entanglement with a third polymer network formed in situ. Strong adhesion is achieved without requiring any functional groups in the two preexisting polymer networks. The third network acts like a suture at the molecular level. Various topologies of adhesion greatly proliferate the methods of strong adhesion, and enable additional functions to adhesion (Yang et al., 2018a). Such a functional adhesion is illustrated by the recent discovery of photodetachable adhesion (Gao et al., 2018). Peel from strong adhesion is hard and sometimes painful. Topological adhesion enables both strong and easy detachment. The latter is triggered, on-demand, through an exposure to a light of a certain frequency range. This photodetachable adhesion has been demonstrated for hydrogels, elastomers, inorganic solids, and living tissues.

The development of strong adhesion between hydrogels and other materials has just opened an enormous field of opportunities. Composites have been developed by integrating hydrogels with other materials, such as plastics (Agrawal et al., 2013; Guo et al., 2017; He et al., 2016; Liao et al., 2013; Lin et al., 2014a; Xu et al., 2018), metals (Illeperuma et al., 2014), glass (Huang et al., 2017), and elastomers (Visser et al., 2015; Xiang et al., 2019). Such a water matrix composite has three main constituents: water molecules, one or more sparse polymer networks, and some other material in the form of fibers or sheets. The water molecules dissolve ions and small molecules and transport them, the sparse polymer networks retain the water molecules and bind the fibers and sheets, and the fibers and sheets carry much of mechanical loads. This division of labors—mass transport and load bearing—among dissimilar materials will greatly span the applications of hydrogels. The mechanical behavior of these composites depends on the adhesion between the sparse polymer networks and the fibers and sheets.

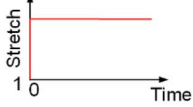
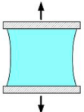
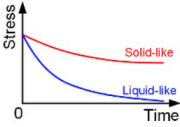
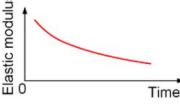
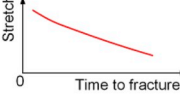
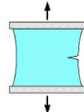
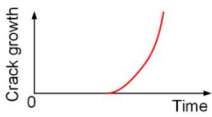
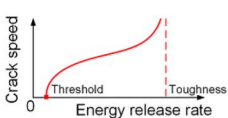
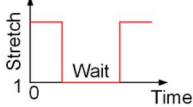
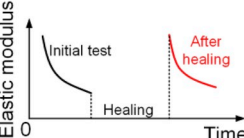
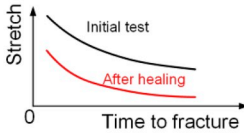
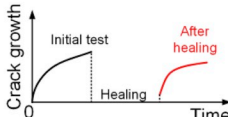
Hydrogels have been tested to function under unusual conditions. Hydrogels can retain water in the open air when they dissolve hygroscopic salts (Bai et al., 2014), or are coated with hydrophobic elastomers (Sun et al., 2014; Yang et al., 2018a; Yuk et al., 2016b). Hygroscopic salts and hydrophobic elastomers in combination enable hydrogels to be washable and wearable conductors for active textiles (Le Floch et al., 2017). Hydrogels containing specific salts can remain soft at temperatures far below 0 °C (Bai et al., 2014; Morelle et al., 2018). Hydrogels coated with hydrophobic elastomers can sustain temperatures above 100 °C without boiling (Liu et al., 2018b). It is possible to develop conductive hydrogel textiles that one can wear, wash, and iron.

3. Symptoms of fatigue and efficacy of heal

The word *fatigue* has been used to describe many symptoms observed in materials under prolonged loads. Symptoms of fatigue vary with profiles of the prolonged loads (i.e., loads as functions of time). Two idealized profiles of loads are commonly used to characterize fatigue: static loads and cyclic loads. Fatigue under prolonged static loads is called *static fatigue* (Table 1), and fatigue under prolonged cyclic loads is called *cyclic fatigue* (Table 2). A testing machine can prescribe either stretch or stress as a function of time. This section assumes that the testing machine prescribes stretch as a function of time. One can similarly test fatigue by prescribing stress as a function of time.

Fatigue may refer to the degradation of properties (e.g., modulus, toughness, conductivity, and swelling ratio). The degradation of properties is associated with distributed damage, may or may not cause the material to fracture, and is commonly studied using samples with no

Table 1
Static fatigue and heal.

<p>Fatigue under static stretch</p> 	 <p>Stress Relaxation</p>  <p>Static fatigue damage</p>  <p>Static fatigue fracture</p> 	 <p>Static fatigue crack growth</p>  <p>The speed of crack is a function of the energy release rate</p> 
<p>Heal after static fatigue</p> 	<p>Heal after static fatigue damage</p>  <p>Heal after static fatigue fracture</p> 	<p>Heal after static fatigue crack growth</p> 

precut crack. Distributed damage under prolonged loads is called *fatigue damage*.

Fatigue may also refer to the nucleation and growth of cracks in hydrogels. The nucleation of cracks is commonly studied using samples with no precut cracks, whereas the growth of cracks is commonly studied using samples with precut cracks. Fracture under prolonged loads is called *fatigue fracture*. When a crack is observed to grow under prolonged load, the growth is called *fatigue crack growth*.

When a sample without precut crack is subject to a prolonged static stretch, the stress may relax over time (Table 1). This symptom is called *stress relaxation*. The material is called liquid-like if the stress relaxes to zero after a long time, and is called solid-like if the stress relaxes to a finite level after a long time. Before the stress is fully relaxed, however, the sample may fracture. As the magnitude of the static stretch reduces, the time to fracture increases. This symptom is called *static fatigue fracture*. Other names include delayed fracture, subcritical fracture, stress-relaxation fracture, and stress corrosion. The last two names are specific to mechanisms of fracture. If the load is small and the time is short, the sample does not fracture, but its properties may change with time due to distributed damage. This symptom is called *static fatigue damage*.

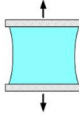
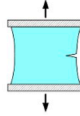
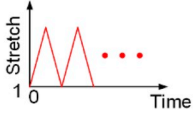
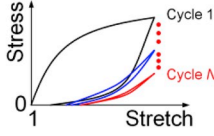
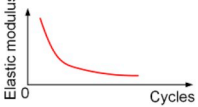
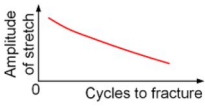
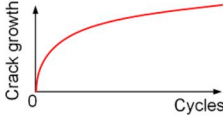
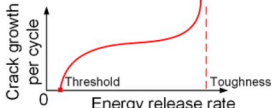
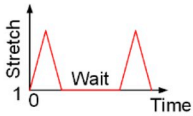
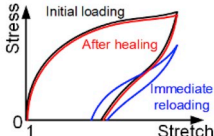

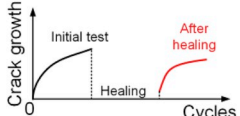
After a hydrogel is subject to a period of prolonged load, one may remove the load, and *heal* the hydrogel for some time under conditions such as a compressive stress, an elevated temperature, an exposure of light of certain frequencies, and an immersion in a solution. A hydrogel may even heal at room temperature for some time, subject to no other stimuli. Healing a hydrogel is analogous to healing a thermoplastic, annealing a metal, or sintering a ceramic. Of course, the range of temperature accessible to a hydrogel is more limited than many other

materials. Nonetheless hydrogels are particularly amenable to heal for several reasons. Like life itself, a hydrogel has abundant water, which mediates many molecular processes. Water in hydrogels also transports molecules from external solutions, so that one may design “drugs” to heal hydrogels. Many hydrogels are transparent, so that light can be a stimulus for heal. The efficacy of heal is characterized by subject the sample to another period of prolonged load.

When a sample with a precut crack is subject to a static stretch, the crack may extend as a function of time, at a speed much below the speed of sound in the material. This symptom is called *static fatigue crack growth*. Depending on the time-dependent process, this symptom may be called viscoelastic, poroelastic, or stress-corrosion crack growth. The speed of the crack is a function of the energy release rate. A hydrogel with a precut crack under a static stretch exhibits a threshold and a toughness. The crack does not grow when the energy release rate is below the threshold, and grows rapidly when the energy release rate approaches the toughness. After a period of crack growth, the sample may be allowed to heal for a period of time. The efficacy of heal is characterized by subjecting the sample to another period of prolonged static stretch, and measure the re-growth of the crack as a function of time.

When a sample without precut crack is subject to a cyclic stretch, the sample may fracture after some cycles (Table 2). As the amplitude of the cyclic stretch reduces, the number of cycles to fracture increases. This symptom is called *cyclic fatigue fracture*. The sample may not fracture if the stretch is small or the number of cycles is low, but its properties may change with cycles. This symptom is called *cyclic fatigue damage*. After a period of prolonged cyclic stretch, one can subject the sample to a condition to heal, and then characterize the efficacy of heal

Table 2
Cyclic fatigue and heal.

		
<p>Fatigue under cyclic stretch</p> 	<p>Hysteresis</p>  <p>Cyclic fatigue damage</p>  <p>Cyclic fatigue fracture</p> 	<p>Cyclic fatigue crack growth</p>  <p>The crack growth per cycle is a function of the amplitude of the energy release rate</p> 
<p>Heal after cyclic fatigue</p> 	<p>Heal after cyclic fatigue damage</p>  <p>Heal after cyclic fatigue fracture</p> 	<p>Heal after cyclic fatigue crack growth</p> 

by testing the sample under another period of prolonged cyclic stretch. When a sample with a precut crack is subject to a cyclic stretch, the crack may extend as a function of the number of cycles. This symptom is called *cyclic fatigue crack growth*. The crack growth per cycle is a function of the amplitude of energy release rate. A hydrogel with a precut crack under a cyclic stretch also exhibits a threshold and a toughness. The crack does not grow when the amplitude of energy release rate is below the threshold, and grows rapidly when the amplitude of energy release approaches the toughness. One can similarly try to heal the sample and characterize the efficacy of heal.

4. Samples without precut crack under prolonged static and cyclic loads

This section summarizes tests using samples without precut cracks, under five types of loading profiles: monotonic stretch, constant stretch, constant stress, cyclic stretch, and heal. In such a test, the stress and stretch are taken to be homogeneous in the sample. Uniaxial tensile test is often conducted if the hydrogel is tough enough to be fixed to the testing machine. Alternatively, uniaxial compression test is conducted, and the hydrogel is made slippery enough between the stiff plates to avoid lateral constraint. Another common experimental setup uses a hydrogel of a rectangular shape, with the thickness much smaller than the height, and the height much smaller than the length. The sample is rigidly clamped along the length, and pulled in the direction of the height. The rigid clamps suppress the deformation in the direction of

length, except for the edges of the sample. The setup is called the “pure shear test”. This name and its justification have caused pointless confusion, but no other name is commonly used.

Water can migrate in a hydrogel. The hydrogel can lose water to the environment, or gain water from the environment. One can ascertain the loss or gain of water by weighing the sample before and after the mechanical test. For a thin sample tested over a long time in the open air, the loss or gain of water will affect the stress-stretch curve. One should enclose the sample in a humidity-controlled chamber (Tang et al., 2017), or in a bath of oil or water (Illeperuma et al., 2013). The migration of water is negligible if the hydrogel is homogenized during preparation, and if the time of the test is much smaller than the time of migration of water in the hydrogel. The latter is estimated by L^2/D , where L is a representative length of the sample, and D is the effective diffusivity of water in hydrogels. The relevant length of a sample with no precut crack is the smallest dimension of the sample (e.g., the thickness of the sample). The effective diffusivity of water in hydrogels can be measured, for example, using indentation (Hu et al., 2010). Taking representative values, $L = 10^{-3}$ m and $D = 10^{-10}$ m²/s, we estimate the time of diffusion as 10^4 s.

Under a hydrostatic state of stress, the elastic modulus of a hydrogel is comparable to that of polymers and water, on the order of GPa. This bulk modulus is much larger than the shear modulus and applied stress, both on the order of 10–100 kPa. When the migration of water in the hydrogel is negligible, the hydrogel is taken to be incompressible, like an elastomer.

4.1. Monotonic stretch test

In this test, the testing machine prescribes a displacement to a sample of a material. Because hydrogels are soft materials, the compliance of testing machines is negligible. One grip of the machine remains stationary, and the other grip moves at a prescribed velocity. The stretch is defined by the length of the sample in a deformed state divided by the length of the sample in the undeformed state. The rate of stretch is defined by the velocity of moving grip divided by the length of the sample in the undeformed state. A sensor records the force acting on the sample. The nominal stress is defined by the force in a deformed state divided by the cross-sectional area of the sample in the undeformed state.

The initial slope of the stress-stretch curve measures the elastic modulus of the material. In a uniaxial tensile or compressive monotonic stretch, the initial slope of the stress-stretch curve measures Young's modulus, which is three times the shear modulus for an incompressible material. In a pure shear test, the initial slope of the stress-stretch curve is four times the shear modulus for an incompressible material.

Beyond the initial linear region of small deformation, the stress-stretch curve is nonlinear. The slope of the curve changes with the stretch, and becomes steep when the hydrogel approaches its limiting stretch. This stretch-stiffening is due to the finite length of the polymer chains. The area under the stress-stretch curve is the work applied by the testing machine to a unit volume of the sample. When the stress-stretch curve is measured till the sample ruptures, the stress defines the *strength*, the stretch defines the *stretchability*, and the work defines the *work of fracture*. For samples of a given material, the measured strength, stretchability and work of fracture often scatter considerably, likely due to imperfections of samples or testing conditions. For example, stress concentration often causes a sample to fracture at its end in a uniaxial tensile test. If the stress concentration is reduced by making the sample of dog bone shape, or tying knots instead of gripping the sample at the two ends, or rolling the sample to a rigid rod in a pure shear test, the measured strength, stretchability and work of fracture will increase (Chen et al., 2017; Pharr et al., 2012). For materials with the flaw-sensitivity length larger than, say, 0.1 mm, these procedures can eliminate stress concentration, and lead to small scatter in the measured strength, stretchability, and work of fracture (Chen et al., 2017). In such a case, these quantities are material properties.

The stress-stretch curve may depend on the loading rate. Such rate-dependence, for example, may come from the breaking of the sacrificial bonds, which may or may not reform. Necking has been observed in some tough hydrogels under uniaxial tension (Gong, 2010; Gong et al., 2003; Hu et al., 2015; Na et al., 2006).

4.2. Constant stretch test

In this test, the testing machine rapidly deforms a sample, and then holds the displacement constant in subsequent time. Meanwhile the force sensor records the stress as a function of time. The stress rises quickly, then drops over time, and eventually approaches either zero or a constant stress. The constant stretch test is also called the *stress relaxation test*. If the stress approaches a nonzero level, the hydrogel is said to be *solid-like*. If the stress approaches zero, the hydrogel is said to be *liquid-like*. The characteristic time for the relaxation is called the relaxation time. A hydrogel containing a covalently crosslinked polymer network is solid-like. A hydrogel only has a network cross-linked by physical associations can be either solid-like or liquid like, depending on whether the physical associations can sustain finite force under prolonged load.

A sample with or without precut crack may sustain a constant stretch for a period of time, but then fracture all of a sudden (Bonn et al., 1998). The mechanism of this delayed fracture for most hydrogels remains inconclusive (Tang et al., 2017). Culprits include pullout of chains in a hydrogels of polymer chains in physical entanglement

(Baumberger et al., 2006b), time-dependent migration of solvent (Tanaka et al., 2016; Wang and Hong, 2012), and progressive damage of the network (Karobi et al., 2016). In hard materials such as metals and ceramics, delayed fracture is often caused by chemical reaction at crack fronts, and the rate of reaction is possibly assisted by the high stress (Evans and Wiederhorn, 1974; Lawn and Wilshaw, 1993; Wei, 2010). Similar phenomenon occurs in natural rubber, where abundant carbon double bonds are prone to the chemical attack of oxygen and ozone (Lake, 2003). Stress corrosion has not been reported for hydrogels.

4.3. Constant stress test

In this test, the stress is held constant, and the stretch is recorded with time. The constant stress test is called the *creep test*. Subject to a constant stress, a solid-like hydrogel approaches a nonzero stretch, but a liquid-like hydrogel deforms indefinitely. Of course, the hydrogel may suffer delayed fracture, also called *creep fracture*.

4.4. Cyclic stretch test

Cyclic stretch is extensively used to measure the stress-stretch hysteresis. The hysteresis is small for nearly elastic hydrogels, such as polyacrylamide, but is large and usually rate-dependent for hydrogels with tougheners. A hydrogel without precut crack suffers fatigue fracture under cyclic stretch. A sample is subject to a cyclic stress of amplitude s , and the test records the number of cycles to fracture, N . The data, called the s - N curves, scatter greatly even when the tests are carefully conducted. This scatter is due to uncontrolled flaws in different samples of the material. Indeed, the s - N curves may as well be called s - N clouds.

Cyclic fatigue damage measures the irreversible change of material property over cycles in a material without precut crack. In the cyclic stress-stretch curves, a steady state is commonly observed after many cycles, where the curves do not change anymore. This steady state may result from the complete damage of the irreversible sacrificial bonds from the toughener, or the continuous breaking and reforming of reversible bonds.

4.5. Heal test

To test the efficacy of the heal of distributed damage, properties such as elastic modulus, stress-stretch hysteresis, and fracture stress are compared between tests conducted before and after the healing period. To test the efficacy of the heal of a crack, the fatigue crack growth is measured again and is compared to that measured in the initial loading. Both damage-healing and crack-healing experiments for many materials date back to antiquity. Quantitative crack-healing experiments were first conducted in mica (Obreimoff, 1930), and have been conducted extensively in developing the wafer-bonding technology (Gösele and Tong, 1998).

5. Samples with precut crack under prolonged static and cyclic loads

In a hard material (a metal, a ceramic, or a plastic), a crack grows typically when small deformation prevails in the main part of the sample, where linear elasticity applies. By contrast, in a soft material (a hydrogel or an elastomer), a crack typically grows when large deformation prevails in the main part of the body, where nonlinear elasticity applies. For elastomers, the use of samples with precut cracks was initiated by Rivlin and Thomas (1953) to study crack growth under monotonic loads, by Thomas (1958) to study crack growth under cyclic loads, and by Mullins (1959) to study crack growth under static loads. The practice introduced by these classic papers has remained the same since, and has been adopted in the study of crack growth in hydrogels.

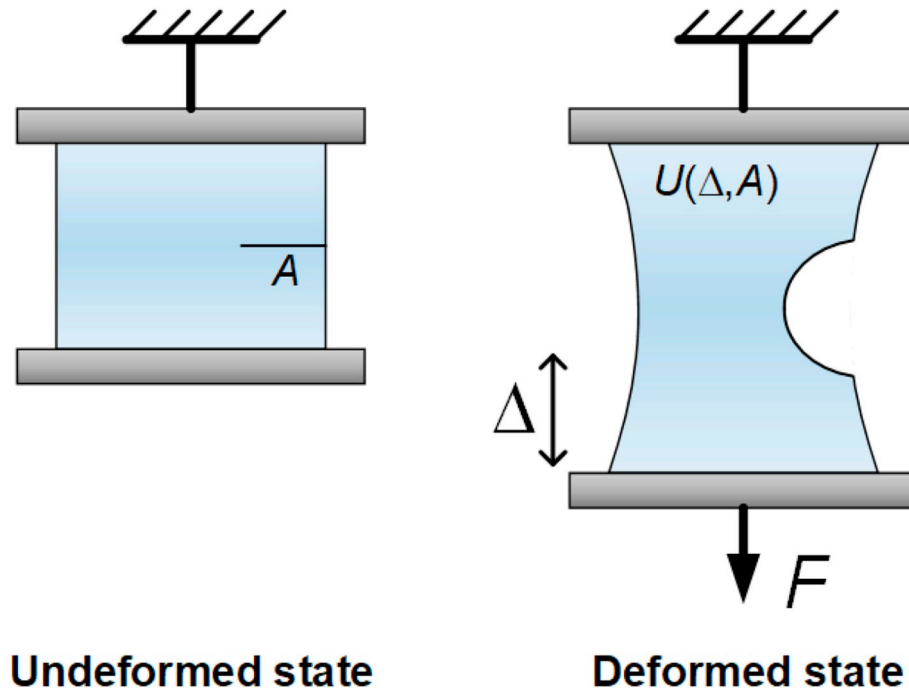


Fig. 1. A body has a crack of area A measured in the undeformed state. The body is subject to an applied force F and displacement Δ . The elastic energy of the body in the deformed state is a function of the displacement and the crack area, $U(\Delta, A)$.

The two papers that initiated the study of cyclic and static fatigue crack growth in elastomers predate the corresponding literature on metals. The three classic papers, along with other papers by them and their colleagues at British Rubber Producers' Research Association, deserve close reading. The remainder of this section describes the practice of using samples with precut crack, as well as the theoretical underpinning that was obscure in the classic papers, but has since become prominent.

5.1. Energy release rate

The deformation in the sample with a precut crack is inhomogeneous and concentrates at the front of the crack. Because the precut crack is typically much longer than any crack-like imperfections in the sample, the fracture typically initiates from the precut crack. Fracture is a process of inelasticity, accompanied by the scission of polymer chains, as well as possibly the breaking and reforming of sacrificial bonds. Indeed, inelasticity is inherent in fracture of all materials: "elastic fracture" never happens and is a misleading phrase.

In defining the energy release rate, however, we ignore the presence of inelasticity, regard the entire sample with a precut crack as an elastic body, all the way to the crack front (Fig. 1). Denote the elastic energy of the body by U . The area of the crack, A , is measured when the body is in the undeformed state. The body is subject to an applied force F and displacement Δ . When the displacement changes by $d\Delta$, the applied force does work $Fd\Delta$. The elastic energy of the body in the deformed state is a function of the displacement and the crack area, $U(\Delta, A)$, and is the area under the force displacement curve when the area of crack is fixed. The energy release rate G is defined by the equation $Fd\Delta = dU + GdA$. Thus, $F = \partial U(\Delta, A)/\partial \Delta$ and $G = -\partial U(\Delta, A)/\partial A$. The energy release rate has the unit of energy per unit area.

The energy release rate is a loading parameter, not a material property. In defining G , we picture two bodies identical in every other way, except for a slight difference in the areas of the precut cracks when the bodies are in the undeformed states, A' and A'' . Both cracks are precut using, say, a razor blade. When the bodies are loaded, the precut cracks do not grow. The energy release rate is $G = -[U(\Delta, A'') - U(\Delta, A')]/(A'' - A')$. The energy release rate is fully

determined by the elastic boundary value problems associated with the two bodies, and requires no information of fracture.

5.2. Toughness

By contrast, the toughness Γ is a material property that measures the energy dissipation associated with the growth of a crack. That is, Γ is defined by the equation $Fd\Delta = dU + \Gamma dA$. By this definition, the applied work is the sum of the change in the elastic energy and the dissipated energy. The toughness Γ also has the unit of energy per unit area. When a sample of a precut crack is subject to a monotonic force F , the loading parameter G increases with the applied load, and the front of the crack blunts, but the crack does not extend if the applied force is small. When the applied force reaches a critical value, the crack grows, and the loading parameter G reaches the material property Γ .

The definition of G and Γ are nearly identical except for the meaning of the phrase "the change in crack area dA ". In defining G , the change in the crack area, dA , refers to samples of precut cracks of different areas, and the cracks do not grow under the applied load. In defining Γ , the change in the crack area, dA , is the growth of the crack under the applied load.

Rivlin and Thomas (1953) noted that their measured toughness of rubber was much larger than the surface energy of rubber. The toughness is on the order of 10^5 J/m^2 , whereas the surface energy is on the order of 10^{-2} J/m^2 . The reason for this large difference was obscure in the original paper, but has since come to light. Toughness and surface energy are unrelated quantities. Toughness measures the dissipation of energy due to the scission of the polymer chains on the crack plane and the inelastic deformation off the crack plane. Surface energy measures the bonds between monomer units, and is the same as the surface energy of an uncrosslinked polymer liquid. Surface energy has nothing to do with the scission of the polymer chains or the inelastic deformation of the rubber.

Rivlin and Thomas (1953) measured the toughness of a rubber using specimens of several types: a long sheet with a short crack in the center, a long sheet with a short crack at one edge, a tear specimen with a long crack, and a pure shear specimen with a long crack. All these specimens

gave a similar value of toughness. Their experiments established that toughness is a material property, independent of the types of specimens used to measure it. We now know that this specimen-independent toughness results from the concentration of deformation at the front of the crack. The following line of arguments parallels that for metals (Hutchinson, 1983; Rice, 1968). Also see a review on the measurement and interpretation of toughness of hydrogels (Long and Hui, 2016).

5.3. Elasticity around a crack front

The deformation of a body is described by a map $\mathbf{x}(\mathbf{X})$, where \mathbf{X} is the coordinate of a material particle when the body is in the undeformed state, and \mathbf{x} is the coordinate of the same material particle when the body is in the deformed state. Define the deformation gradient by $F_{iK} = \partial x_i(\mathbf{X})/\partial X_K$. The elasticity of every material particle of the body is characterized by the Helmholtz function per unit volume, $W(\mathbf{F})$. Here we list the deformation gradient as the independent variable, and assume that the temperature is held constant. The tensor of nominal stress relates to the deformation gradient as $s_{iK} = \partial W(\mathbf{F})/\partial F_{iK}$. In the absence of any body force, the nominal stress satisfies the equation of equilibrium, $\partial s_{iK}/\partial X_K = 0$. These equations, along with the boundary conditions, determine the elastic field in the body. These equations have no length scale.

Now consider a semi-infinite crack in an infinite body, and assume that the body is elastic everywhere, all the way to the front of the crack. The boundary conditions also have no length scale. Regard the energy release rate G as the loading parameter of the boundary value problem. Recall that W has the unit of energy per unit volume, and G has the unit of energy per unit area. Let R be the distance of a material particle from the crack front, measured when the body is in the undeformed state. Because the boundary value problem has no length scale, dimensional considerations dictate that the elastic field should scale as $W \sim G/R$, with the pre-factor independent of R , but dependent on the polar angle. See a review of crack-front fields in materials modeled with specific

Helmholtz functions (Long and Hui, 2015).

5.4. Inelasticity around a crack front

The elastic field $W \sim G/R$ is singular as R approaches the crack front, and must break down near the crack front. Assume that inelasticity occurs when W exceeds some representative value W_1 . Consequently, for a semi-infinite crack in an infinite body, the size of the inelastic zone scales as G/W_1 . Outside the inelastic zone, the material is elastic, with the stress-stretch relation derived from the Helmholtz function $W(\mathbf{F})$.

Now consider a sample of a finite size (Fig. 2). When inelasticity is localized around the crack front, in a zone small compared to the size of the sample, with the remaining part of the sample being elastic, the sample is said to be under a condition of *small-scale inelasticity*. When small-scale inelasticity prevails, an annulus exists, its internal radius being larger than the inelastic zone size G/W_1 , and its external radius being smaller than the sample size. Within this annulus, the elastic field $W \sim G/R$ is valid. This elastic field is the same for a body of the same material (i.e., characterized by the same Helmholtz function $W(\mathbf{F})$), but of different shapes. The load applied on the external boundary of the body communicates to the fracture process at the crack front through the elastic field in the annulus, with G as the only messenger. This annulus is called the *G-annulus*. Consequently, the condition of small-scale inelasticity ensures that the energy release G is a single loading parameter. This fact explains why the toughness Γ is a material property independent of types of specimens.

Large-scale inelasticity prevails when major portion of the sample undergoes inelastic deformation. In a tough hydrogel, despite large-scale inelasticity, toughness determined using samples of various sizes and geometries is about the same (Sun et al., 2012). This experimental fact is likely due to the practice that the toughness is determined near the onset of the crack growth, before the growth of the crack forms a steady-state wake, so that much of the sample only experiences loading,

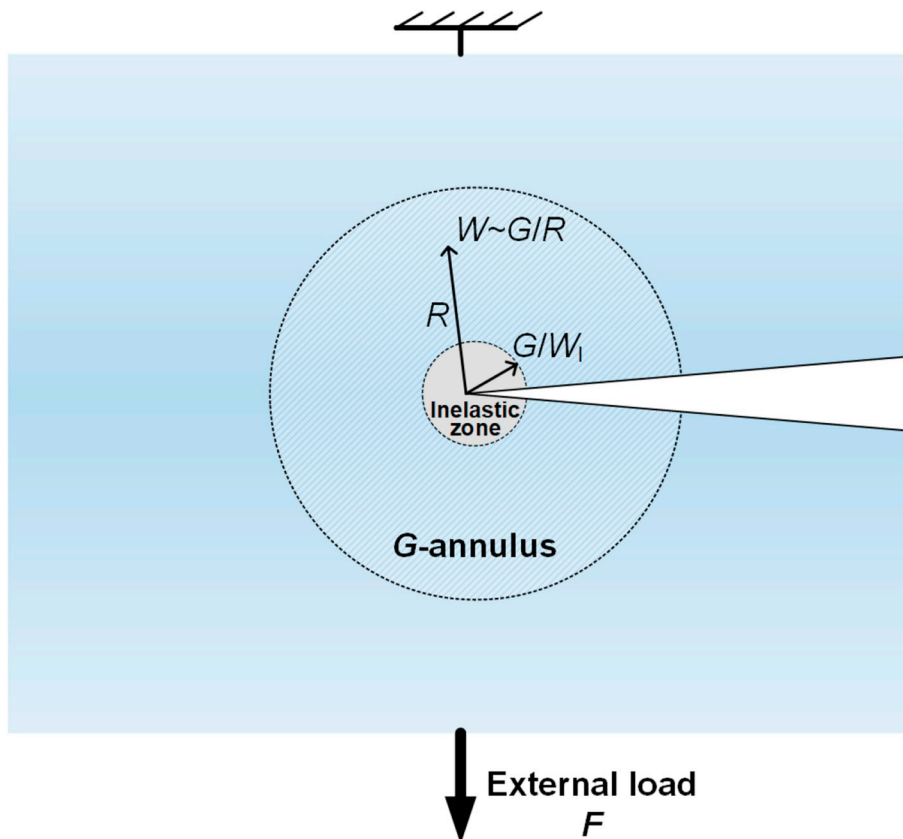


Fig. 2. When small-scale inelasticity prevails, a *G-annulus* exists, with the internal radius being larger than the inelastic zone size G/W_1 , and the external radius being smaller than the sample size. Within the annulus, the elastic field $W \sim G/R$ is valid. The external load communicates with the inelastic zone through a single messenger, G .

without unloading. Under such a condition the inelastic stress-stretch relation may be approximately expressed by an energy function, in the same spirit of the deformation theory of plasticity. Similar independence of sample size and shape has long been established in the fracture of metals under the conditions of large-scale plasticity (Begley and Landes, 1972; Landes and Begley, 1972).

5.5. Flaw sensitivity

A polyacrylamide hydrogel can be stretched several times its original length, but ruptures at a small stretch when the sample is precut with a crack of length exceeding a few millimeters. This flaw sensitivity happens to all materials, but the flaw size that begins to knock down stretchability appreciably is material specific, from nanometers for silica, to centimeters for ductile steel.

The flaw-sensitivity length can be estimated from the scaling of the elastic field $W \sim G/R$ (Chen et al., 2017). Let W_f be the work of fracture measured using a “perfect sample” containing no cracks, and Γ be the toughness measured using a sample with a long precut crack. The ratio Γ/W_f defines a length, called the flaw-sensitivity length, which is a material property. When the precut crack in a sample is short compared to the flaw-sensitivity length, the crack has negligible effect on the stretchability of the sample. When the precut crack is long compared to the flaw sensitivity length, the crack reduces the stretchability of the sample. This reduction is estimated by $W(\lambda_f) \sim \Gamma/a$, where a is the length of the crack, λ_f is the stretch that ruptures the sample with the precut crack, and $W(\lambda_f)$ is the area under the stress-stretch curve up to fracture. For silica, the flaw-sensitivity length is on the order of nanometer, and the “perfect samples” can only be prepared under special conditions, such as ultra-thin fibers. For many elastomers and hydrogels, the flaw-sensitivity length is larger than 0.1 mm, and samples prepared with some care measure the work of fracture with relatively small scatter.

Flaw-sensitivity lengths for representative materials are plotted in the diagram of toughness and work of fracture (Fig. 3) (Chen et al., 2017). The representative values of a polyacrylamide hydrogel are $\Gamma \sim 10^2 \text{ J/m}^2$, $W_f \sim 10^5 \text{ J/m}^3$, and $\Gamma/W_f = 10^{-3} \text{ m}$. By contrast, representative values for a tough hydrogel are $\Gamma \sim 10^4 \text{ J/m}^2$, $W_f \sim 10^5 \text{ J/m}^3$, and $\Gamma/W_f = 0.1 \text{ m}$. Such a large flaw-sensitivity length makes the tough hydrogel flaw-insensitive in most applications. Some authors call the quantity W_f toughness. This designation is ill advised: of all materials surveyed, silica glass has the highest work of fracture W_f (Fig. 3).

To design hydrogels that resist fatigue fracture for samples with no precut cracks, we should estimate the flaw-sensitivity length under prolonged loads. Under static loads, Γ_0 corresponds to the static-fatigue threshold, and W_f is the work of fracture measured in a sample without

precut crack at a vanishingly low loading rate. Under cyclic loads, Γ_0 corresponds to the cyclic-fatigue threshold, and W_f is the work of fracture measured in a sample without precut crack after a large number of loading cycles to break all the bonds in the toughener. A hydrogel is flaw-insensitive under static or cyclic loads if the size of any crack-like defect in the hydrogel is smaller than the flaw-sensitivity length. No work has been reported on the study of short cracks in hydrogels under prolonged loads. These brief comments are inadequate for this significant topic, but may serve as a reminder to instigate serious work.

Kim et al. (2018) have studied the growth of a liquid phase in an elastomeric gel. A liquid drop grows by rupturing the network of the gel. When the size of the liquid drop is small compared to the flaw-sensitivity length of the gel, the scission of polymer chains is not localized, but distributed around the entire liquid/gel interface. Distributed scission may have also occurred around the vapor bubbles in a deep-fried hydrogel (Liu et al., 2018b). By contrast, a worm burrows in a brittle hydrogel by wedging a sharp crack (Dorgan et al., 2005).

As noted in Section 2, the monomers of cyanoacrylate adhere two pieces of hydrogels by polymerization into a glassy polymer network, in topological entanglement with the networks of the two hydrogels (Chen et al., 2018). When the adhered hydrogels are stretched in a direction in the plane of the interface, the glass phase ruptures, which causes the hydrogels to rupture if the glass phase is thick. However, if the glass phase takes the form of drops small compared to the flaw-sensitivity length of the hydrogels, the adhered hydrogels are highly stretchable without damage. The glass drops function as staples.

5.6. Monotonic load

For samples containing precut cracks subject to a monotonic load, the interpretation of experimental data is simplified for materials of time-independent stress-stretch behavior. In a pure shear test, the energy release rate in a precut sample is $G = HW(\lambda)$, where $W(\lambda)$ is the elastic energy density of the uncut sample (i.e., the area under stress-stretch curve of an uncut sample stretched from 1 to λ), and H is the height of the sample in the undeformed state (Rivlin and Thomas, 1953).

Toughness of a hydrogel can be determined by using two samples of the hydrogel, one without precut crack, and the other with a precut crack (Sun et al., 2012). The sample without precut crack is used to measure the stress-stretch curve without fracture, and the area under the stress stretch curve determines the function $W(\lambda)$ (Fig. 4a). The sample with a precut crack is stretched to fracture, and the critical stretch λ_{cr} is recorded (Fig. 4b). The toughness of the hydrogel is given by $\Gamma = HW(\lambda_{cr})$.

Alternatively, one determines the toughness of a hydrogel using a single sample with a precut crack (Bernardi et al., 2018). If the sample is sufficiently long, the presence of the crack affects the stress-stretch curve negligibly, so that the sample itself can be used to determine the function $W(\lambda)$ up to λ_{cr} .

In peel (Fig. 5a) or tear (Fig. 5b), the sample is often attached with two inextensible backing layers, which suppress the deformation far away from the crack front (Gent and Lai, 1994). When the loading machine prescribes a displacement to the arms of the sample, a force sensor records the applied force F as a function of displacement (Fig. 5c). When the force is small, the crack does not extend but blunts. As the force increases, the crack blunts further. At some level of the force, the crack extends by the scission of polymer chains. Upon further loading, the crack may grow into a steady state, and the force may reach a plateau. In the steady state, the extension of the crack is half of the displacement prescribed by the loading machine to one arm relative to the other, and the energy release rate is $G = 2F/w$ for peel, and $G = 2F/h$ for tear, where w is the width and h is the thickness of the sample. In the steady state, the plateau force F gives the toughness $\Gamma = 2F/w$ for peel and $\Gamma = 2F/h$ for tear. For a hydrogel of time-

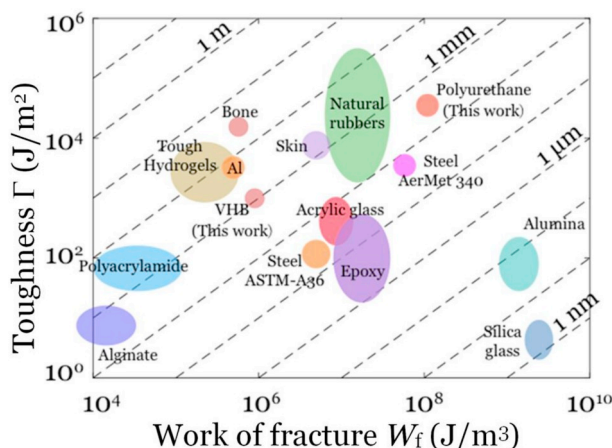


Fig. 3. A diagram of toughness Γ and work of fracture W_f , along with the flaw-sensitivity length Γ/W_f (Chen et al., 2017).

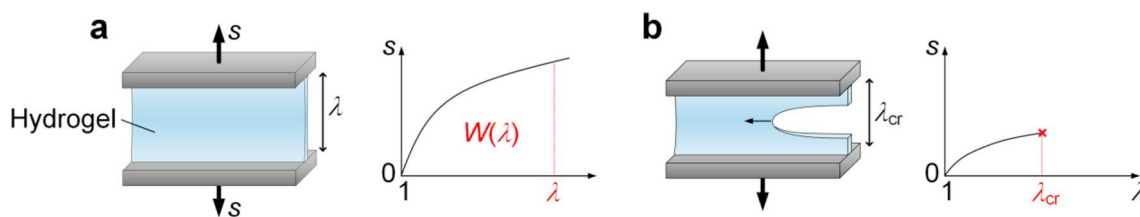


Fig. 4. Pure shear. (a) A sample without a precut crack is used to measure the stress-stretch curve and the energy density as a function of stretch, $W(\lambda)$. (b) A sample with a precut crack is used to measure the critical stretch for fracture, λ_{cr} .

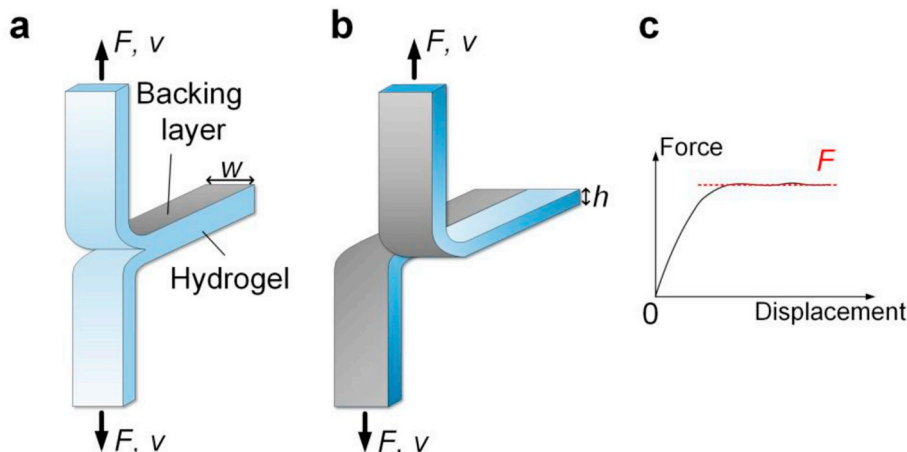


Fig. 5. (a) Peel. (b) Tear. (c) Force-displacement curve.

independent stress-stretch behavior, the measured force-displacement curve negligibly depends on the loading speed.

Because the thickness of the sample can be readily adjusted over a large range in peel and tear, the two experimental setups can be used to probe the scale of inelasticity (Bai et al., 2018a). The toughness is measured as a function of the thickness of the sample (Fig. 6). For a thick sample, the inelastic zone is small compared to the thickness h , small-scale inelasticity prevails, and the toughness Γ does not depend on the thickness h . For a thin sample, the inelastic zone is large compared to the thickness h , large-scale inelasticity prevails, and the toughness Γ increases with the thickness h . In materials like elastomers, plastics and metals, the dependence of peel force on thickness has long been observed experimentally (Gent and Hamed, 1977) and analyzed theoretically (Kim and Aravas, 1988; Wei and Hutchinson, 1998).

The three experimental setups—pure shear, peel, and tear—allow cracks to run over long distance, in a steady state. However, the steady state may be unstable, and gives way to jerky crack extension (Gent and Pulford, 1984; Kolvin et al., 2017; Tanaka et al., 2000, 2016). The crack path may also deviate from a straight line and form branches (Baumberger and Ronsin, 2010; Gent et al., 2003; Livne et al., 2005; Papadopoulos et al., 2008). Fingering instabilities have been observed in peel of elastomers and hydrogels (Shull et al., 2000; Yuk et al., 2016a). When a crack runs in a steady state, the energy release rate is well defined for the three experimental setups. When instability occurs, it is still a good practice to report the peel/tear force-displacement curve, with loading speed specified.

5.7. Static fatigue crack growth

Static fatigue crack growth is a common way to study hydrogels of complex rheology. Such an experiment records the crack speed v as a function of the energy release rate G (Table 1). When the crack runs rapidly, the energy release rate approaches the toughness, Γ . When the crack speed vanishes, the energy release rate approaches the threshold.

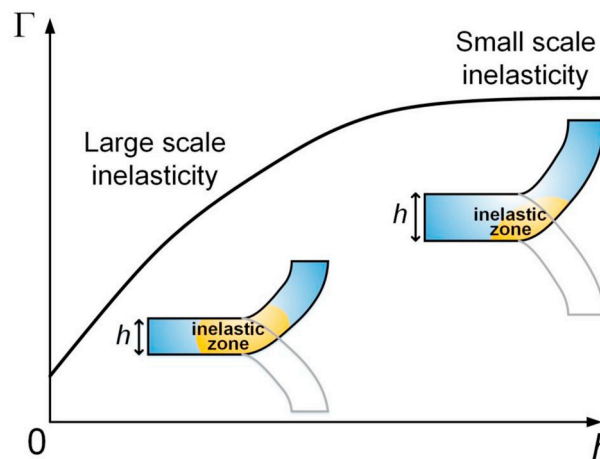


Fig. 6. The measured toughness is thickness-dependent under the condition of large-scale inelasticity, but is thickness-independent under the condition of small-scale inelasticity.

The threshold is the toughness of the hydrogel after the rate-dependent inelasticity is completely relaxed. For example, a polyacrylamide-calcium-alginate hydrogel has large rate-dependent inelasticity from the calcium-alginate network. The energy release rate is $\sim 4000 \text{ J/m}^2$ at a crack speed of 10 mm/s , and is $\sim 200 \text{ J/m}^2$ at a crack speed of $1 \mu\text{m/s}$ (Bai et al., 2018a).

Static fatigue crack growth can be characterized using the pure shear test. For a hydrogel of complex rheology, when a precut sample is held at a constant stretch λ for a long time, the materials far ahead and far behind the crack front are fully relaxed, and can be modeled as an elastic material. The crack speed v can be recorded using a video camera. When the extension of the crack reaches a steady state, the crack speed is constant independent of time. Recall the equation that

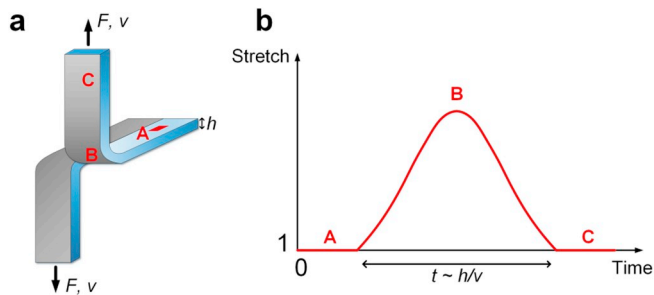


Fig. 7. In tear, active deformation is localized around the tear front in a volume scales as h^3 . (a) Points A, B, and C represent material particles in the sample. (b) The loading and unloading history of a material particle during a tear test. The time of active deformation is estimated by h/v .

defines the energy release rate: $Fd\Delta = dU + GdA$. In the steady state, the clamps are held fixed, so that $d\Delta = 0$. Furthermore, $dU = -HW(\lambda)dA$, where $W(\lambda)$ is the area under the stress-stretch curve of a sample without precut crack, measured in a pure shear test, at a low enough loading rate to allow stress relaxation. The energy release rate is $G(\lambda) = HW(\lambda)$. The ν - G curve is measured by conducting experiments by holding the applied stretch λ at different values.

Even when the crack extends at a low speed, the material is inelastic around the crack front. If the inelastic zone is small compared to the height of the sample, small-scale inelasticity prevails, and the ν - G curve is independent of the height of the specimen. When the loading speed is not small enough, or the specimen is not high enough, large-scale inelasticity prevails. So long as the specimen is fully relaxed far ahead and far behind the crack front, energy release rate is still given by $G(\lambda) = HW(\lambda)$. Under large-scale inelasticity, the ν - G curve depends on the height of the sample. For pure shear, to ensure that the sample far ahead the crack front is fully relaxed, the sample needs to be held at a fixed stretch for a long enough time.

By comparison, peel and tear have some advantages in studying static fatigue crack growth in hydrogels of complex rheology (Bai et al., 2018a). Take tear for example (Fig. 7a). When the tear front extends in the steady state, the speed of the tear front is half of the speed prescribed by the loading machine on one arm relative to the other. Consequently, there is no need to videotape the tear front. Once again recall the equation that defines the energy release rate: $Fd\Delta = dU + GdA$. In the steady state, the zone of active deformation travels at the crack speed, so that the elastic energy in the sample remains invariant, $dU = 0$. Furthermore, the change in the crack area relates to the displacement prescribed by the loading machine as $dA = (h/2)d\Delta$. Consequently, the energy release rate relates to the tear force by $G = 2F/h$. This expression holds at any tear speed, and is independent of the rheology of the hydrogel. During tear, a material particle undergoes a history of load and unload. The active deformation is localized around the tear front, in a volume scales with h^3 . A material particle is initially far ahead the crack front, and is undeformed (Point A). The material particle deforms as it approaches the crack front, within a distance about h (Point B). Finally, the material particle moves far behind the crack front, and does not deform further (Point C). When the crack extends at velocity ν , the time of active deformation is estimated by $t \approx h/\nu$ (Fig. 7b). When the time of active deformation is small compared to the relaxation time of the hydrogel, the tear speed is high, and the energy release rate is above the threshold. When the time of active deformation is large compared to the relaxation time of the hydrogel, the tear speed is low, and the energy release rate approaches the threshold.

Both peel and tear require a precut crack to be made before the test. For peel, the precut crack is required to stay well in the mid-plane of the sample, which is challenging in practice if the thickness of the sample becomes sub-millimeter scale. For tear, the precut crack is easily performed for any thickness of sample.

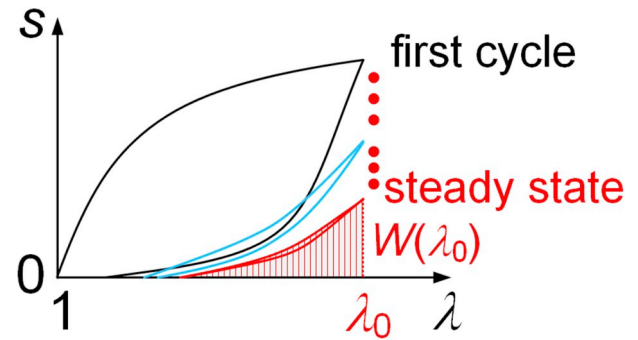


Fig. 8. For cyclic fatigue crack growth using a pure shear test, the energy release rate in the steady state is calculated using the area under the stress-stretch curve of the uncut sample in the steady state (Bai et al., 2017). The amplitude of the cyclic stretch is λ_0 .

5.8. Cyclic fatigue crack growth

Cyclic fatigue crack growth in hydrogels can be characterized using pure shear. A precut sample is subject to cyclic stretch of a prescribed amplitude λ_0 , while the extension of the crack is videotaped. A steady state is often observed after many cycles, when the extension of crack is linear in the number of cycles. The crack extension per cycle in the steady state is a function of the amplitude of the energy release rate. The crack extension per cycle increases steeply when the energy release rate approaches the toughness, and approaches zero when the energy release rate approaches the threshold (Table 2).

For an inelastic hydrogel, the energy release rate is calculated as follows. Because the period of each cycle is relatively short, on the order of a second, the breaking of most sacrificial bonds in the toughener is irreversible. Such bond breaking progresses cycle by cycle, and the stress-stretch curve keeps changing until it reaches a steady state (Fig. 8). This progressive damage over many cycles is called *shakedown* (Bai et al., 2017). Since the toughener is significantly damaged in the steady state after many cycles, the stress-stretch hysteresis is relatively small, and the hydrogel can be assumed as elastic. The energy release rate is well defined in the steady state, $G = HW(\lambda_0)$, where W is the area of the stress-stretch curve in the steady state (Bai et al., 2017).

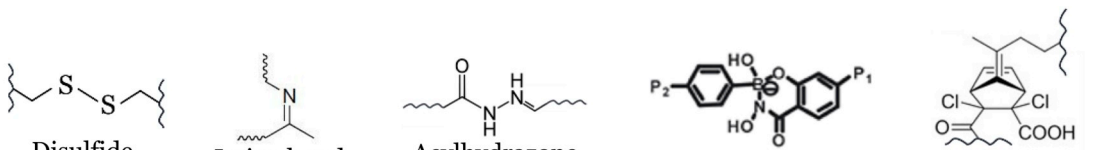
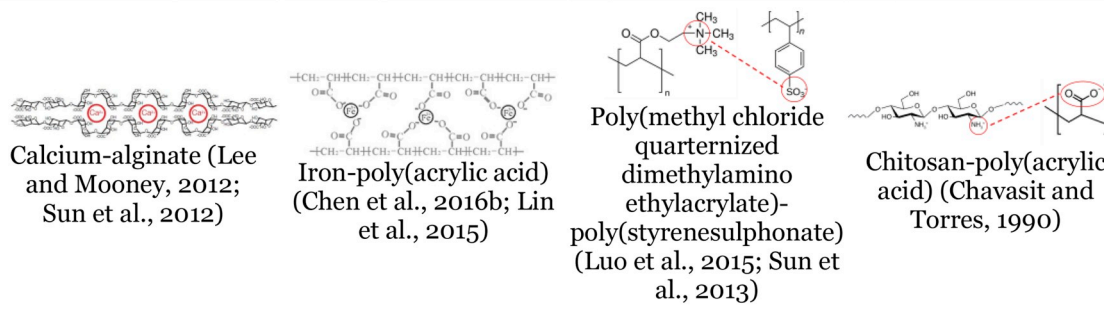
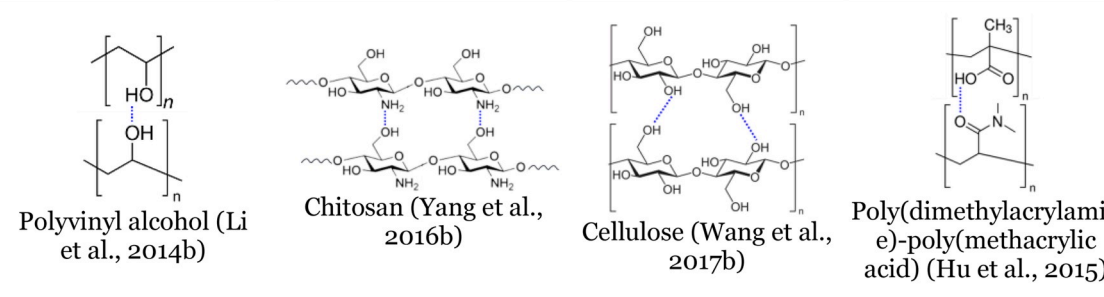
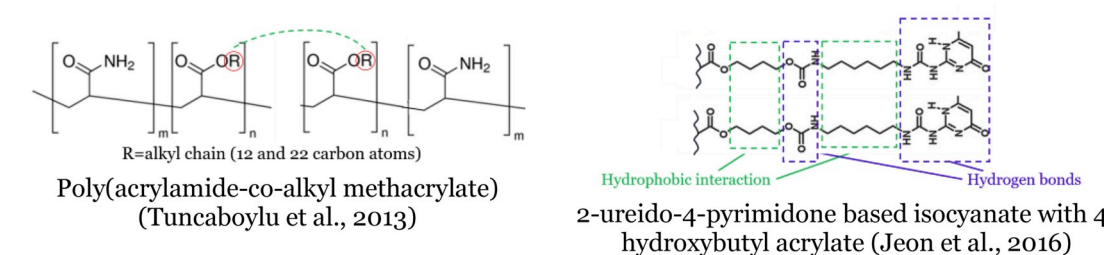
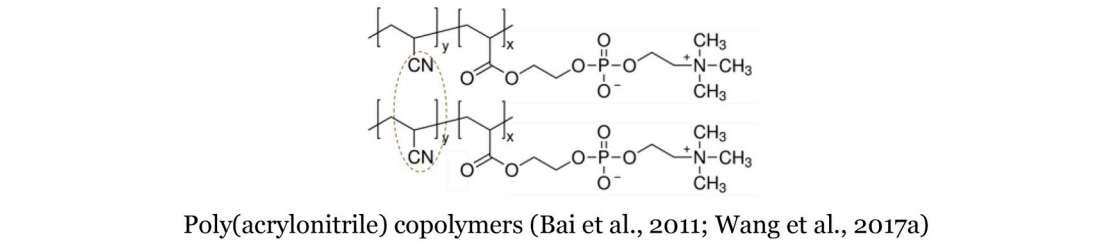
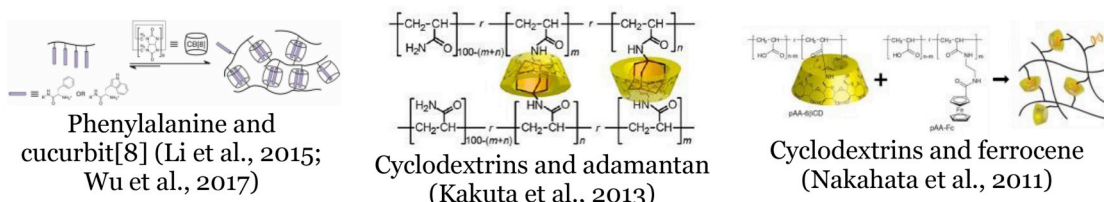
The stress-stretch curve of the uncut sample may still exhibit a small hysteresis in the steady state. In the literature of cyclic fatigue crack growth in elastomers, to calculate $W(\lambda_0)$, some authors integrated the loading part of the curve (Thomas, 1958), while others integrated the unloading part of the curve (Gent and Lai, 1994; Gent, 2012). Indeed, the hysteresis loop becomes relatively small in the steady state, and the difference induced by the two ways of calculation becomes even smaller as the crack extension per cycle approaches zero.

Cyclic fatigue crack growth in elastomers has been characterized by tear (Thomas, 1958) and peel (Baumard et al., 2012). In such a test, loading and unloading are prescribed by a constant velocity, and each cycle is controlled with a constant peak force. The crack growth per cycle can be calculated as the distance between two consecutive force peaks in the force-displacement curve recorded by the machine. The energy release rate is calculated using the same equations for tear and peel, with the peak force replacing the plateau force. The experimental data are evaluated after thousands of cycles, so that the fatigue crack growth has reached the steady state. So far, no work has reported on cyclic fatigue crack growth in hydrogels by peel or tear. It is significant to conduct cyclic peel and tear experiments, and compare them to the cyclic pure-shear experiments. This comparison is urgent for hydrogels of complex rheology.

6. Chemistries of bonds

In hydrogels, various bonds link monomer units into polymer

Table 3
Representative chemistries of reversible bonds.

<p>Dynamic covalent bonds</p>	 <p>Disulfide bond (Deng et al., 2012)</p> <p>Imine bond (Zhang et al., 2011)</p> <p>Acylhydrazone bond (Deng et al., 2012, 2010)</p> <p>Phenylboronate ester complexations (Roberts et al., 2007)</p> <p>Bonds formed by Diels–Alder reactions (Wei et al., 2013)</p>
<p>Ionic bonds</p>	 <p>Calcium-alginate (Lee and Mooney, 2012; Sun et al., 2012)</p> <p>Iron-poly(acrylic acid) (Chen et al., 2016b; Lin et al., 2015)</p> <p>Poly(methyl chloride quaternized dimethylamino ethylacrylate)-poly(styrenesulphonate) (Luo et al., 2015; Sun et al., 2013)</p> <p>Chitosan-poly(acrylic acid) (Chavasit and Torres, 1990)</p>
<p>Hydrogen bonds</p>	 <p>Polyvinyl alcohol (Li et al., 2014b)</p> <p>Chitosan (Yang et al., 2016b)</p> <p>Cellulose (Wang et al., 2017b)</p> <p>Poly(dimethylacrylamide)-poly(methacrylic acid) (Hu et al., 2015)</p>
<p>Hydrophobic interaction</p>	 <p>Poly(acrylamide-co-alkyl methacrylate) (Tuncaboylu et al., 2013)</p> <p>2-ureido-4-pyrimidone based isocyanate with 4-hydroxybutyl acrylate (Jeon et al., 2016)</p>
<p>Dipole-dipole interaction</p>	 <p>Poly(acrylonitrile) copolymers (Bai et al., 2011; Wang et al., 2017a)</p>
<p>Host-guest interaction</p>	 <p>Phenylalanine and cucurbit[8] (Li et al., 2015; Wu et al., 2017)</p> <p>Cyclodextrins and adamantane (Kakuta et al., 2013)</p> <p>Cyclodextrins and ferrocene (Nakahata et al., 2011)</p>

chains, and crosslink the polymer chains to polymer networks. Common bonds in hydrogels include covalent bonds, ionic bonds, hydrogen bonds, hydrophobic interaction, dipole-dipole interaction, and host-guest interaction (Table 3). So far as the mechanical behavior is concerned, the main characteristics of the bonds are their strengths, as well as their reversibility under the conditions of load and heal.

All bonds can reform after breaking under suitable conditions, such as long time, elevated temperature, proper pH, presence of an enzyme, and light of specific wavelength. Some covalent bonds and many non-covalent bonds are reversible under conditions applicable to hydrogels under load or heal. Reversible bonds have enabled the healing of hydrogels after distributed damage and growth of cracks (Picchioni and Muljana, 2018; Taylor and in het Panhuis, 2016; Wei et al., 2014). To limit the scope of this review, we regard a bond as irreversible if its reformation requires conditions beyond useful time and temperature for hydrogels, and will not consider the effect of any other stimuli.

6.1. Covalent bonds

Most hydrogels are composed of covalent bonds such as C-C and C-O bonds. Examples include polyacrylamide, polyethylene glycol, and poly (N-isopropylacrylamide). These bonds are irreversible. Once broken in distributed damage or crack growth, these bonds do not reform. Hydrogels formed by dynamic covalent bonds are able to heal after breaking in a time scale ranging from seconds to hours. Examples include disulfide bonds (Deng et al., 2012), imine bonds (Zhang et al., 2011), acylhydrazone bonds (Deng et al., 2012, 2010), phenylboronate ester complexations (Roberts et al., 2007), and bonds formed by Diels-Alder reactions (Wei et al., 2013). Hydrogels composed of acylhydrazone bonds can heal the crack within 24–48 h (Deng et al., 2012). Extran-poly(ethylene glycol) hydrogels can heal the crack after 7 h at 37 °C (Wei et al., 2013).

6.2. Ionic bonds

Ionic bonds are formed by the electrostatic interaction between ions of positive and negative charges. For example, alginate chains form ionic bonds with divalent calcium ions (Braccini and Pérez, 2001; Lee and Mooney, 2012), as well as other multivalent ions (Yang et al., 2013). Once broken in a hydrogel under cyclic fatigue damage, the bond is almost irreversible even after one day at room temperature. However, if the hydrogel is rest at a temperature of 60 °C for one day, the stress-stretch curve heals to more than 50% of its initial level (Sun et al., 2012). On the other hand, when forming a calcium-alginate hydrogel, the calcium ions are able to replace the sodium ions in the sodium-alginate chains within hours at room temperature. This difference in the kinetics of reaction has not been studied.

Enhancing the intermolecular interaction between ionic bonds can promote the reversibility. Ferric ions and carboxylic acid can form strong Fe^{3+} -COO⁻ coordination complex. A hydrogel without pre-cut crack formed by such complex is able to heal more than 90% of its initial mechanical property within hours without heating following the initial cyclic loads (Chen et al., 2016b; Lin et al., 2015). Mixing positively charged trimethylammonium and negatively charged sulfonate into two different polymer chains can lead to random formation of ionic bonds of different strength, and the stress-stretch curve almost completely heals after 30 min at room temperature (Luo et al., 2015; Sun et al., 2013). Other examples of ionic bonds include electrostatic interaction between chitosan chains and poly(acrylic acid) chains (Chavasit and Torres, 1990).

6.3. Hydrogen bonds

Hydrogen bonds are created between a more electronegative functional group and an adjacent functional group bearing a lone pair of electrons. A single hydrogen bond is usually weak. However, a densely

and well-packed group of hydrogen bonds can significantly amplify the bond strength. Examples include hydrogen bonds between hydroxyl groups on polyvinyl alcohol (Li et al., 2014b) and cellulose (Wang et al., 2017b), amine groups and hydroxyl groups on chitosan chains (Yang et al., 2016b), and dimethylamide groups and methacrylic acid groups (Hu et al., 2015). Because a large amount of functional groups participate in forming the hydrogen bonds, the healing from fatigue damage of such a hydrogel may be relatively easier. The healing time from fatigue damage is usually about 1–4 h at room temperature.

6.4. Hydrophobic interaction

In an aqueous solution, hydrophobic molecules aggregate and form weak interaction. When hydrophobic molecules are linked to hydrophilic polymer chains, two or more polymer chains tend to form interaction at the hydrophobic sites. Typical hydrophobic moieties are alkyl chains with length of 12 and 22 carbon atoms. The healing time of a hydrogel formed by these chains from fatigue damage is about 60 min at room temperature (Tuncaboylu et al., 2013). Combination of hydrogen bonds and hydrophobic interaction gives rise to even faster healing. A hydrogel formed by a crosslinker of an acrylic head, a hydrophobic alkyl spacer connected by carbamate, and a 2-ureido-4-pyrimidone tail has a healing time from fatigue damage as short as 1–2 min at room temperature (Jeon et al., 2016).

6.5. Dipole-dipole interaction and host-guest interaction

Dipole-dipole interaction and host-guest interaction are less common compared to the other bonds, possibly because they require uncommon matching functional groups. Strong dipole-dipole interaction is observed between nitrile groups (Bai et al., 2011; Jia et al., 2017; Wang et al., 2017a). Host-guest interaction can be established through phenylalanine and cucurbit[8] (Li et al., 2015; Wu et al., 2017), cyclodextrins and adamantane (Kakuta et al., 2013), and cyclodextrins and ferrocene (Nakahata et al., 2011).

7. Topologies of networks

Irreversible bonds can be relatively strong, but do not reform after breaking (e.g., C-C bonds). Reversible bonds are typically weak, and may reform after breaking (e.g., some ionic bonds). By a topology of networks we mean an arrangement of bonds of various types to link monomer units into polymer chains, and crosslink the polymer chains into polymer networks. The difference in the topologies of networks causes difference in the symptoms of fatigue. We next describe several representative topologies of networks.

A hydrogel of a single network crosslinked by irreversible bonds exhibits near-perfect elasticity before the bonds break (Fig. 9a). A sample without pre-cut crack keeps stress-stretch curves nearly unchanged after many cycles of load. A sample with pre-cut crack does suffer fatigue crack growth under prolonged static and cyclic loads. Because the crack extends by the scission of the irreversible network, the hydrogel after fatigue crack growth does not heal to its original state. Because the topology of the bonds of such a hydrogel is the same as that in a ceramic, the mechanical behavior of such a hydrogel is ceramic-like, even though stretch of the hydrogel is much larger than the ceramic.

A hydrogel of a single network crosslinked by reversible bonds exhibits viscoelasticity (without yield stress) or viscoplasticity (with yield stress) (Fig. 9b). In such a hydrogel, monomer units link into polymer chains by irreversible bonds (e.g., C-C covalent bonds), but polymer chains crosslink into a network by reversible bonds. Provided the intrachain irreversible bonds are much stronger than the inter-chain reversible bonds, when the hydrogel is subject to a load, the polymer chains do not break, but the network changes connectivity by breaking and reforming the reversible bonds. A sample without pre-cut crack will

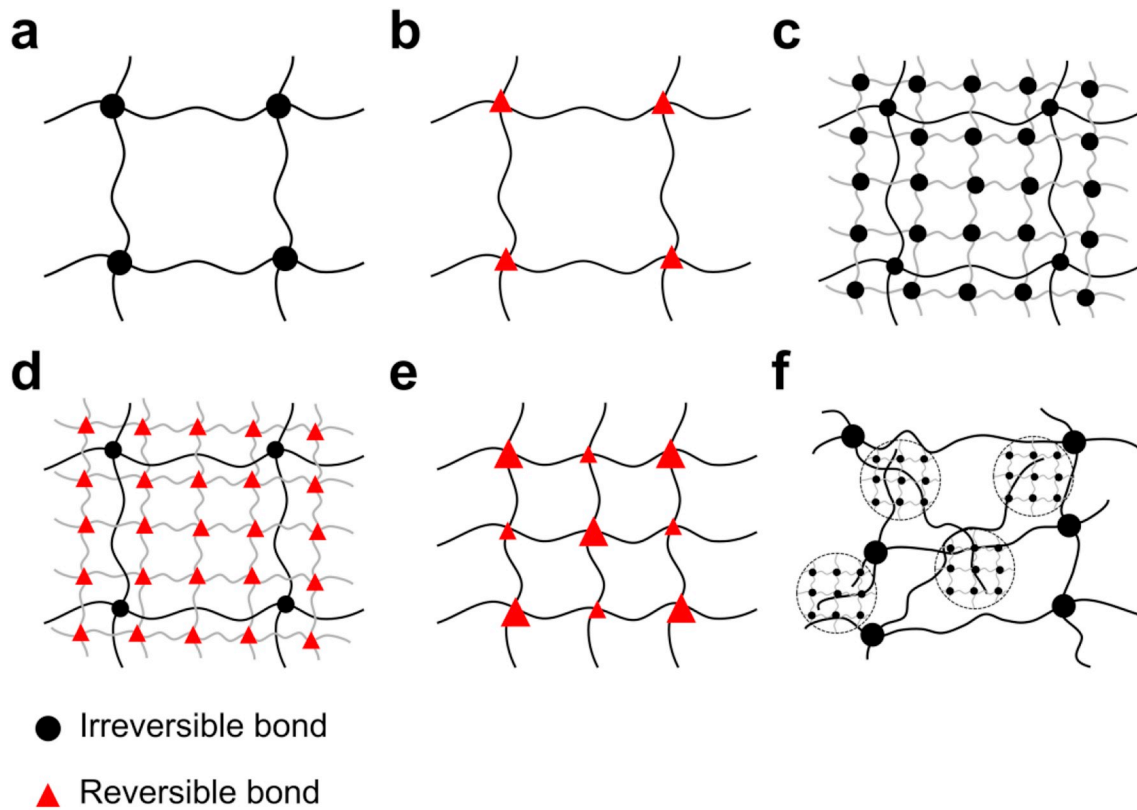


Fig. 9. Representative topologies of networks. (a) A hydrogel of a single network crosslinked by irreversible bonds. (b) A hydrogel of a single network crosslinked by reversible bonds. (c) A hydrogel of double networks crosslinked by irreversible bonds. (d) A hydrogel of two networks, one being crosslinked by irreversible bonds, and the other being crosslinked by reversible bonds. (e) A hydrogel of a single network, with two types of reversible bonds of different strengths. (f) A hydrogel of a single network crosslinked by irreversible bonds, in topological entanglement with particles of hydrogels crosslinked by irreversible bonds.

suffer fatigue damage, but damage may recover, even though the sample may suffer permanent change in shape. A sample with a precut crack may or may not suffer fatigue crack growth, depending on whether the material can concentrate stress at crack front. Honey does not suffer crack growth at ordinary loading rate, but silly putty does. Because the topology of the bonds of such a hydrogel is the same as that in a metal, the mechanical behavior of such a hydrogel is metal-like, even though stretch of the hydrogel is much larger than the metal.

In a double-network hydrogel, each network is crosslinked by irreversible bonds, the two networks are in topologically entanglement and need not have inter-network bonds, and one network is more stretchable than the other (Fig. 9c). Subject to prolonged static and cyclic loads, a sample with no precut crack exhibits near-perfect elasticity when the amplitude of stretch is small. At a larger amplitude of stretch, one network breaks in many sites, but the other network remains intact. The damage will not heal. A sample with precut crack suffers fatigue crack growth under prolonged static and cyclic loads. The cyclic fatigue threshold is below static fatigue threshold, and both thresholds are below the toughness. After fatigue crack growth, the hydrogel cannot heal to its original state. Such a double-network hydrogel is reminiscent of a ceramic-ceramic composite.

Next consider a hydrogel of two networks, one being crosslinked by irreversible bonds, and the other being crosslinked by reversible bonds (Fig. 9d). The two networks are in topological entanglement and need not have inter-network bonds. Subject to prolonged static and cyclic loads, a sample with no precut crack suffers fatigue damage, which may heal. The static network provides elasticity, which may retain the shape of the sample after the heal. A sample with precut cracks suffer both static and cyclic fatigue crack growth. After fatigue crack growth, the hydrogel cannot heal to its original state. Such a double-network hydrogel is reminiscent of a metal-ceramic composite.

Then consider a hydrogel of a single network, but with two types of reversible bonds of different strengths (Fig. 9e). Subject to prolonged static and cyclic loads, a sample with no precut crack suffers fatigue damage. The hydrogel may recover its properties, but may not recover its shape. A sample with precut cracks suffer both static and cyclic fatigue crack growth. After fatigue crack growth, the hydrogel may heal to its original state. The behavior is expected to be similar if the hydrogel has multiple species of polymer chains, crosslinked in various ways by dynamic bonds of various strengths. Such a hydrogel is reminiscent of a metal-metal composite.

In the next section, we review experimental data for hydrogels of the above five topologies. As yet another example, a hydrogel can be formed by an irreversible single network, in topological entanglement with particles of hydrogels of irreversible bonds (Hu et al., 2012a, 2012b) (Fig. 9f). This topology leads to similar mechanical behavior of the double-network hydrogel (Fig. 9c), but gives considerable flexibility in casting, coating, and printing. Many other topologies of networks are conceivable, but their effects on mechanical behavior and manufacturing are not well explored.

8. Data of five representative hydrogels

The five hydrogels represent different topologies of networks (Fig. 9a–e): polyacrylamide (a single-network hydrogel crosslinked by irreversible bonds), calcium-alginate (a single-network hydrogel crosslinked by reversible bonds), polyacrylamide-poly(2-acrylamido-2-methylpropane sulfonic acid) (a double-network hydrogel crosslinked by irreversible bonds), polyacrylamide-calcium-alginate (a double-network hydrogel crosslinked by irreversible and reversible bonds), and polyampholytes (a single-network hydrogel with two types of reversible bonds of different strengths).

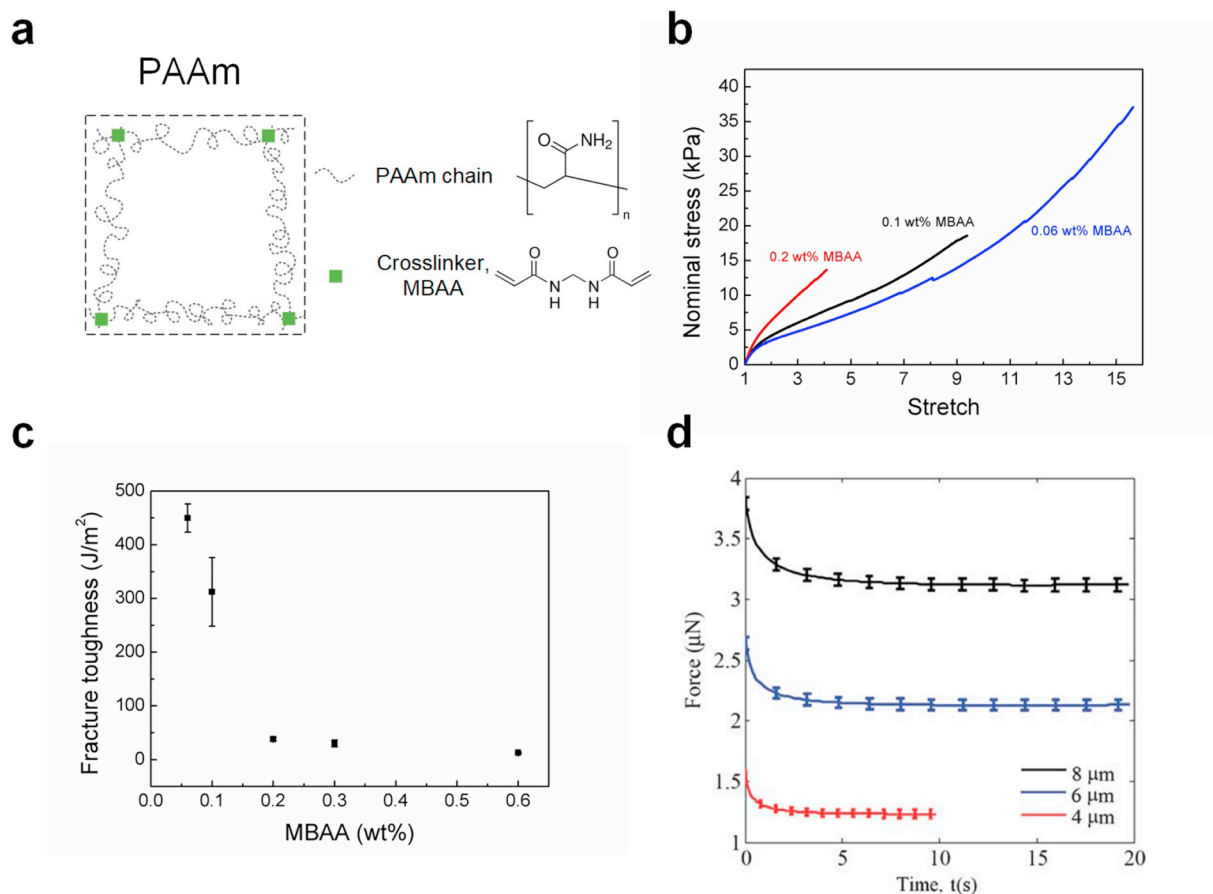


Fig. 10. Mechanical characterization of PAAm hydrogels. (a) The molecular structure of a PAAm hydrogel. (b) The stress-stretch curve of the hydrogel depends on the amount of crosslinkers MBAA added in the precursor. Each experiment is terminated when the sample ruptures. (c) The toughness of the hydrogel depends on the amount of crosslinkers. (d) Stress-relaxation of a PAAm hydrogel under an indenter (Kalcioğlu et al., 2012). (b) and (c) are plotted from a collection of data from (Bai et al., 2018b; Yang et al., 2018a), and unpublished data from Zhengjin Wang. Each data point in (c) represents an average measurement of three samples.

8.1. Polyacrylamide

A polyacrylamide (PAAm) hydrogel has a single polymer network of irreversible crosslinks (Fig. 10a). Because water has low viscosity and the PAAm network is sparse, the PAAm hydrogel has near-perfect elasticity. PAAm hydrogels are readily synthesized at many research laboratories using radical polymerization. PAAm hydrogels are used in water treatment, oil recovery, agriculture, medicine (Caulfield et al., 2002), as well as in most recently developed ionotronic devices (Lee et al., 2018; Yang and Suo, 2018). Many of these devices directly benefit from the high water content, high stretchability, elasticity, and transparency of PAAm hydrogels. Many tough hydrogels use PAAm as the primary network. The chemical and physical properties of PAAm hydrogels have been extensively characterized, including kinetics of polymerization (Candau et al., 1985; Gelfi and Righetti, 1981a, b; Tobita and Hamielec, 1990), long-time stability (Caulfield et al., 2002; Cheng, 2004; Smith et al., 1997), thermodynamics of mixing (Day and Robb, 1981; Hochberg et al., 1979), large deformation and swelling (Cai and Suo, 2012; Li et al., 2012), fracture (Foegeding et al., 1994; Livne et al., 2010; Tanaka et al., 2000; Zhang et al., 2005), and phase separation (Sato et al., 2015). All these facts together make PAAm an excellent model material for the study of the mechanical behavior of hydrogels, just like silica for the study of the mechanical behavior of glass and ceramics (Griffith, 1921; Orowan, 1944; Wiederhorn and Bolz, 1970), and copper for the study of the mechanical behavior of metals (Basinski et al., 1980; Katagiri et al., 1977; Thompson et al., 1956).

The modulus, stretchability, and toughness of PAAm hydrogels

depend on the polymer chain length, which can be controlled by the amount of the crosslinkers *N,N'*-Methylenebis(acrylamide) (MBAA) (Fig. 10b&c). For a PAAm hydrogel synthesized with 1.9 M of the monomer acrylamide, adding 0.2 wt% of MBAA relative to acrylamide makes a stretchable but brittle hydrogel. The hydrogel has a Young's modulus of 9.3 kPa, can be stretched to four times its initial length before fracture, and has a toughness of $38.2 \pm 3.4 J/m^2$. With 0.06 wt% of MBAA, the hydrogel becomes much more stretchable and tougher. The hydrogel has a Young's modulus of 6.7 kPa, can be stretched over 15 times its initial length without fracture, and has a toughness of $449 \pm 26 J/m^2$.

As noted before, the effective diffusivity of water in hydrogels can be measured using indentation (Hu et al., 2010). The indenter is pressed onto the hydrogel to a prescribed depth and then held over a long time. The depth of indentation is large enough so that the measured relaxation is limited by poroelasticity (Hu and Suo, 2012). A force sensor records the force on the indenter as a function of time, $F(t)$. The force has an initial value of $F(0)$, decreases with time t , and reaches a plateau $F(\infty)$ after a long time. Different indentation depths lead to different force-relaxation curves (Fig. 10d). The curves are then plotted using a normalized force $(F(t) - F(\infty))/(F(0) - F(\infty))$ and a normalized loading time t/a^2 , where a is the indentation depth of the experiment. In this way, all the curves collapse onto one curve. The time scale of viscoelastic relaxation is assumed to be independent of the indentation depth, whereas the time scale of poroelastic relaxation is proportional to the square of the length scale a . This collapse of data indicates that the relaxation of hydrogel is due to poroelasticity, not viscoelasticity. The effective diffusivity of PAAm is on the order of $D \sim 10^{-10} m^2/s$

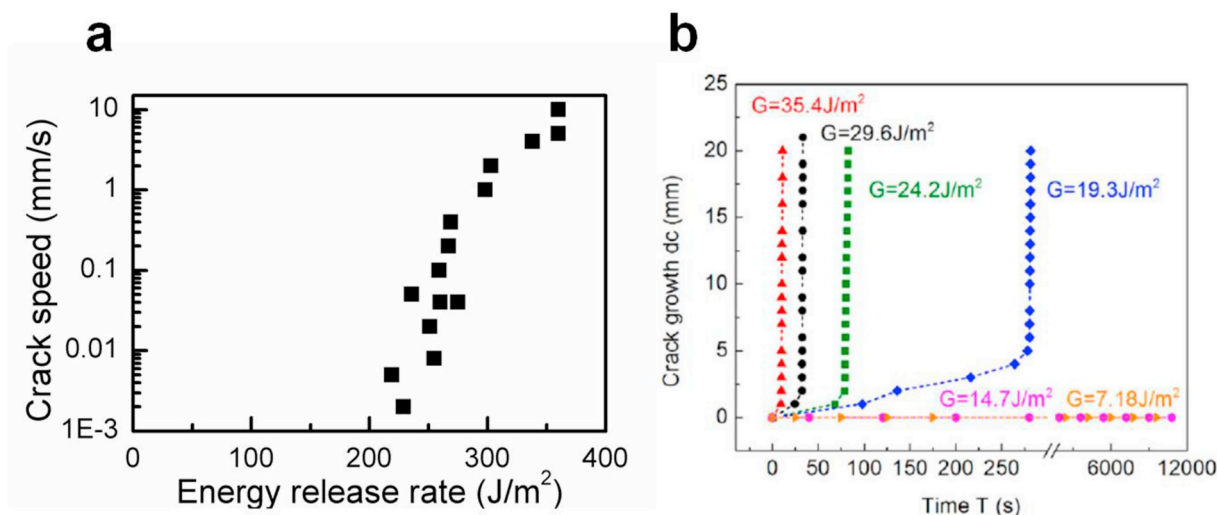


Fig. 11. Static fatigue of samples of PAAm hydrogels with pre-cut cracks. (a) Static fatigue crack growth in PAAm. Data replotted from (Yang et al., 2018b). (b) Delayed fracture in PAAm (Tang et al., 2017). The two sets of data in (a) and (b) use PAAm hydrogels prepared under different conditions, and should not be compared.

(Kalcioğlu et al., 2012). The time needed to homogenize a material over a length scale 1 mm is 10^4 s. For comparison, the viscoelastic relaxation time of polyacrylamide chains has been measured to be typically less than 1 s (Heemskerk et al., 1984; Pavesi and Rigamonti, 1995; Tian et al., 2018; Weiss and Silberberg, 1977).

Whereas PAAm hydrogels without pre-cut cracks exhibit near-perfect elasticity, PAAm hydrogels with pre-cut cracks do suffer both static and cyclic crack growth. The study of static fatigue crack growth in hydrogels was initiated by Tanaka et al. (2000), using PAAm hydrogels and the peel test. The ν - G curve depends on the concentration of the crosslinker. As the concentration of the crosslinker reduces, the length of PAAm chains increase, and the energy release rate increases for a constant crack speed. The ν - G curve is also expected to depend on the volume fraction of polymer in the hydrogel, but this dependence has not been reported. For a PAAm hydrogel, with 0.06 wt% of MBAA relative to acrylamide, and with the volume fraction of polymer at 10.7%, the energy release rate is about 350 J/m^2 at a high speed of 10 mm/s, and approaches about 200 J/m^2 at a low speed of $1 \mu\text{m/s}$ (Fig. 11a) (Yang et al., 2018b).

Delayed fracture has been observed using PAAm hydrogels with pre-cut cracks (Tang et al., 2017). The delay time, i.e. the period between the start of loading and fracture, is longer under lower energy release rate (Fig. 11b). When the energy release rate is below a threshold, denoted as the *threshold for delayed fracture*, the crack does not grow within the observable time window of the experiment.

Under cyclic loads, samples of PAAm hydrogels without pre-cut cracks exhibit near perfect elasticity, free from cyclic fatigue damage. The stress-stretch curves exhibit little hysteresis, and change negligibly after thousands of loading cycles (Fig. 12a) (Bai et al., 2017).

The study of cyclic fatigue crack growth in hydrogels was initiated by Tang et al. (2017), using PAAm hydrogels and the pure shear test. The cyclic-fatigue threshold increases with the volume fraction of polymer (Zhang et al., 2018a). The threshold is also expected to increase with length of polymer chains, but no experimental data is reported.

For the same PAAm hydrogel, the cyclic-fatigue threshold is lower than the delayed-fracture threshold (Tang et al., 2017). The relation between the two thresholds is still under study. Both the static and cyclic fatigue of PAAm indicate that PAAm hydrogels contain some kind of mechanism of energy dissipation, despite low hysteresis in the stress-stretch curves of samples without pre-cut cracks. A likely mechanism is poroelasticity (Section 12).

8.2. Calcium-alginate

Alginate hydrogels are broadly used in medical applications such as drug delivery, tissue engineering, and cell transplantation (Augst et al., 2006; Lee and Mooney, 2012; Li and Mooney, 2016; Rowley et al., 1999). Sodium-alginate dissolves in water as a polyelectrolyte, with mobile ions (Na^+), along with mobile alginate chains containing fixed charges (carboxyl group COO^-). By contrast, a calcium-alginate (Ca-alginate) hydrogel consists of alginate polymer chains crosslinked by Ca^{2+} ions (Fig. 13a). Ca-alginate hydrogels have elastic modulus ~ 10 – 100 kPa (Fig. 13b), and toughness $\sim 10 \text{ J/m}^2$ (Fig. 13c) (Sun et al., 2012).

In Ca-alginate hydrogels, the alginate chains and Ca^{2+} ions form “egg box”-like interactions, with the energy of ionic bonds on the order of kT , where kT is the temperature in the unit of energy (Braccini and Pérez, 2001; Fang et al., 2007; Sikorski et al., 2007). Such ionic bond is two orders of magnitude weaker compared to the covalent bond forming alginate chains. As a result, the ionic bond is reversible at elevated temperature (Sun et al., 2012). Subject to a constant compressive strain, Ca-alginate relaxes to zero stress when the hydrogel is compressed in the phosphate-buffered saline (PBS) solution (Fig. 13d) (Zhao et al., 2010), but relaxes to a finite stress when the hydrogel is compressed in the silicone oil (Fig. 13e) (Bai et al., 2018a). Such a difference may result from the known degradation of Ca-alginate network in PBS due to ion exchange or bacteria (Bajpai and Sharma, 2004; Hashimoto et al., 2005), which may have damaged the Ca-alginate network over the long time.

Because of the relatively weak ionic bonds forming the crosslinks, the fracture of the Ca-alginate hydrogel results from the unzipping of the ionic bonds and pullout of the alginate chains. The energy release rate for crack propagation depends on the crack speed (Fig. 14a) (Baumberger and Ronsin, 2009). The threshold for static fatigue crack growth in Ca-alginate is only a few J/m^2 . In comparison, the threshold of a crack growing in PAAm is 10 – 100 J/m^2 , where the fracture is due to the scission of polymer chains.

The mechanical behavior of Ca-alginate hydrogels under many cycles of loading has not been reported. Considerable stress-stretch hysteresis has been observed during an initial loading cycle with a stretch amplitude of 1.2 (Fig. 14b) (Sun et al., 2012).

Static fatigue fracture and crack growth have been studied in other physical hydrogels with networks crosslinked by reversible bonds. Examples include agar hydrogels (Bonn et al., 1998; Lefranc and

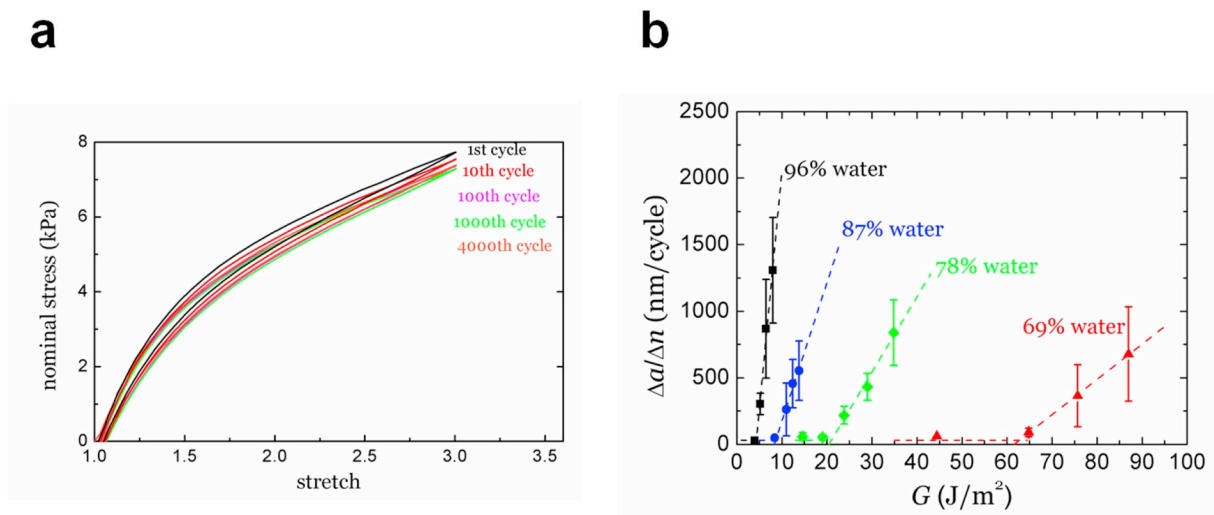


Fig. 12. (a) Samples of PAAm hydrogels without pre-cut cracks do not suffer cyclic fatigue damage and have small stress-stretch hysteresis (Bai et al., 2017). (b) Samples of PAAm hydrogels with pre-cut cracks suffer cyclic fatigue fracture. The cyclic fatigue crack growth depends on the intrinsic variables of the hydrogel, such as the water content (Zhang et al., 2018a).

Bouchaud, 2014), and gelatin hydrogels (Baumberger et al., 2006a, 2006b; Leocmach et al., 2014; Naassoui et al., 2018). Cyclic fatigue crack growth in any physical gel has not been reported. Such a study would provide an excellent contrast with that for a chemical gel like polyacrylamide. A physical gel is metal-like, and a chemical gel is ceramic-like.

8.3. Polyacrylamide-poly(2-acrylamido-2-methylpropane sulfonic acid)

The polyacrylamide-poly(2-acrylamido-2-methylpropane sulfonic acid) (PAAm-PAMPS) hydrogel is the first double-network hydrogel that exhibits high toughness (Gong et al., 2003). The hydrogel consists of a more stretchable PAAm network and a less stretchable PAMPS network, with the two networks interpenetrating in topological entanglement (Fig. 15a). When the hydrogel is subject to a uniaxial tensile stretch, the stress-stretch curve shows a yielding point, accompanied by a necking phenomenon observed in the hydrogel (Fig. 15b) (Gong, 2010; Na et al., 2006; Nakajima et al., 2013; Yu et al., 2009). In Region (i) of the stress-stretch curve, as the hydrogel is stretched, the PAAm network remains nearly intact, but the PAMPS network breaks progressively. The deformation is homogeneous with no strain localization. The stress increases with the stretch. In Region (ii), the accumulated damage of the PAMPS network leads to a yielding point in the stress-stretch curve. A portion of the hydrogel sample forms a neck. A subsequent plateau in the stress-stretch curve is observed, just like ideal plasticity in metal. The necking zone in the sample gradually develops with the increase of stretch over the plateau. In Region (iii), the PAMPS network has broken extensively, the elasticity of the PAAm network dominates, the hydrogel sample regains a homogeneous deformation, and the stress starts to increase again.

The toughness of the PAAm-PAMPS hydrogel is higher when the crosslink density of the PAAm network decreases, similar to the PAAm hydrogel. On the other hand, if the crosslink density of PAAm in the double-network hydrogel is too low to form a homogeneous and well-crosslinked network, the toughness will decrease again (Fig. 15c) (Gong, 2010; Nakajima et al., 2009).

Because both networks are covalently crosslinked, the PAAm-PAMPS hydrogels are less susceptible to static fatigue than PAAm-calcium-alginate hydrogels. For a PAAm-PAMPS hydrogel of a particular composition, the energy release rate is about 600 J/m^2 at a crack speed of 10^3 mm/min , and about 200 J/m^2 at 10^{-1} mm/min (Fig. 16a) (Tanaka et al., 2005; Yu et al., 2009).

The scission of the covalent PAMPS network is completely irreversible. As a result, an uncut PAAm-PAMPS hydrogel severely suffers cyclic fatigue damage under cyclic loads. The stress-stretch curve has pronounced hysteresis during the first cycle of loading, but almost no hysteresis in the following loading cycles (Fig. 16b&c) (Webber et al., 2007; Zhang et al., 2018b). The hydrogel does not recover its mechanical property even after one week staying in the unstressed state (Fig. 16b). The stress-stretch curve in the second loading cycle follows the unloading curve of the initial cycle, but behaves as a fresh material once exceeding the maximum stretch in the first cycle. Such observation is denoted as the Mullins effect (Mullins, 1948, 1969; Webber et al., 2007). The hysteresis and the stress level keeps decreasing over thousands of loading cycles before reaching a steady state (Fig. 16c). This phenomenon is called *shakedown* (Bai et al., 2017), and has been observed in other hydrogels (Bai et al., 2011, 2018c). A pre-cut PAAm-PAMPS hydrogel suffers cyclic fatigue crack growth. The threshold can reach over 400 J/m^2 (Fig. 16d) when the crosslink density of the PAAm network is low. This is the highest cyclic-fatigue threshold among hydrogels reported so far, but still much lower than the toughness ($\sim 4000 \text{ J/m}^2$) of the hydrogel.

Although the toughness of a PAAm-PAMPS hydrogel is often lower than many other hydrogel systems due to the finite dissipation from the covalently crosslinked PAMPS toughener, it has potential advantage in specific applications. Both networks in the PAAm-PAMPS hydrogel are covalently crosslinked, inert and stable, making the hydrogel stable in biological environment, such as being implanted in a living body (Haque et al., 2012b; Nonoyama et al., 2016). The PAAm-PAMPS hydrogel can be a good candidate for development of hydrogel biological applications that require both robustness of load bearing and stability in biological environment.

8.4. Polyacrylamide-calcium-alginate

In a polyacrylamide-calcium-alginate (PAAm-Ca-alginate) hydrogel, PAAm forms a network of covalent crosslinks, Ca-alginate forms a network of ionic crosslinks, and the two networks interpenetrate in topological entanglement (Fig. 17a). Sun et al. (2012) discovered that the hydrogel can be stretched more than 20 times its initial length, and has toughness above 8000 J/m^2 . Further improvements have increased the toughness of PAAm-Ca-alginate hydrogels beyond $10,000 \text{ J/m}^2$ (Li et al., 2014a). The hydrogel has been developed for applications including soft robots (Yuk et al., 2017), tough adhesives (Li et al., 2017a),

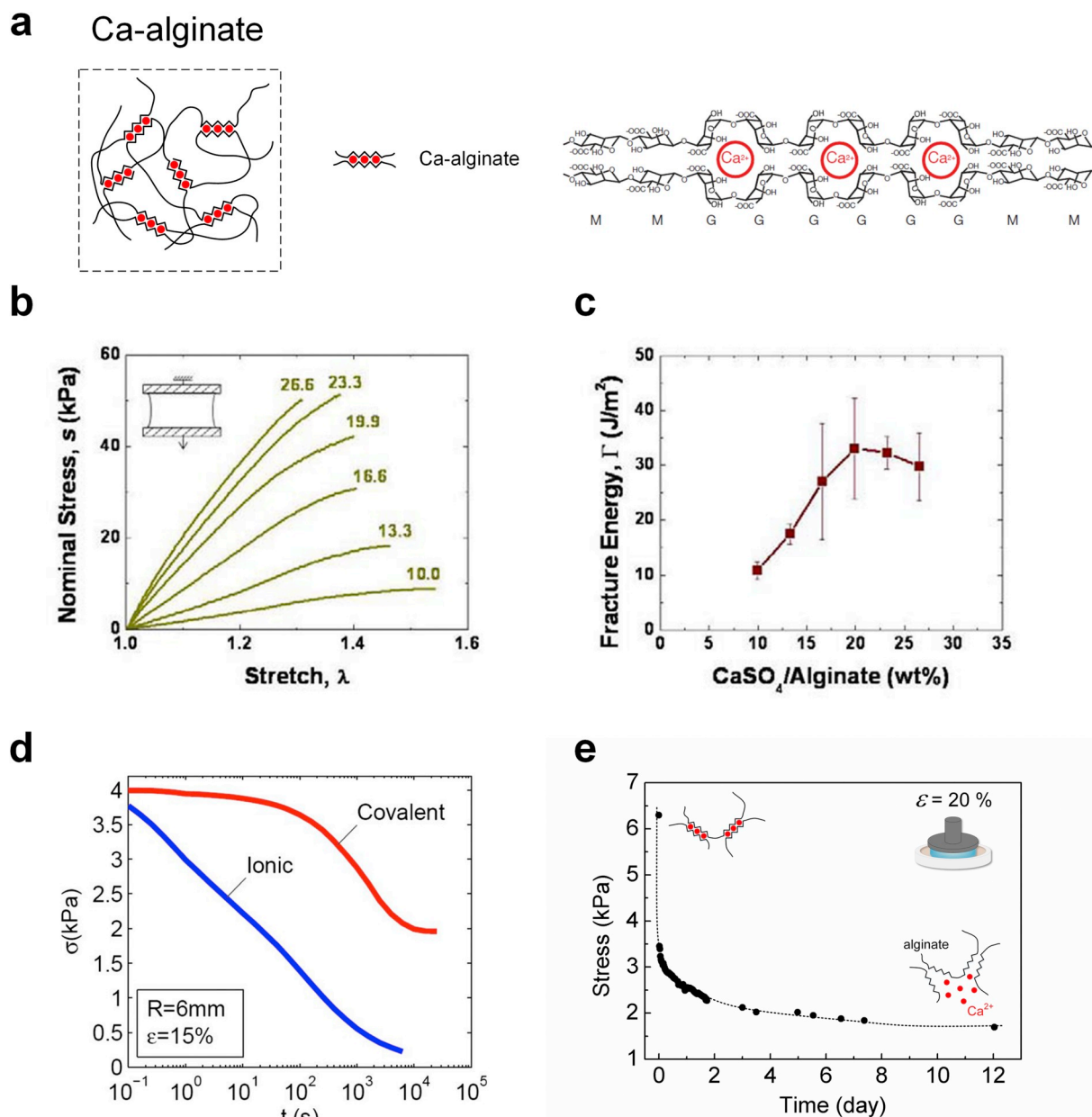


Fig. 13. Mechanical characterization of Ca-alginate hydrogels. (a) The molecular structure of the Ca-alginate hydrogel. (b) The stress-stretch curve depends on the ratio between Ca²⁺ ions and alginate chains (Sun et al., 2012). (c) The toughness depends on the ratio between Ca²⁺ ions and alginate chains (Sun et al., 2012). (d) Stress relaxation of the Ca-alginate hydrogel (blue) and the covalently crosslinked alginate hydrogel (red) immersed in PBS (Zhao et al., 2010). (e) Stress relaxation of the Ca-alginate hydrogel immersed in silicone oil (Bai et al., 2018a). (For interpretation of the references to colour in this figure legend, the reader is referred to the Web version of this article.)

and drug delivery systems (Liu et al., 2017a).

Upon stretching, the long-chain PAAm network provides elasticity and ensures high stretchability, while the Ca-alginate network unzips through its ionic crosslinks and dissipate energy. The stress-stretch curves depend on the proportions of the two networks (Fig. 17b). When a pre-cut PAAm-Ca-alginate hydrogel is stretched, the PAAm network bridges the crack front, while the Ca-alginate network unzips in a large volume surrounding the crack front. The synergy of the two processes leads to large energy dissipation. The toughness peaks when the amount of alginate is neither too low nor too high (Fig. 17c).

Because of the rate-dependent unzipping of Ca-alginate, the PAAm-Ca-alginate hydrogel is also rate-dependent (Lu et al., 2016; Mao et al., 2017; Xin et al., 2015). The elastic response of the stress-stretch curves after relaxation is identical under a range of loading rate (Fig. 17d&e),

but does not coincide with the stress-stretch curve directly measured at a lower loading rate (Fig. 17e). Such an over-drop of the relaxed elastic response has been modeled as the viscoelastic Mullins effect of PAAm-Ca-alginate hydrogels (Lu et al., 2016).

Static fatigue crack growth is pronounced in PAAm-Ca-alginate hydrogels (Fig. 18) (Bai et al., 2018a). At a high crack speed, the unzipping of Ca-alginate dissipates a large amount of energy and toughens the hydrogel. For the hydrogel with a specific composition and thickness, the energy release rate is over 4000 J/m² at a crack speed of 0.01 m/s, but only about 200 J/m² at a crack speed of 1 μ m/s (Fig. 18a). The large amount of unzipping Ca-alginate induces large-scale inelasticity. The inelastic zone grows with increasing crack speed. Such rate-dependent inelastic zone can be probed by testing samples of identical composition but different thicknesses, as discussed before

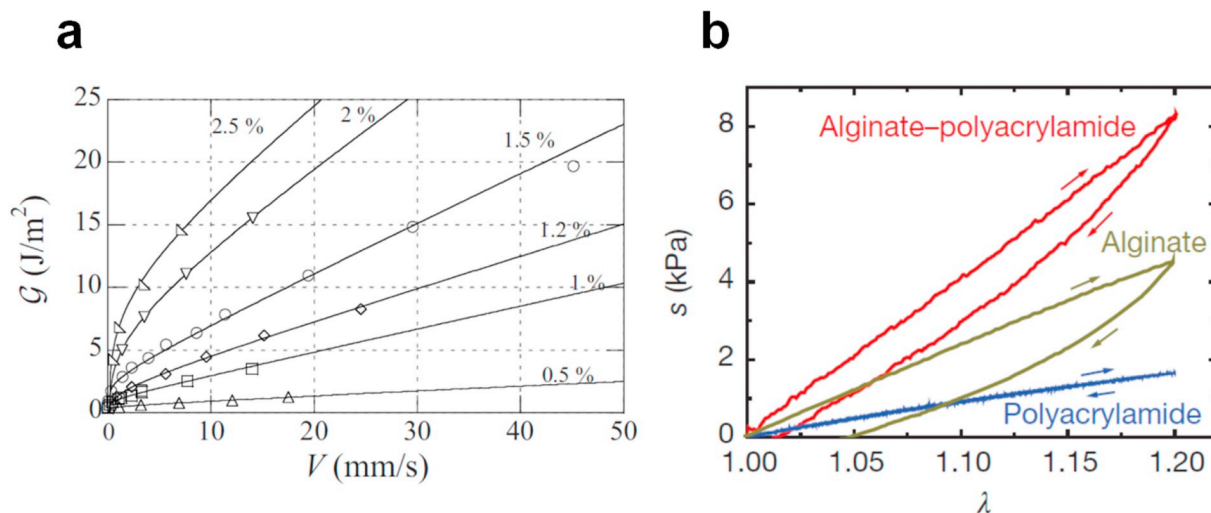


Fig. 14. Static and cyclic fatigue of Ca-alginate hydrogels. **(a)** Static fatigue crack growth of the Ca-alginate hydrogel (Baumberger and Ronsin, 2009). The different curves correspond to different alginate/water weight fractions. **(b)** Cyclic hysteresis of the Ca-alginate hydrogel, together with the PAAm hydrogel and the hybrid hydrogel of the two networks (Sun et al., 2012).

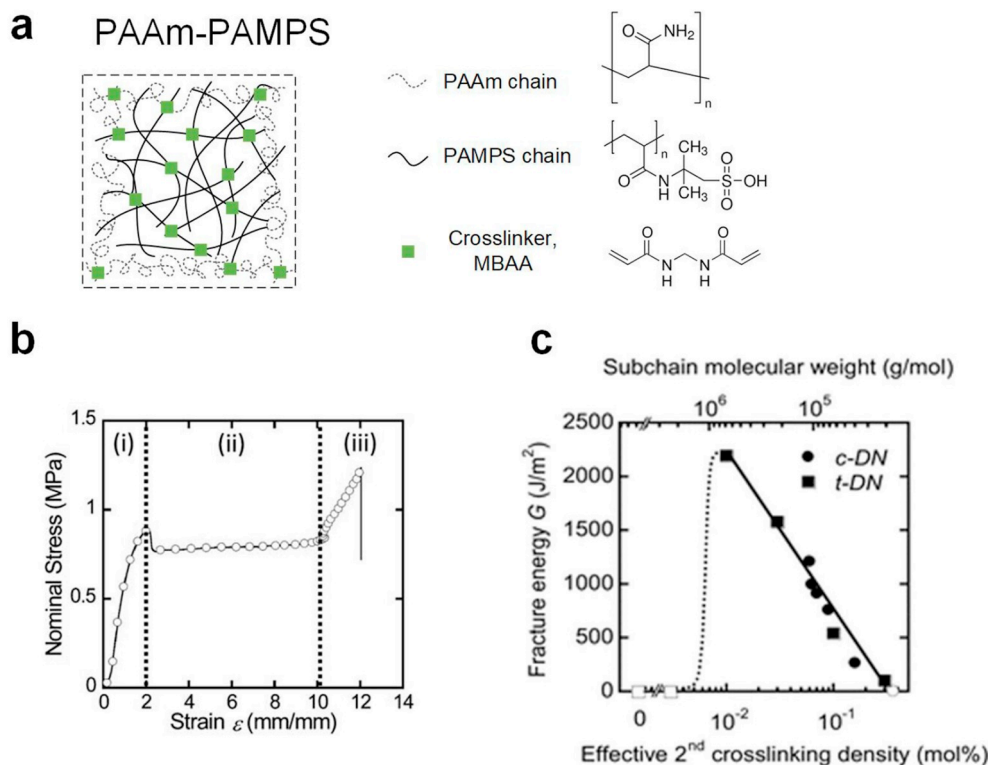


Fig. 15. Mechanical characterization of PAAm-PAMPS hydrogels. **(a)** The molecular structure of the PAAm-PAMPS hydrogel. **(b)** The stress-stretch curve shows a yielding point (Nakajima et al., 2013). **(c)** The toughness is a function of the crosslinking density of the PAAm network (Nakajima et al., 2009).

(Section 5.6, Fig. 6). In the tear test, at a tear speed of 0.5 $\mu\text{m/s}$, the energy release rate depends negligibly on the thickness (Fig. 18b), indicating the condition of small-scale inelasticity, and the size of the inelastic zone is smaller than the smallest thickness tested, 0.4 mm. At tear speeds higher than 0.5 $\mu\text{m/s}$, the energy release rate increases with the thickness from 0.4 mm, 0.7 mm, 1.0 mm–1.5 mm, but reaches a plateau from 1.5 mm to 3.0 mm, indicating that small-scale inelasticity only holds for the thickness of 1.5 mm and 3.0 mm. Under the condition of small-scale inelasticity, the size of the inelastic zone at these speeds is between 1.0 mm and 1.5 mm.

The solid-like Ca-alginate network at low speed still toughens the static-fatigue threshold. For PAAm-alginate hydrogels with the same

PAAm-alginate, but different concentrations of calcium, 0 (0-Ca), 2.2 wt % of AAm (1-Ca) and 4.4 wt% of AAm (2-Ca), the threshold is 59, 173, and 952 J/m^2 , respectively (Fig. 18c).

Under cyclic loads, an uncut PAAm-Ca-alginate hydrogel suffers cyclic fatigue damage (Bai et al., 2017; Sun et al., 2012). The dissociation of Ca-alginate ionic bonds is almost irreversible at room temperature, but is reversible at elevated temperature. The stress-stretch hysteresis decreases drastically in the second loading cycle even if the hydrogel stays unstressed for one day at room temperature (Fig. 19a), but the hydrogel substantially heals from fatigue damage at an elevated temperature (Fig. 19b) (Sun et al., 2012). The large reduction of hysteresis indicates that the majority of sacrificial bonds

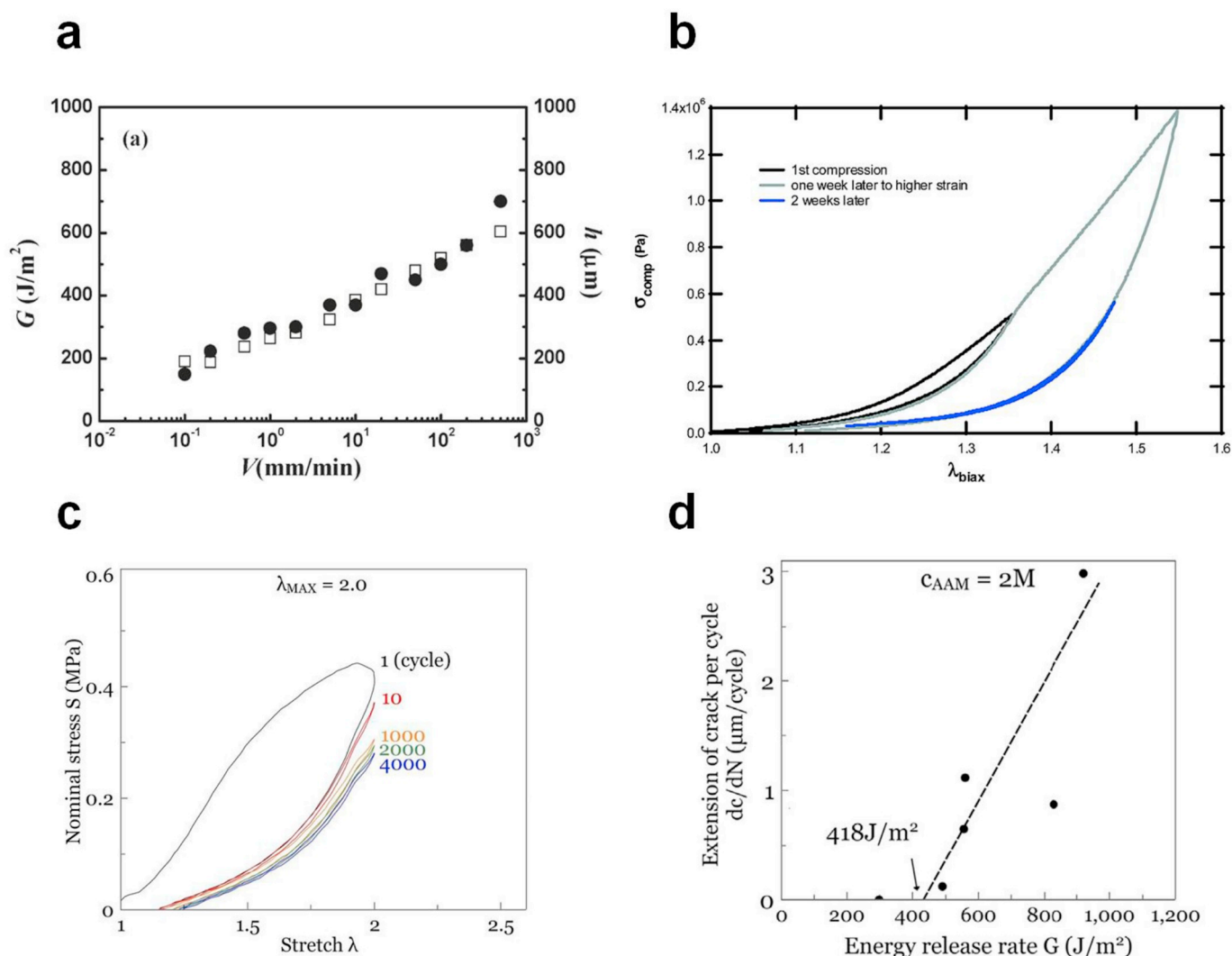


Fig. 16. Static and cyclic fatigue of PAAm-PAMPS hydrogels. (a) Static fatigue crack growth (Yu et al., 2009). (b) The hydrogel shows significant stress-stretch hysteresis during the first loading, but shows almost no hysteresis in the following loading (Webber et al., 2007). Mullins effect is observed in the hydrogel. The hydrogel cannot recover its material property at all, even after one week staying in the undeformed state. (c) Cyclic fatigue damage of the PAAm-PAMPS hydrogel. The hydrogel reaches a steady state with negligible hysteresis after thousands of cycles (Zhang et al., 2018b). (d) The cyclic-fatigue threshold can reach over 400 J/m², higher than any other hydrogels reported so far, but still much lower than the toughness of the hydrogel (~4000 J/m²) (Zhang et al., 2018b).

already break after the initial loading. The hysteresis is rate-dependent as expected from Ca-alginate dissociation (Fig. 19c) (Mao et al., 2017). Shakedown of the stress-stretch curve is observed under thousands of cycles of loads (Fig. 19d) (Bai et al., 2017).

A precut PAAm-Ca-alginate hydrogel suffers cyclic fatigue crack growth under cyclic loads (Bai et al., 2017). Under a constant amplitude of cyclic stretch, the crack extension per cycle is steep at the beginning, but becomes smaller when reaching the steady state (Fig. 19e). Due to the cyclic fatigue damage in the hydrogel, the energy release rate corresponding to the fixed stretch amplitude is large at the beginning, but decreases with cycles. For a relatively brittle type of PAAm-Ca-alginate hydrogel with toughness of about 1500 J/m², the threshold is 53 J/m² (Fig. 19f).

In addition to PAAm-Ca-alginate hydrogels, many hydrogels have been developed to heal using networks of irreversible bonds and tougheners of reversible bonds. The reversible tougheners include networks crosslinked by hydrogen bonds (Hu et al., 2015; Liu and Li, 2016; Yang et al., 2016b), hydrophobic interaction (Haque et al., 2011, 2012a; Jeon et al., 2016; Tuncaboylu et al., 2013), dipole-dipole interaction (Bai et al., 2011), and ionic bonds (Chen et al., 2016b; Du et al., 2014; Lin et al., 2015; Liu and Li, 2016; You et al., 2016). In these

hydrogels, the properties such as modulus, strength, area of hysteresis loop, and toughness typically reduce by 10%–50% immediately following an initial loading. Most of these hydrogels can completely heal from cyclic fatigue damage and recover their properties at room temperature. The time of complete heal ranges from a few minutes to almost a day, depending on the type of reversible bonds. For example, creating well-organized and densely-packed hydrogen bonds among multiple polymer chains can improve the inter-chain interaction, and lead to a heal time of 1–4 h at room temperature (Hu et al., 2015; Yang et al., 2016b). Linking hydrophobic moieties to hydrophilic chains also improves the inter-chain interaction, and the heal time is about 60 min at room temperature (Haque et al., 2011, 2012a; Tuncaboylu et al., 2013). Compared to calcium ions, ferric ions can form stronger coordination with alginate or poly(acrylic acid), and the heal time is about 20 min at room temperature (Chen et al., 2016b; Lin et al., 2015). A combination of hydrogen bonds and hydrophobic interaction gives rise to even shorter heal time of 1–2 min at room temperature (Jeon et al., 2016).

Bai et al. (2018c) have studied both cyclic fatigue crack growth and cyclic fatigue damage in a hydrogel with PAAm network and uncrosslinked polyvinyl alcohol (PVA) chains. The PVA chains interact with themselves

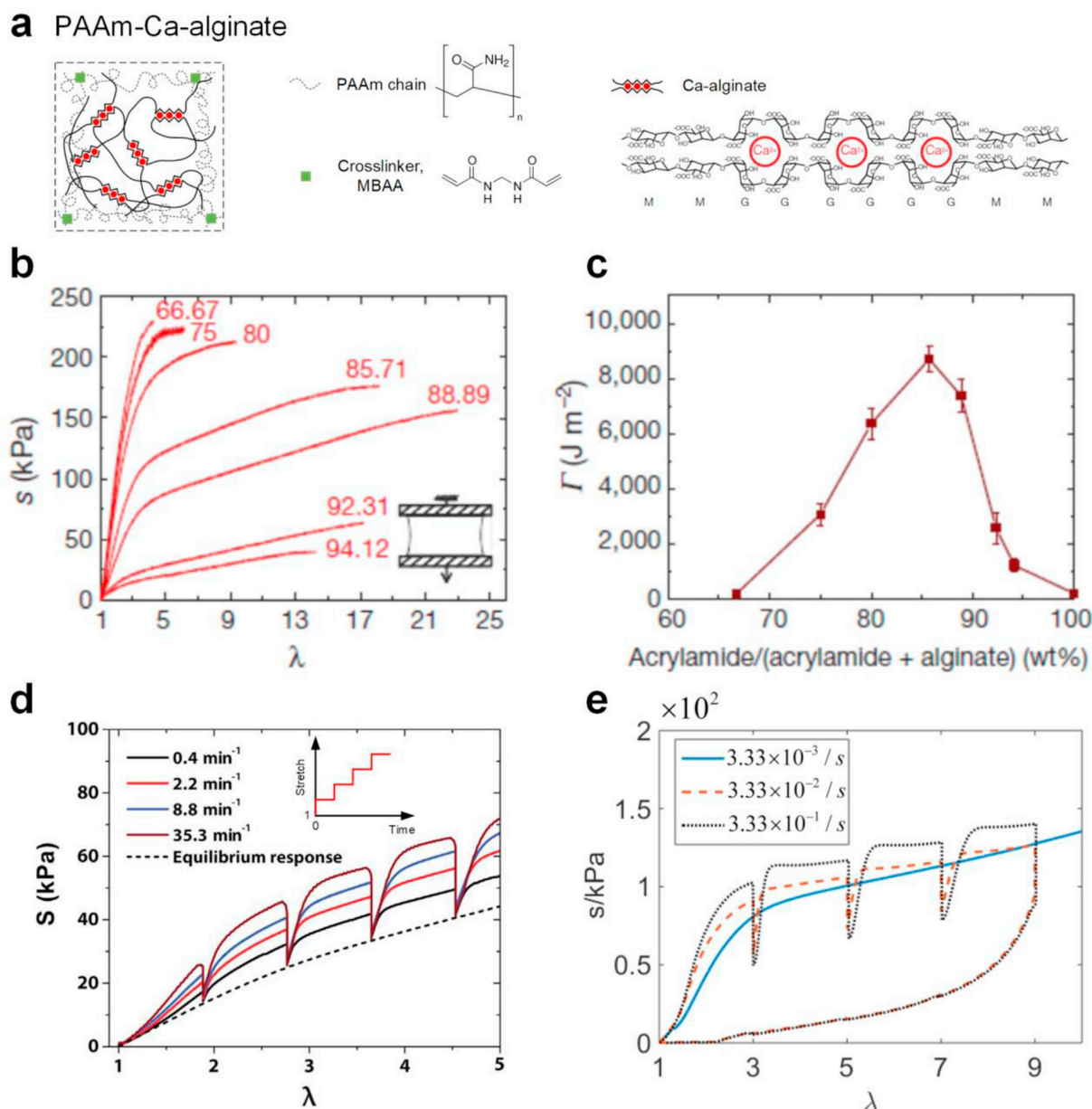


Fig. 17. Mechanical characterization of PAAm-Ca-alginate hydrogels. (a) The molecular structure of the hydrogel. (b) The stress-stretch curve depends on the ratio between the acrylamide and alginate (Sun et al., 2012). (c) The toughness depends on the ratio between the acrylamide and alginate (Sun et al., 2012). (d) Stress relaxation of the hydrogel under different initial loading rate (Mao et al., 2017). (e) The elastic response of the stress-stretch curves after relaxation is lower than the stress-stretch curve directly measured at a lower loading rate (Lu et al., 2016).

and with PAAm chains through hydrogen bonds. When a sample with no precut crack is tested under cyclic loads, the hydrogel heals from cyclic fatigue damage completely after 3 min staying in the unstressed state. When a sample with precut crack is tested under cyclic load, the crack extends cycle by cycle, and the hydrogel cannot heal from cyclic fatigue crack growth afterwards. That is, the hydrogel does not suffer cyclic fatigue damage given some time of heal, but does suffer cyclic fatigue crack growth. Because the crack extends by the scission of the irreversible network, the cracked hydrogel cannot heal to the original state.

8.5. Polyampholytes

A polyampholyte chain contains dissimilar charged monomer units (Zurick and Bernards, 2013). A polyampholyte hydrogel is synthesized by random copolymerization of two kinds of oppositely charged monomers. The effective energy of an ionic group in the hydrogel is a

collection of many individual ionic pairs that are chemically identical. The ionic groups have a wide distribution of strength in the hydrogel, where the stronger ionic groups build a solid-like network, and the weaker ionic groups act as a toughener (Fig. 20a) (Sun et al., 2013). The bond energy of each ionic pair may be much lower than that of a C-C covalent bond, but the energy of an ionic group as a sum can be built up and tuned by the concentrations of ionic pairs, as well as the combinations of different pairs. Such combinations bestow the polyampholyte hydrogel high stiffness, strength, toughness, as well as efficacy for heal (Sun et al., 2017a). The complex mechanical behavior of a polyampholyte hydrogel reflects its complex molecular topologies.

The solid-like strong ionic groups ensure that the hydrogel has a high strength of MPa, while the easily reversible weak ionic groups make the stress-stretch curve rate-dependent (Fig. 20b). The toughness can reach as high as thousands of J/m^2 , increasing with the fraction of polymers in the hydrogel (Fig. 20c) (Sun et al., 2013). The toughening

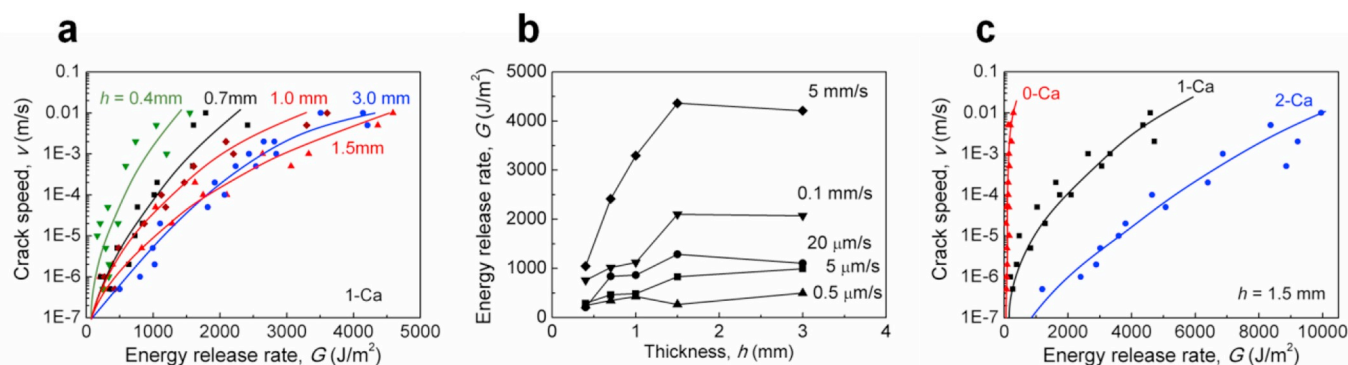


Fig. 18. Static fatigue of PAAm-Ca-alginate hydrogels (Bai et al., 2018a). (a) The v - G curves of samples of different thickness. (b) The energy release rate G depends negligibly on the thickness h at a tear speed of $0.5 \mu\text{m/s}$. At higher tear speeds, G increases with h from 0.4 mm, 0.7 mm, 1.0 mm–1.5 mm, but reaches a plateau from 1.5 mm to 3.0 mm. (c) The threshold depends on the concentration of calcium.

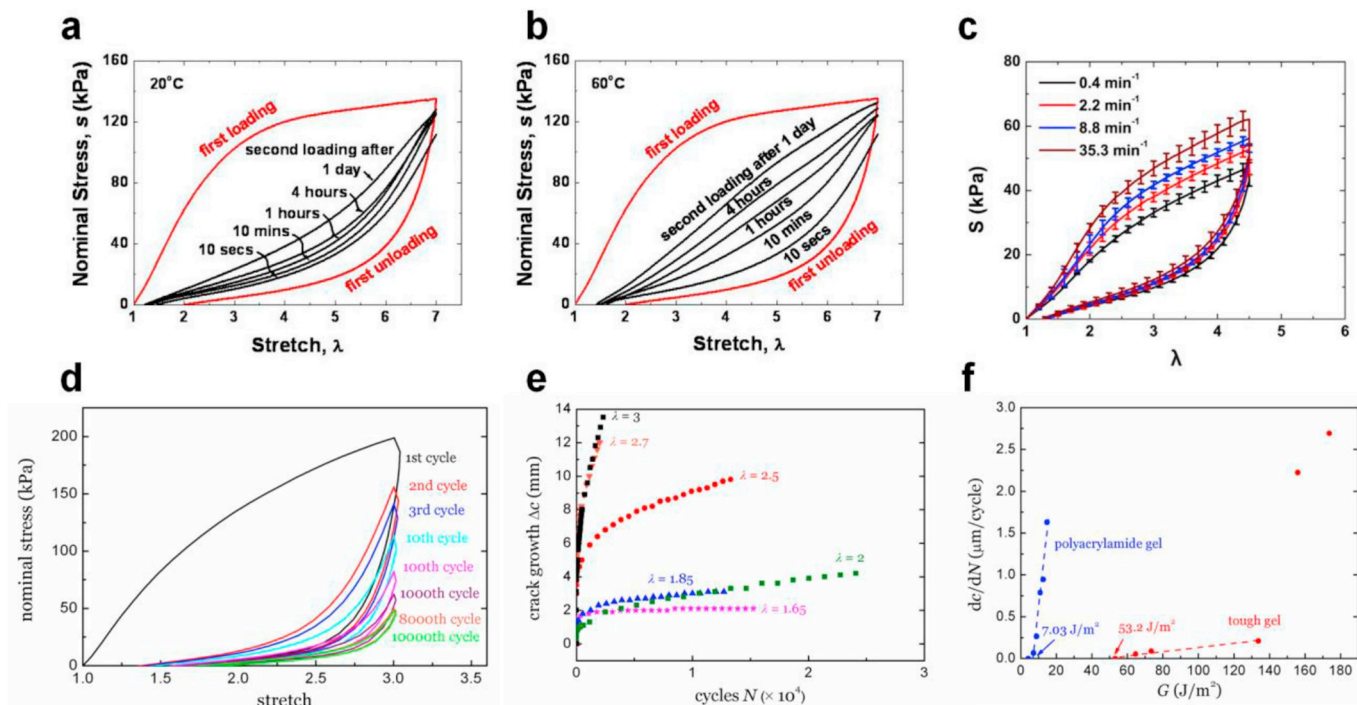


Fig. 19. Cyclic fatigue of PAAm-Ca-alginate hydrogels. (a) The hydrogel cannot self-recover after an initial loading, even if being in the unstressed state for one day at room temperature (Sun et al., 2012). (b) The hydrogel is able to partially self-recover if staying in the unstressed state for one day at an elevated temperature (60°C) (Sun et al., 2012). (c) The stress-stretch hysteresis is rate-dependent (Mao et al., 2017). (d) The hydrogel suffers cyclic fatigue damage. The stress-stretch curve reaches a steady state after thousands of loading cycles, denoted as *shakedown* (Bai et al., 2017). (e) Because of shakedown, in a precut hydrogel under cyclic stretch of constant amplitude, the crack growth per cycle is large at the initial cycles, and is smaller when reaching a steady state after thousands of cycles (Bai et al., 2017). (f) A precut hydrogel suffers cyclic fatigue crack growth. The threshold is on the order of 10 J/m^2 , higher but close to the threshold in the PAAm hydrogel itself (Bai et al., 2017).

results from energy dissipation of the multiscale structure formed by the polymer chains and the ionic groups in a polyampholyte hydrogel (Cui et al., 2018).

Static fatigue crack growth and creep fracture have been reported in the polyampholyte hydrogel. The v - G curve above the threshold is governed by the viscoplastic ionic dissociation, and has been studied using the time-temperature superposition principle derived from elastomers (Sun et al., 2017b). The energy release rate is about 200 J/m^2 at a crack speed of 10^{-6} m/s (Fig. 21a). Under a constant stress of 0.1–1 MPa, a polyampholyte hydrogel keeps elongating, and finally fractures after several hours, denoted as the creep fracture (Fig. 21b) (Karobi et al., 2016). The failure time of creep fracture inversely depends on the loading stress (Fig. 21c).

The ionic groups in a polyampholyte hydrogel are reversible. The

polyampholyte hydrogel heals its crack after cutting. When a hydrogel is cut to two pieces, attached together again, and allowed for 24 h of healing, the hydrogel completely regains its original stress-stretch curve (Ihsan et al., 2016). The polyampholyte hydrogel also heals from cyclic fatigue damage (Fig. 22a) (Sun et al., 2013). Because of the rate-dependent ionic dissociation, the stress-stretch hysteresis increases with the strain rate (Fig. 22b). The hydrogel can almost recover its initial stress-stretch curve after staying unloaded for 30 min. The time scales of the healing of uncut sample and the healing of completely cut sample are dramatically different. The possible reason is that many strong ionic groups do not break in an uncut hydrogel during cyclic loads, and still provide elasticity to motivate the fast heal of the weak ionic groups. When the hydrogel is cut into two pieces, these strong ionic groups completely break, and their heal takes a much longer time.

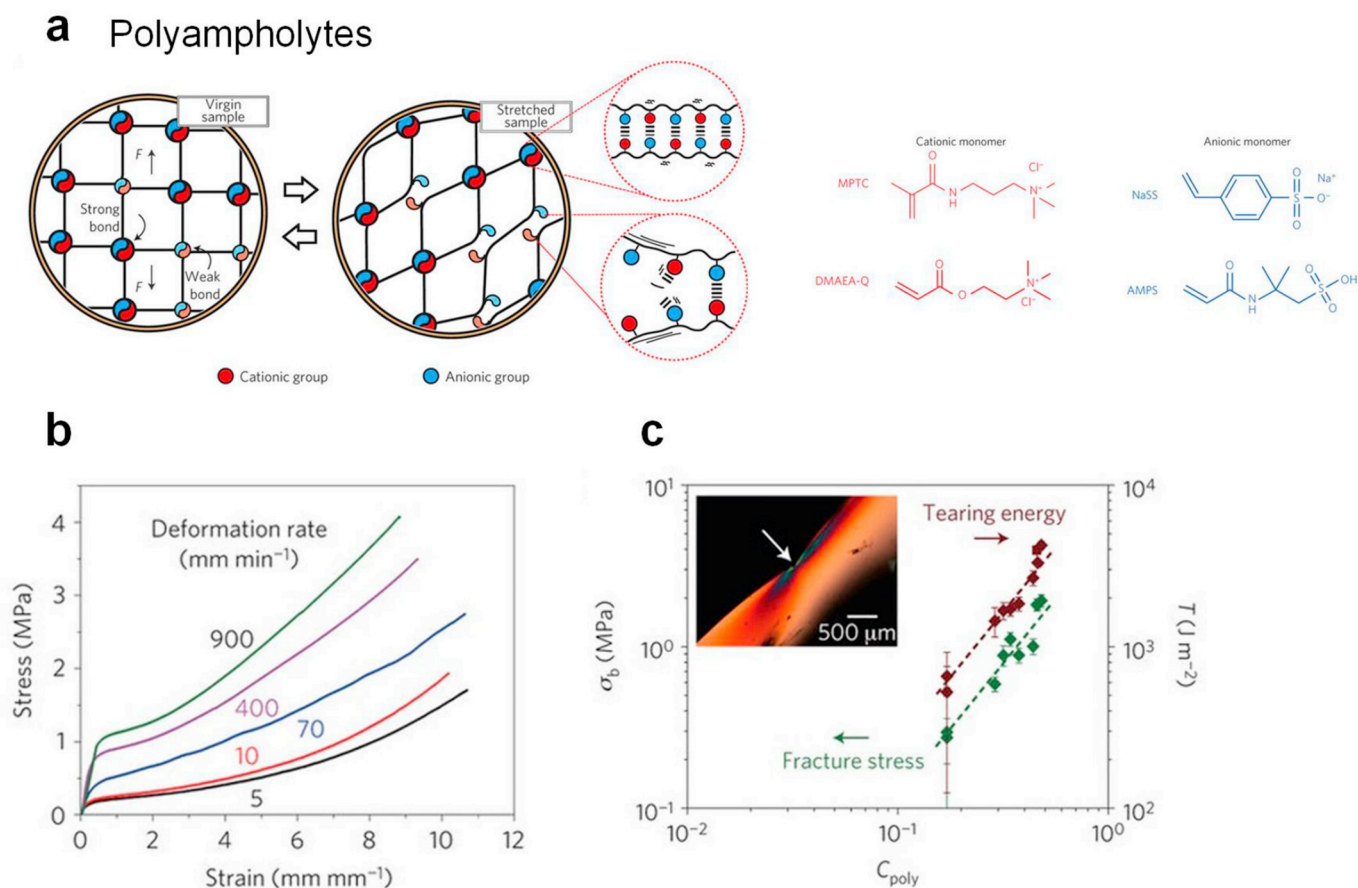


Fig. 20. Mechanical characterization of polyampholyte hydrogels (Sun et al., 2013). (a) The molecular structure of the hydrogel. (b) The stress-stretch curve is rate-dependent. The stress level is on the order of MPa. (c) The toughness can reach as high as thousands of J/m², increasing with the fraction of polymers in the hydrogel. Inset: a polarized microscope image of a polyampholyte hydrogel being torn, with the arrow indicating the crack front.

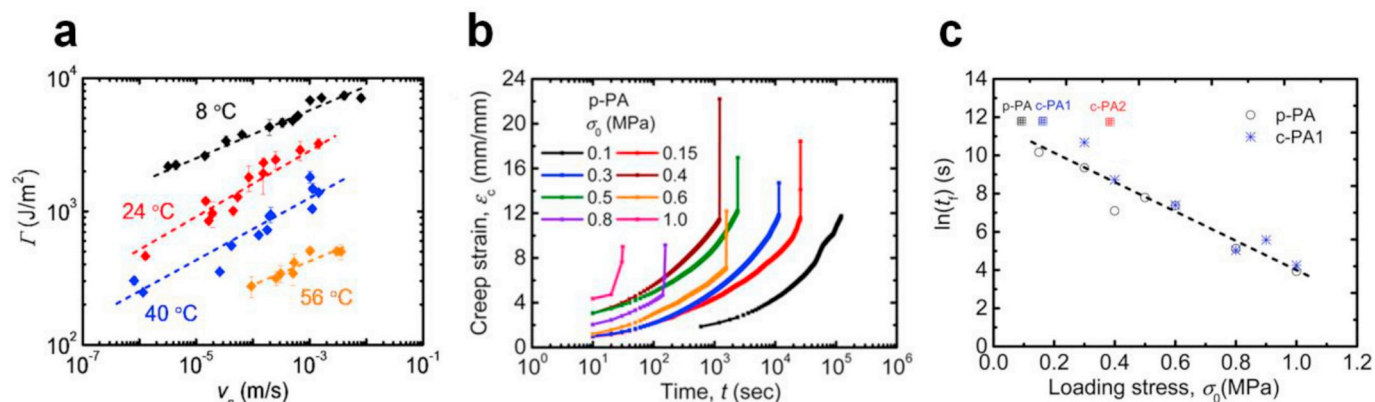


Fig. 21. Static fatigue of Polyampholyte hydrogels. (a) Static fatigue crack growth. Above the threshold, the static fatigue crack growth is governed by the viscoplastic process (Sun et al., 2017b). (b) Under a constant stress, the stretch in the hydrogel keeps increasing, and leads to fracture of the entire sample after some time (Karobi et al., 2016). (c) The failure time of the creep fracture inversely depends on the loading stress (Karobi et al., 2016).

Fatigue damage, crack growth, and heal have also been studied in hydrogels formed by oppositely charged homopolyelectrolytes (Luo et al., 2015, 2016). Such a hydrogel only forms inter-chain ionic bonds, whereas a polyampholyte hydrogel forms both inter- and intra-chain ionic bonds.

Other than the cyclic fatigue damage and healing in a polyampholyte hydrogel after one loading cycle, cyclic fatigue of polyampholyte hydrogels over many cycles has not been reported. The hydrogel has no covalently crosslinked network, which differs it from all the other hydrogels reported so far in cyclic fatigue tests. The

hydrogel has a metal-like rheology, and is expected to still suffer crack growth under cyclic loads. In principle, this hydrogel may heal to its original state after fatigue crack growth.

9. The Lake-Thomas model and its extensions

9.1. The scaling of a truss-like model of elastomer

Lake and Thomas (1967) noted that the experimentally determined cyclic-fatigue threshold of several elastomers is $\Gamma_0 = 50$ J/m². These

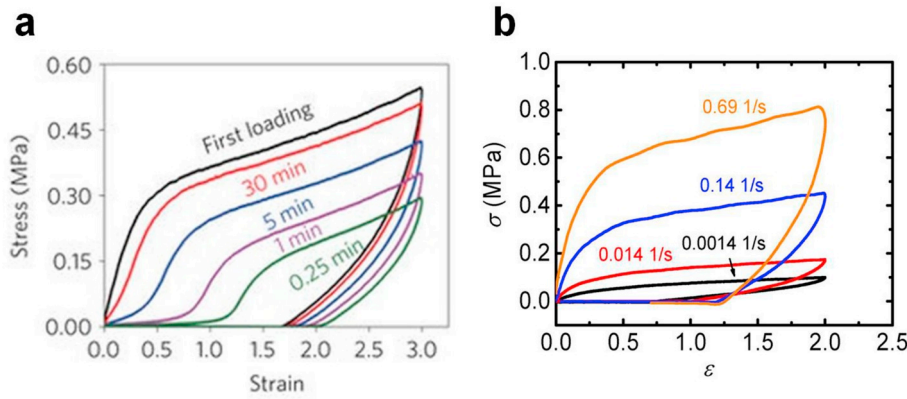


Fig. 22. Cyclic fatigue damage of polyampholyte hydrogels. (a) The hydrogel without precut crack is able to heal its material property after 30 min (Sun et al., 2013). (b) The cyclic stress-stretch hysteresis is rate-dependent (Sun et al., 2017b).

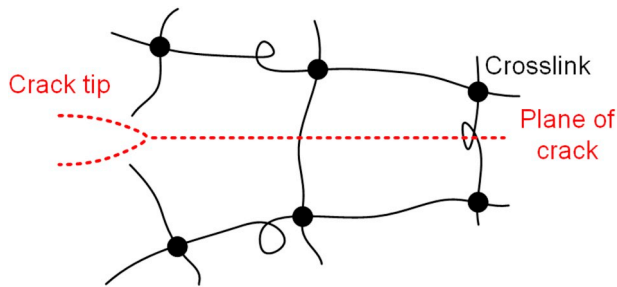


Fig. 23. The Lake-Thomas model.

authors hypothesized that the vanishingly small crack extension per cycle at the threshold no longer activates the inelastic deformation in the bulk of the material, so that the threshold is entirely due to the scission of the polymer chains lying across the crack plane (Fig. 23). They further hypothesized that just before scission every covalent bond along a polymer chain is stretched close to the covalent energy of the bond, and the scission causes the chain to dissipate the energy of the entire chain. In this Lake-Thomas model, the threshold is the bond energy of a single layer of polymer chains, divided by the area of the elastomer in the undeformed state. The bond energy per unit volume of an elastomer is J/V , where J is the C-C bond energy, and V is the volume of each monomer unit. The thickness of a layer of chain in the undeformed state is estimated by the equilibrium distance between the two ends of the chain in the freely-jointed chain model, $l\sqrt{n}$, where l is the length of each monomer unit, and n is the number of monomer units in a polymer chain. The Lake-Thomas model estimates the threshold of an elastomer as $\Gamma_0 = \alpha l\sqrt{n}J/V$, where α is a pre-factor of order unity.

The pre-factor α in the Lake-Thomas model is undetermined. The main uncertainty comes from the estimate of the thickness of the layer that dissipates energy. Why should we limit to a single layer of chains? How about multiple layers of chains? How about the arrangement of the chains, or chains of different lengths? A polymer chain does not behave as the ideal model of a freely-jointed chain. To resolve these issues will require a model of a crack in a more realistic network, similar to a model of a crack in a stiff truss (Tankasala et al., 2015). Indeed, the Lake-Thomas model is simply a scaling analysis of a truss-like model. Of course, an elastomer network is a condensed phase, and does not have open space between chains. Taking representative values, $V = 10^{-28} \text{ m}^3$, $J = 3.3 \times 10^{-19} \text{ J}$, $l = 5 \times 10^{-10} \text{ m}$, and $n = 100$, a threshold $\Gamma_0 = 50 \text{ J/m}^2$ corresponds to $\alpha = 3$.

9.2. A gel as a solvent-filled truss

We now consider several extensions of the Lake-Thomas model to

gels. Let ϕ be the volume fraction of the polymer in the gel. If the network is formed in a solvent, the equilibrium distance between two ends of a chain is still $l\sqrt{n}$. The bond energy per unit volume of the gel reduces to $\phi J/V$. Consequently, the threshold is estimated by $\Gamma_0 = \alpha \phi l\sqrt{n}J/V$ (Akagi et al., 2013).

Next consider a network formed in a dry state, which then imbibes the solvent to form a gel. The equilibrium distance between the two ends of a chain in the gel increases to $\phi^{-1/3}l\sqrt{n}$, and the bond energy per unit volume of the gel reduces to $\phi J/V$. Consequently, the threshold is estimated by $\Gamma_0 = \alpha \phi^{2/3}l\sqrt{n}J/V$ (Ahagon and Gent, 1975; Mueller and Knauss, 1971; Tang et al., 2017).

As yet another example, consider a network initially formed in a solvent, with ϕ_0 being the volume fraction of the polymer. The gel then imbibes or loses solvent to form the final gel, with ϕ being the volume fraction of the polymer. The equilibrium distance between the two ends of a chain is $l\sqrt{n}$ in the initial gel, and is $(\phi_0/\phi)^{1/3}l\sqrt{n}$ in the final gel. The bond energy per unit volume of the final gel is $\phi J/V$. Consequently, the threshold is estimated by $\Gamma_0 = \alpha \phi^{2/3}\phi_0^{1/3}l\sqrt{n}J/V$.

The initial volume fraction of the polymer is tunable by the concentration of monomers in the precursor. The final volume fraction of the polymer is tunable by swelling or drying the gel. The number of monomers per polymer chain is tunable by the concentration of the crosslinker. So long as Γ_0 is measured as a function of each tunable parameter, the validity of the Lake-Thomas model can be tested.

Next consider a hydrogel crosslinked by bonds that are weaker than the bonds forming its polymer chains. Examples include a gelatin hydrogel crosslinked by hydrogen bonds, or a Ca-alginate hydrogel by ionic bonds. Each crosslink typically involves a group of such weak bonds. Still, the bond energy of a crosslink is typically smaller than that of a C-C covalent bond. Just before a polymer chain breaks from a weak crosslink, each monomer unit of the polymer chain is stretched to the energy comparable to the bond energy of the crosslink, so that the Lake-Thomas model still applies, with J interpreted as the bond energy of the weak crosslink.

When the bond energy of the weak crosslink is much smaller than that of the bond forming the polymer chain, we propose an alternative modification of the Lake-Thomas model. A polymer chain is an entropic spring. Right before the chain breaks from a weak crosslink, the force pulling the chain equals the strength of the weak crosslink. For example, we can model the polymer chain by a freely-jointed chain (Kuhn and Gr \ddot{u} n, 1942; Rubinstein and Colby, 2003). The elastic energy per monomer unit is $J = kT[\beta/\tanh \beta + \log(\beta/\sinh \beta)]$, where kT is the temperature in the unit of energy, $\beta = fl/kT$, l is the length of each monomer unit, and f is the force needed to break the weak crosslink. The Lake-Thomas model still applies, with J replaced by the above expression.

9.3. Synergy of the primary network and sacrificial bonds

As described in Section 2, a hydrogel can achieve high toughness through the synergy of two mechanisms of energy dissipation: the scission of the primary network on the crack plane, and the breaking of the sacrificial bonds in the bulk of the hydrogel. The synergy sets up a boundary-value problem in continuum mechanics, i.e., the cohesive-zone model or the crack-bridging model, analogous to that in metals (Needleman, 1987; Tvergaard and Hutchinson, 1992), polymers (Du et al., 2000; Hui et al., 2003; Schapery, 1975), ceramics (Evans, 1990; McMeeking and Evans, 1982), and composites (Bao and Suo, 1992; Marshall et al., 1985; Sørensen and Jacobsen, 2003). Such a model represents crack bridging by a traction-separation relation, and background dissipation by a stress-strain relation in rheology. The same model has been used to analyze tough hydrogels (Brown, 2007; Qi et al., 2018; Tanaka, 2007; Zhang et al., 2015).

The thresholds for static and cyclic fatigue crack growth are often called the *intrinsic toughness*. Zhang et al. (2015) measured the intrinsic toughness of PAAm-Ca-alginate by pre-stretching a sample to large deformation to unzip most of the Ca-alginate bonds, and measuring the toughness afterwards. The notion of intrinsic toughness is used in studying tough hydrogels (Creton, 2017; Creton and Ciccotti, 2016; Long and Hui, 2016; Zhang et al., 2015; Zhao, 2014).

In the next two sections, we will review the experimental data on the static and cyclic fatigue thresholds. In the literature, it has been unclear whether the two thresholds measured under static and cyclic loads are identical and corresponding to a single material constant. As described in subsequent subsections, our own experimental data indicate the two thresholds can differ greatly.

10. Cyclic-fatigue threshold

For PAAm hydrogels, the experimental data and theoretical prediction of the cyclic-fatigue threshold agree well for hydrogels with higher water content, but deviate for hydrogels with low water content (Zhang et al., 2018a) (Fig. 24). For the composition of PAAm hydrogels used in the experiments, the volume of each monomer unit is $V = M/(A\rho) = 1.0 \times 10^{-28} \text{ m}^3$, where M is the molecular weight of acrylamide (71.08 g/mole), ρ is the density of acrylamide (1.13 g/cm³), and A is the Avogadro number (6.02×10^{23} /mole). The length of the acrylamide monomer is estimated by $l = V^{1/3} = 0.47 \text{ nm}$. The C-C bond energy is $J = 3.3 \times 10^{-19} \text{ J}$. The number of monomers between two crosslinks can be estimated by $n = 1/(VN)$, where N is the number of chains per unit volume of the dry polymer. Two ways of calculating N can be

adopted. In one way, N can be experimentally estimated through the shear modulus $\mu = \phi^{1/3}NkT$, assuming the hydrogel follows the Gaussian chain model (Cai and Suo, 2012). The calculated N varies greatly with the water content, and an averaged value of N is taken for the analysis. Alternatively, N can be calculated by assuming that all the added crosslinkers have formed crosslinks, so that $N = 2n_{cl}$ since each crosslink connects two chains on average. The number of crosslinker per unit volume of the dry polymer, n_{cl} , is prescribed by experiments. The calculated values of N from these two ways are close, and we take $n = 2175$. The threshold was fitted to $\Gamma_0 = \alpha\phi^{2/3}l\sqrt{n}J/V$ in the original paper (Zhang et al., 2018a). This assumes that the network is formed in the dry state and then swollen. Here we fit the experimental data using $\Gamma_0 = \alpha\phi^{2/3}\phi_0^{1/3}l\sqrt{n}J/V$, where $\phi_0 = 12\%$ corresponds to the volume fraction of the polymer network when it is prepared. The fitting curve remains the same, and gives the pre-factor $\alpha = 1.8$.

In addition, the Lake-Thomas model indicates that the threshold increases with the polymer chain length. This dependence seems consistent with the experimental observation, but no systematic experimental characterization has been reported. Cyclic-fatigue thresholds have also been measured for other hydrogels, including PAAm-Ca-alginate (Bai et al., 2017; Zhang et al., 2019), PAAm-PAMPS (Zhang et al., 2018b), and PAAm-polyvinyl alcohol (Bai et al., 2018c). The measured cyclic-fatigue thresholds in all these hydrogels are found to be close to the estimated values using the Lake-Thomas model. In all cases, the cyclic-fatigue threshold is much smaller than the toughness of the hydrogel, by one or two orders of magnitude.

A hypothesis has emerged recently that tougheners increase the toughness of a hydrogel greatly, but contribute little to the cyclic-fatigue threshold (Bai et al., 2018c). Cyclic fatigue crack growth has been studied in hydrogels of two kinds, identical in all aspects except for tougheners. A PAAm-polyvinyl alcohol hydrogel has liquid-like, uncrosslinked polyvinyl alcohol chains as the toughener, resulting in a toughness of 448 J/m^2 , much higher than the toughness of the PAAm hydrogel without polyvinyl alcohol (71 J/m^2). However, the cyclic-fatigue thresholds of the two hydrogels, 8.4 and 9.5 J/m^2 , are nearly identical (Fig. 25). This hypothesis is also ascertained in the PAAm-Ca-alginate hydrogel (Zhang et al., 2019), where the large amount of ionic bonds crosslinking the Ca-alginate network act as solid-like tougheners. The toughness of the hydrogel is 3375 J/m^2 , while the cyclic-fatigue threshold is 35 J/m^2 . For comparison, a PAAm-alginate hydrogel identical in all other aspects but without calcium has a toughness of 169 J/m^2 and a cyclic-fatigue threshold of 17 J/m^2 .

All the measurements of cyclic-fatigue threshold available so far are conducted in hydrogels containing at least one covalent network of C-C bonds (i.e., PAAm). Cyclic fatigue crack growth in hydrogels with no covalent network has not been explored. A special group of them is the *self-healing* hydrogel. By self-healing we mean the bonds of the polymer network of a hydrogel are completely reversible after being fractured. The reforming of bonds in a self-healing hydrogel often depends on the magnitude and the speed of loading. As a result, a self-healing hydrogel behaves as a non-Newtonian fluid or plastic liquid (Balmforth et al., 2014; Barnes, 1999; Huang et al., 2016; Morelle et al., 2017). Most self-healing hydrogels do not contain networks to provide strong elasticity, so they hardly recover their original shape after a relatively large deformation, or subject to a static load for a long time.

Whether a self-healing hydrogel suffers cyclic fatigue crack growth depends on the loading condition of the experiment. Take the polyampholyte hydrogel as an example. The hydrogel completely heals its crack if the two pieces of cracked materials are firmly attached and stored in the unstretched state for 24 h (Ihsan et al., 2016). When a sample of polyampholyte hydrogel with a pre-cut crack is subject to cyclic loads, if the period of each cycle is much longer than 24 h, the hydrogel will not suffer cyclic fatigue crack growth, since the fractured network has enough time to heal. In contrast, if the period is shorter than 24 h, the hydrogel will still suffer cyclic fatigue crack growth.

In a pure shear test, to characterize the energy release rate related to

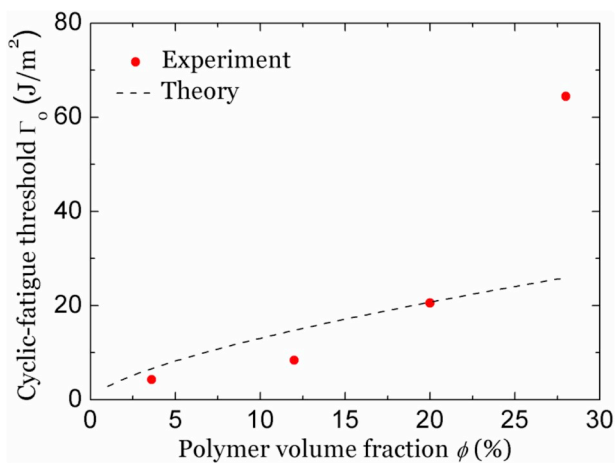


Fig. 24. The cyclic-fatigue threshold of PAAm hydrogels with different water content. The first three points of experimental data (Zhang et al., 2018a) is fitted using $\Gamma_0 = \alpha\phi^{2/3}\phi_0^{1/3}l\sqrt{n}J/V$. The four data points correspond to PAAm hydrogels of 96, 87, 78, and 69 wt% of water, from left to right.

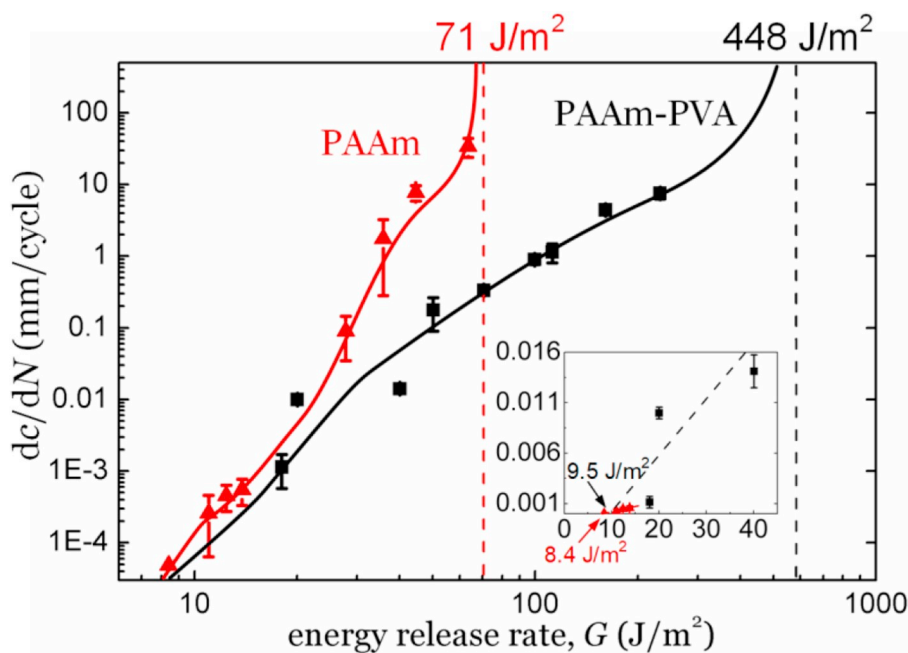


Fig. 25. The cyclic-fatigue threshold of a PAAm-polyvinyl alcohol hydrogel negligibly depends on the polyvinyl alcohol (PVA) chains as tougheners (Bai et al., 2018c).

the cyclic fatigue crack growth, the cyclic stress-stretch curves of an uncut sample are measured, and shakedown has been observed in most hydrogels. Shakedown of the PAAm-Ca-alginate hydrogel takes thousands of loading cycles (Fig. 19d). By comparison, shakedown of the PAAm-PAMPS is swift, completed mostly in the first few cycles (Fig. 16c). Shakedown of hydrogels has been analyzed using the phenomenological model of viscoelastic Mullins effect (Wang et al., 2018a). Such a large difference in the number of cycles to reach the steady state calls for further study.

11. Static-fatigue threshold

Static-fatigue thresholds have been measured for non-covalently crosslinked hydrogels such as gelatin and Ca-alginate (Baumberger et al., 2006b; Baumberger and Ronsin, 2009). The energy dissipation from pullout of polymer chains has no contribution to the threshold. Rather, the threshold is determined by breaking the crosslinks of hydrogen bonds in the hydrogel network. Because the bond energy of hydrogen bonds is much smaller than that of C-C covalent bonds in these hydrogels, the static-fatigue threshold is on the order of 1 J/m².

We can compare the threshold to our modified Lake-Thomas model proposed in Section 9, with the J estimated from a freely-jointed chain. The mesh size of the network is $l\sqrt{n} = 10^{-8}m$, the volume of each monomer unit is $V = l^3 = 2.7 \times 10^{-29}m^{-3}$, and the bond energy of the hydrogen bond is $fl = 1.6 \times 10^{-20}J$. At room temperature, $kT = 4.2 \times 10^{-21}J$. Taking these together, and dropping the pre-factors in the Lake-Thomas model, we estimate the threshold to be $\Gamma_0 = 3.1 J/m^2$, which is close to the experimental value of (Baumberger et al., 2006b), $\Gamma_0 = 2.5 J/m^2$.

Static-fatigue thresholds have also been measured for PAAm-Ca-alginate hydrogels (Bai et al., 2018a). While tougheners contribute little to the cyclic-fatigue threshold, experiments show that they can contribute greatly to the static-fatigue threshold (Bai et al., 2018a). To explain this observation, here we summarize two hypotheses about the static-fatigue threshold of a hydrogel with a primary solid-like network and a toughener. First, a liquid-like toughener does not contribute to the static-fatigue threshold. The threshold is estimated by the Lake-

Thomas model, determined by the primary network. Second, a solid-like toughener amplifies the static-fatigue threshold. The threshold is contributed by both the scission of the primary network and the rate-independent dissipation of the toughener in the inelastic zone around the crack front. If the size of such inelastic zone is comparable or larger than the size of the sample, large-scale inelasticity will take place, and the measured threshold will depend on the sample size.

To test the hypotheses, static-fatigue thresholds have been measured for PAAm-Ca-alginate hydrogels identical in all aspects except for the concentration of calcium (Bai et al., 2018a). The static-fatigue threshold of a PAAm-alginate hydrogel with no calcium is 59 J/m², whereas the static-fatigue threshold is 173 and 952 J/m², when the concentration of calcium in the hydrogel increases (Fig. 18c).

The difference between the cyclic-fatigue threshold and static-fatigue threshold of a hydrogel with solid-like tougheners is reminiscent of the fatigue of rate-independent ductile metals, where the cyclic-fatigue threshold is much smaller than the toughness – in this case the static-fatigue threshold – of a ductile metal.

The cyclic-fatigue threshold and static-fatigue threshold, however, are not distinguished in the study of elastomers. In the static-fatigue crack growth of elastomers, the energy release rate is considered as the Lake-Thomas threshold amplified by a factor due to viscoelasticity, $G = \Gamma_0(1 + f(v, T))$, where $f(v, T)$ is a function of the crack speed v and temperature T , and approaches zero as v approaches zero or T is high enough (Bhowmick, 1988; de Gennes, 1996; Gent, 1996; Gent and Schultz, 1972). Indeed, the measured static-fatigue thresholds of various rubbers are close to values predicted by the Lake-Thomas model, and such expression has been extensively used in the literature of fracture of soft materials (Creton, 2017; Creton and Ciccotti, 2016; Knauss, 2015; Persson et al., 2005; Persson and Brener, 2005). The large difference between the measured static-fatigue threshold and the estimated Lake-Thomas threshold was observed and clarified for the first time recently in hydrogels with solid-like tougheners (Bai et al., 2018a).

In the study of fatigue of hydrogels with complex rheology, the various compositions of hydrogels not only motivate the development of theoretical models, but also challenge the good agreement between

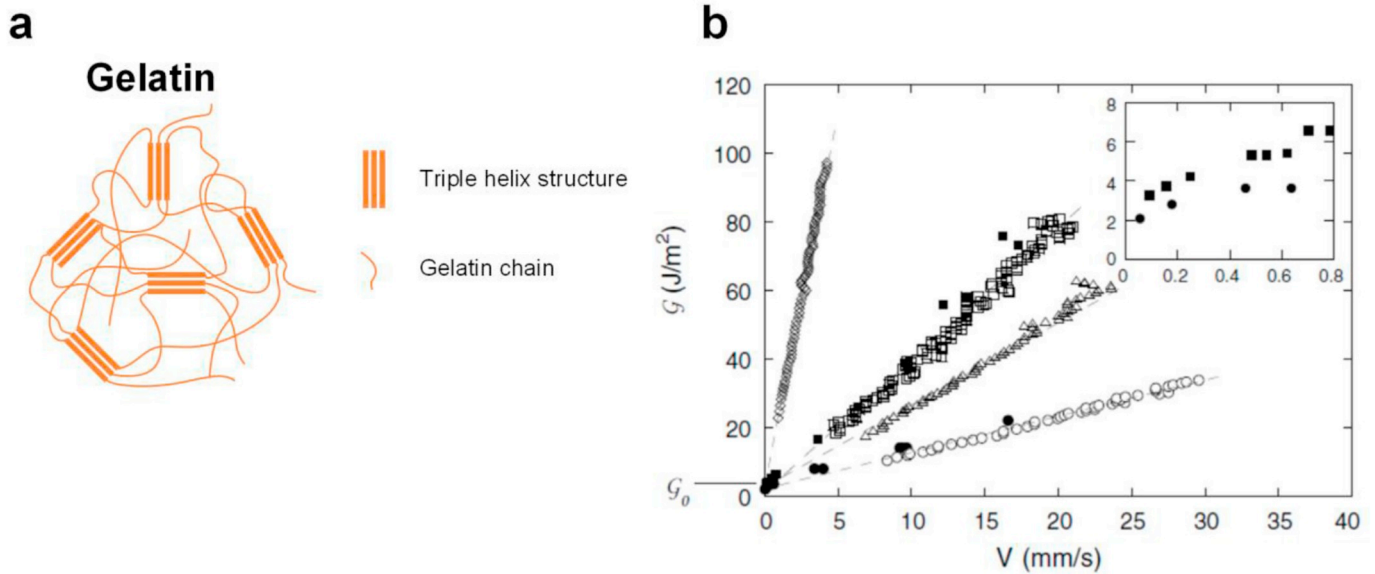


Fig. 26. Static fatigue crack growth of gelatin hydrogels. (a) The molecular picture of a gelatin hydrogel. (b) The G - V curves of gelatin hydrogels with the same gelatin network but solvents of different viscosity (Baumberger et al., 2006b).

theoretical models and experimental observations. After all, a quantitative agreement between theory and experiments is not common in fatigue. Here we highlight one example of such study in hydrogels: the static fatigue crack growth of gelatin hydrogels (Baumberger et al., 2006b).

A gelatin hydrogel is crosslinked by the collagen triple helix formed by hydrogen bonds (Fig. 26a) (Bigi et al., 2004; Higgs and Ross-Murphy, 1990). To vary the composition of gelatin hydrogels, different concentrations of glycerol are added to the hydrogel to modify the viscosity of the solvent. Pure shear tests are conducted on hydrogels immersed in solvent, to measure the v - G curves (Fig. 26b). The thresholds are identical in all hydrogels with different viscosity, on the order of 2.5 J/m^2 . Above the threshold, the energy release rate increases linearly with the crack speed, and becomes larger when the concentration of glycerol is higher.

A theoretical model is derived to capture the relationship between G and v . The theory hypothesizes that the static-fatigue threshold is determined by the breaking of hydrogen bonds that form the triple helix crosslinks. Above the threshold, the crack growth is determined by the pullout of polymer chains from the hydrogel matrix with water/glycerol solvents. To show that the threshold is not induced by the scission of polymer chains described in the original Lake-Thomas model, the author measures the threshold in experiments to be two orders of magnitude smaller than that estimated by the scission of polymer chains. The threshold G_0 is estimated as $G_0 \sim J/(l\xi^2)L$, where l is the length of each monomer unit as defined before, ξ is the average mesh size, J is the bond energy of a hydrogen bond, and L is the length of a fully stretched chain. The above estimation can be regarded as an alternative modification of the Lake-Thomas model.

Above the threshold, the energy release rate G is a function of crack speed v , $G(v) = G_0 + (L/\xi)^2\eta v$, where η is the viscosity. The experimental results agree quantitatively well with the theoretical model.

Good agreement between theory and experiments has also been found in the dissipation mechanism of static fatigue crack growth of polyampholyte hydrogels above the threshold (Sun et al., 2017b).

All symptoms of fatigue originate from one fundamental cause: molecular unites change neighbors when a material is subject to a prolonged load. Fatigue correlates with rheology. In the following sections, we discuss fatigue crack growth in materials of dissimilar types of rheology.

12. Poroelastic fatigue crack growth

The PAAm and PAAm-PAMPS hydrogels only contain covalent networks. Samples of these hydrogels with no precut cracks have rate-insensitive stress-stretch curves. Yet samples with precut cracks show the energy release rate changes with crack speed (Figs. 11a and 16a). Also observed is the delayed growth of a crack in the PAAm hydrogel in pure shear sample with a precut crack under a constant applied stretch (Fig. 11b). Where does the time-dependent crack growth come from?

One time-dependent process in a hydrogel is the migration of water. The migration of a fluid in an elastic network is described by the theory of poroelasticity (Biot, 1941). Poroelasticity of hydrogels describes concomitant migration of water and large elastic deformation of the polymer network (Hong et al., 2008). Crack growth has long been studied in poroelastic hard solids like rocks (Atkinson and Craster, 1991; Radi et al., 2002; Rice and Cleary, 1976). Wang and Hong (2012) initiated the poroelastic theory of cracks in hydrogels. This theory has been developed in recent years (Böger et al., 2017; Bouklas et al., 2015; Hui et al., 2013; Mao and Anand, 2018; Noselli et al., 2016; Yu et al., 2018). In the remainder of the section, we focus on aspects of the poroelastic theory that can be related to the experiments of static fatigue crack growth.

12.1. Swelling zone

We focus on an ideal experiment conducted in a chamber, with the chemical potential of water vapor in the chamber set to the chemical potential of water in the undeformed hydrogel. Subject a large sample with a long crack to a static applied load. The large stretch near the crack front reduces the local chemical potential of water, so that the hydrogel at the crack front imbibes water from the surrounding hydrogel and from the vapor in the chamber, and becomes more swollen than the hydrogel far away. Because the sample is large and the crack is long, water only migrates near the crack front, in a zone small compared to the size of the sample. We call this zone the *swelling zone*. Outside the swelling zone, migration of water is negligible, and the hydrogel is indistinguishable from an elastic solid. Swelling is a type of inelasticity. Under the condition of small-scale swelling, the static load is characterized by a static energy release rate G .

When the energy release rate does not exceed the threshold, $G \leq \Gamma_0$, the hydrogel, the chamber, and the applied load can reach a state of

thermodynamic equilibrium. In the state of equilibrium, the crack is stationary, and the chemical potential of water is homogeneous everywhere in the hydrogel and in the chamber. However, the concentration of water and the deformation of the polymer network are inhomogeneous in the hydrogel.

Let W_f be the work of fracture (i.e., the area under the stress-stretch curve measured from a sample with no pre-cut crack, under a loading rate low enough to allow the sample to swell, in equilibrium with the chamber and the load). The ratio Γ_0/W_f is the flaw-sensitivity length for samples tested at low loading rate (Section 5.4). Here this length characterizes the size of the swelling zone, in the state of equilibrium when the energy release rate approaches the threshold, $G \rightarrow \Gamma_0$.

When the energy release rate exceeds the threshold, $G > \Gamma_0$, but remains static, the polymer chains break at the crack front. As the crack grows, the hydrogel is out of thermodynamic equilibrium, and water migrates. For a long crack in a large sample, subject to a static energy release rate above the threshold, a steady state is approached. In the steady state, the crack extends as a constant speed v . The field of the concentration of water and the deformation of the polymer network remains invariant in the frame moving at the crack speed. Let D be the effective diffusivity of water in the hydrogel. The ratio D/v defines the size of the swelling zone in a steady state. The higher the crack speed, the smaller the swelling zone around the crack front.

12.2. Poroelastic relaxation speed

We propose a material-specific speed for crack growth in poroelastic gels. When the energy release rate approaches the threshold from the above, the crack speed is small, the steady state approaches the threshold state of equilibrium, and the steadily moving swelling zone approaches the equilibrium swelling zone, $D/v \sim \Gamma_0/W_f$. We now identify a scale of speed, $v_R = D/(\Gamma_0/W_f)$, which we call the *poroelastic relaxation speed*. The relaxation speed is defined by three material properties, and is therefore also a material property. When the crack speed is small compared to the relaxation speed, the energy release rate approaches the threshold, $G \rightarrow \Gamma_0$. When the crack speed is large compared to the relaxation speed, the energy release rate significantly exceeds the threshold, $G > \Gamma_0$.

Taking representative values for PAAm, $D = 10^{-10} \text{ m}^2/\text{s}$, $\Gamma_0 = 10^2 \text{ J/m}^2$, and $W_f = 10^5 \text{ J/m}^3$, we estimate the flaw-sensitivity length to be $\Gamma_0/W_f = 10^{-3} \text{ m}$, and the poroelastic relaxation speed to be $DW_f/\Gamma_0 = 10^{-7} \text{ m/s}$. This estimated relaxation speed is remarkably close to the experimentally observed value (Fig. 11a). Similar relaxation speed is also observed for polyacrylamide-sodium-alginate, in which alginate chains do not crosslink (Fig. 18c).

A hydrogel with a solid-like toughener has a longer flaw-sensitivity length, and therefore a smaller relaxation speed. For such a hydrogel, taking $\Gamma_0 = 10^3 \text{ J/m}^2$ and other values the same, we estimate the flaw-sensitivity length to be $\Gamma_0/W_f = 10^{-2} \text{ m}$, and the poroelastic relaxation speed to be $DW_f/\Gamma_0 = 10^{-8} \text{ m/s}$. This prediction agrees with the experimental observation of polyacrylamide-calcium-alginate hydrogels (Fig. 18c).

The flaw-sensitivity length Γ_0/W_f is the size of the swelling zone under the condition of small-scale inelasticity. When the representative length of the sample, such as the thickness h in peel or tear, is small compare to Γ_0/W_f , large-scale inelasticity takes place. The size of the swelling zone scales with h , and the poroelastic relaxation speed becomes D/h .

If the rheology of a material is not well characterized, one may as well extract the relaxation speed directly from the experimentally measured v - G curve. It might be a good practice to plot $(G - \Gamma_0)/(\Gamma - \Gamma_0)$ as a function of the crack speed v , and define a relaxation speed v_R by setting $G(v_R) = (\Gamma + \Gamma_0)/2$. Of course, without other information the v - G curve by itself will not determine if the time-dependent behavior results from poroelasticity, or from some other time-dependent mechanism, such as viscoelasticity or reaction-assisted chain scission.

12.3. Static fatigue crack growth in a dry environment

Naassaoui et al. (2018) described a “poroelastic signature” in the experiment of static fatigue crack growth in gelatin hydrogels. When a gelatin hydrogel is immersed in water, the threshold is governed by breaking of the crosslinks of hydrogen bonds, and the linear slope of v - G curve is governed by the viscous pullout of polymer chains (Baumberger et al., 2006b). When the gelatin hydrogel is tested in dry air, an increase of energy release rate, $\Delta G(v)$, is observed, which is a constant when the crack speed v is large, but becomes smaller when v approaches zero. The authors hypothesized that, at high crack speed, the energy dissipation associated with the internal water migration is negligible in both the wet and dry environment, and the constant ΔG corresponds to the energy to pull polymer chains from the hydrogel into the dry air. The authors further hypothesized that, at low crack speed, the reduction of $\Delta G(v)$ comes from the water migration from the bulk to the crack front of the hydrogel. To support the second hypothesis, the authors formulated a relaxation speed v_R . Experimental data show that $\Delta G(v)$ approaches a constant, $\Delta G(\infty)$, when $v > v_R$. The author further plots $1 - \Delta G(v)/\Delta G(\infty)$ as a function of v/v_R . For gelatin hydrogels with different weight fraction of gelatin and volume fraction of glycerol as solvent, all the experimental data collapse onto a single curve. This collapse supports the hypothesis that the reduction of $\Delta G(v)$ at low crack speed results from water migration.

12.4. Effect of solvent exchange

Tanaka et al. (2016) peeled a polyacrylamide hydrogel while pouring different types of solvents to the peel front. A hydrogel immersed in water solvent will swell. A hydrogel immersed in an organic good solvent, such as ethylene glycol and glycerol, will first de-swell due to kinetics of diffusion, and then swell to equilibrium. A hydrogel immersed in a poor solvent, such as ethanol, will de-swell to equilibrium. Compared to the hydrogel peeled in air, the hydrogel peeled with water poured to the peel front has similar energy release rate at a high peel speed, but reduced energy release rate at a low peel speed. When an organic good solvent is poured, the energy release rate is larger than that measured in air at a high peel speed, but is not affected by pouring the solvent at a low peel speed. When a poor solvent is poured, the energy release rate is larger than that in air or in any other solvent in the whole range of peel speed.

13. Viscoelastic fatigue crack growth

13.1. Viscoelastic relaxation speed

For a hydrogel with tougheners, in addition to poroelastic relaxation, viscoelastic relaxation also accompanies the static-fatigue crack growth. We now define a relaxation speed associated with viscoelasticity. Consider a long crack in a large sample, subject to a static load for a long time. Remote from the crack front, the material is fully relaxed, and behaves like an elastic material. Consequently, the static load gives a static energy release rate G .

When the energy release rate does not exceed the threshold, $G \leq \Gamma_0$, the hydrogel can reach a state of thermodynamic equilibrium, in which, the crack is stationary, and the hydrogel relaxes to an elastic field. Again, the ratio Γ_0/W_f defines the flaw-sensitivity length for samples tested at a vanishingly low loading rate. Let τ be the viscoelastic relaxation time of the material measured under the relaxation test. These material properties defines a scale of speed, $\Gamma_0/(W_f\tau)$, which we call the *viscoelastic relaxation speed*. When the crack speed is small compared to this relaxation speed, the rate-dependent component of the toughener is completely relaxed, and the energy release rate approaches the threshold.

Viscoelastic fatigue crack growth has long been studied in elastomers. For most rubbers, the threshold is $\Gamma_0 \approx 50 \text{ J/m}^2$, the work of

fracture is $W_f \approx 10^9 \text{ J/m}^3$ (Gent, 1996; Gent and Lai, 1994; Lake and Thomas, 1967), and the relaxation time is on the order of 100 h, $\tau \approx 3.6 \times 10^5 \text{ s}$ (Tobolsky et al., 1944). Putting them together, we estimate the viscoelastic relaxation speed to be $\Gamma_0/(W_f\tau) \approx 10^{-13} \text{ m/s}$. Indeed, in the literature, the slope of ν - G curves at a crack speed $\nu = 10^{-7} \text{ m/s}$ is almost identical to the slope at a higher speed, $\nu = 0.1 \text{ m/s}$ (Mullins, 1959). That is, the two crack speeds are both far above the relaxation speed.

For a hydrogel with a solid-like toughener, such as a polyacrylamide-Ca-alginate, the flaw-sensitivity length is estimated as $\Gamma_0/W_f = 10^{-2} \text{ m}$, the relaxation time is estimated as $\tau = 10^5 \text{ s}$, and the viscoelastic relaxation speed is $\Gamma_0/(W_f\tau) = 10^{-7} \text{ m/s}$. This prediction qualitatively agrees with the experimental observation (Fig. 18c). More careful experiments are needed to separate the poroelastic and viscoelastic relaxation speeds.

13.2. Viscoelastic vs. poroelastic relaxation

When a large sample of a polyacrylamide hydrogel is subject to a homogeneous stress, the hydrogel exhibits near-perfect elasticity, with a slight viscoelastic, over a time scale on the order of 1 s (Heemskerck et al., 1984; Pavesi and Rigamonti, 1995; Weiss and Silberberg, 1977). Assuming a length scale $\Gamma_0/W_f = 10^{-3} \text{ m}$, we estimate the viscoelastic relaxation speed to be 10^{-3} m/s . Recall that the poroelastic relaxation speed of the polyacrylamide hydrogel is estimated to be 10^{-7} m/s (Section 12.2). In a sample of polyacrylamide much larger than 10^{-3} m , the condition of small-scale inelasticity prevails, and the crack approaches the threshold when the crack speed is below 10^{-7} m/s . In this case, poroelasticity, not viscoelasticity, limits the rate to attain the threshold state of equilibrium.

Under the condition of small-scale inelasticity, a comparison of the viscoelastic relaxation speed $(\Gamma_0/W_f)/\tau$ and the poroelastic relaxation speed $D/(\Gamma_0/W_f)$ defines a dimensionless parameter: $(\Gamma_0/W_f)^2/(D\tau)$. When this parameter is small, viscoelasticity sets the relaxation speed to approach the equilibrium state of static threshold. When this parameter is large, poroelasticity sets the relaxation speed.

13.3. Large-scale inelasticity

In peel and tear, the thickness h of the hydrogel is readily changed over a large range. When the flaw-sensitivity length Γ_0/W_f is large compared to the thickness of the hydrogel, the condition of large-scale inelasticity prevails in the threshold state of equilibrium. The viscoelastic relaxation speed becomes h/τ , and the poroelastic relaxation speed becomes D/h . A comparison of the two relaxation speeds defines a dimensionless parameter, $h^2/(D\tau)$. When this parameter is small, viscoelasticity sets the relaxation speed to approach the equilibrium state of static threshold. When this parameter is large, poroelasticity sets the relaxation speed.

14. Elastic-plastic fatigue crack growth

At room temperature, over the time scale in most applications, metals are well characterized by time-independent plasticity. So long as stress-corrosion is suppressed, metals do not suffer static fatigue crack growth, but suffer cyclic fatigue crack growth. The lack of time scale in metal plasticity also explains another experimental fact: the crack growth per cycle is independent of the frequency of the applied load.

All hydrogels have time-dependent rheology. Still, the large body of literature on cyclic fatigue crack growth in metals offers insights. As noted in Section 10, hydrogels with solid-like tougheners have cyclic-fatigue thresholds close to the Lake-Thomas model. As noted in Section 11, hydrogels with solid-like tougheners have static-fatigue thresholds far above the Lake-Thomas thresholds predicted on the basis of the scission of the primary networks. The long-time, slow-crack behavior of hydrogels with solid-like tougheners approaches that of a material of

time-independent plasticity. Qi et al. (2018) have analyzed toughness of soft materials of time-independent hysteresis.

15. Endurant elastomers and gels

A principal aim for the study of fatigue is to create fatigue-resistant (i.e., enduring) materials. The design should address all symptoms of fatigue: change in properties, as well as nucleation and growth of cracks, in samples with and without pre-cut cracks, under prolonged static and cyclic loads. An ideally enduring material should have two characteristics. First, the material exhibits perfect elasticity: the stress-stretch curve of a sample with no pre-cut crack remains unchanged cycle by cycle and has small hysteresis. Second, the material does not suffer fatigue crack growth under prolonged loads: both the static and cyclic fatigue thresholds coincide with the toughness.

For metals, plastics, and most elastomers, cyclic-fatigue thresholds are much below toughnesses. All tough hydrogels exhibit large hysteresis and suffer fatigue crack growth. This low endurance is inherent to the design of the tough hydrogels. They toughen by breaking sacrificial bonds prior to the scission of primary networks. In using a tough material under a prolonged load, a common practice is to minimize hysteresis in large part of the material in normal operation of the material, but maximize hysteresis to resist the growth of cracks at sites of stress concentration. This practice can guide the design of materials (Lin et al., 2014b).

Glasses and ceramics are enduring materials, provided that stress corrosion is suppressed. The perfect elasticity, however, makes these materials brittle. A polyacrylamide hydrogel is close to the ideal of an enduring material. The polyacrylamide hydrogel exhibits near-perfect elasticity: the stress-stretch curve of a polyacrylamide hydrogel with no pre-cut crack is stable cycle by cycle (Fig. 12a). The polyacrylamide hydrogel does suffer fatigue crack growth under prolonged loads, but the threshold is not too much below the toughness (Fig. 11a). The polyacrylamide hydrogel can even achieve respectable toughness, well above 100 J/m^2 (Fig. 10c), but this toughness results from using a polymer network of long chains, following the Lake-Thomas model. A hydrogel of network of long chains has large stretchability, but low elastic modulus (Fig. 10b).

The conflict between the elastic modulus and the Lake-Thomas threshold is well understood. The shear modulus of a polymer network is $\mu = kT/(nV)$, whereas the threshold is $\Gamma_0 = \alpha l \sqrt{n} J/V$. As the number of monomer units per polymer chain, n , increases, the shear modulus reduces, and the threshold increases. This conflict limits the applications of the single-network of elastomers and gels.

Wang et al. (2018b) and Xiang et al. (2019) have demonstrated a principle of enduring elastomers and hydrogels. The principle is illustrated with a composite of a matrix of compliant (long-chain) network and fibers of a stiff (short-chain) network (Fig. 27). The matrix and the fibers are both elastic, have high modulus contrast, and strongly adhere. Because the constituents are elastic and adhere strongly, when the composite with no pre-cut crack is subject to cyclic load, the stress-stretch curve has low hysteresis and is stable cycle by cycle. Because the fibers are much stiffer than the matrix, when the composite with a pre-cut crack is subject to a stretch along the direction of fibers, the soft matrix shears greatly at the crack front, and spreads large stress over a long segment of each fiber. When a fiber ruptures, all the elastic energy stored in the highly stretched segment is released.

This principle of stress de-concentration, of course, operates in all composites of high modulus contrast and strong adhesion. Familiar examples include fiber-reinforced polymers and thread-reinforced elastomers. A three-dimensional lattice of a material in a matrix of a much softer material will resist cracks in all directions. The composites can be self-assembled by phase separation. The fibers can also be replaced by aligned bundles of polymer chains at the molecular level (Bai et al., 2019).

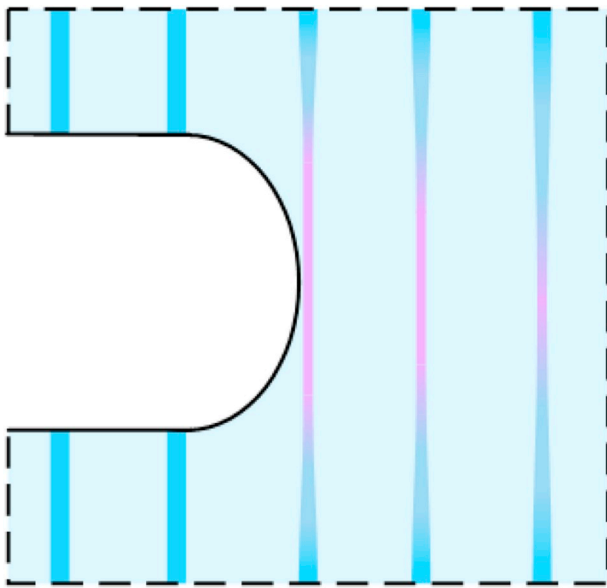


Fig. 27. A composite of a matrix of compliant (long-chain) network and fibers of a stiff (short-chain) network (Wang et al., 2018b).

16. Concluding remarks

This paper reviews the fatigue of hydrogels, characterized by testing samples with and without precut cracks, under prolonged static and cyclic loads. Fatigue is a molecular disease. Various fatigue tests provide lenses to view molecular processes of inelasticity. Symptoms of fatigue and efficacy of heal vary with chemistries of bonds and topologies of networks. We review experimental data of hydrogels of five representative topologies of networks. Reversible bonds may prevent fatigue damage in samples without precut cracks, but do not prevent fatigue crack growth in samples with precut cracks. A liquid-like toughener increases neither static-fatigue threshold nor cyclic-fatigue threshold. A solid-like toughener increases static-fatigue threshold, but does not increase cyclic-fatigue threshold. Near the static-fatigue threshold, the crack speed approaches a material property, which we call the relaxation speed. We give theoretical estimates of the relaxation speed due to poroelasticity and viscoelasticity, under conditions of small-scale and large-scale inelasticity. For a polyacrylamide hydrogel, we show that the experimentally measured relaxation speed agrees with the poroelastic relaxation speed, not the viscoelastic relaxation speed. Poroelastic fatigue is a new type of fatigue, and is specific to gels. The polyacrylamide hydrogel is an excellent model material to study poroelastic fatigue of hydrogels. We outline a strategy to create hydrogels of high endurance. The chemistry of fatigue holds the key to the discovery of hydrogels of properties previously unimagined.

Acknowledgements

This work was supported by MRSEC (DMR-14-20570). Earlier and much shorter versions of this review were presented by R.B. as part of a PhD thesis titled “Fatigue of Hydrogels” at Harvard University on 12 April 2018, and by Z.S. as a plenary lecture titled “Chemistry of Fatigue” at the European Solid Mechanics Conference on 4 July 2018. We thank Zhengjin Wang for providing some of the experimental data in constructing Fig. 10c, and Tongqing Lu for feedback on the manuscript. We thank past and current group members for much of the work described in this paper. Z.S. acknowledges the discussions of polymer networks with Tristan Baumberger, Yongmei Chen, Manoj Chaudhury, Matteo Ciccotti, Costantino Creton, Alan Gent, Jian Ping Gong, Ryan Hayward, Jian Hu, Herbert Hui, John Hutchinson, Ed Kramer, Dave Mooney, Michael Rubinstein, Ken Shull, Joost Vlassak, and George Whitesides.

References

- Acome, E., Mitchell, S.K., Morrissey, T.G., Emmett, M.B., Benjamin, C., King, M., Radakovitz, M., Keplinger, C., 2018. Hydraulically amplified self-healing electrostatic actuators with muscle-like performance. *Science* 359, 61–65.
- Agrawal, A., Rahbar, N., Calvert, P.D., 2013. Strong fiber-reinforced hydrogel. *Acta Biomater.* 9, 5313–5318.
- Ahagon, A., Gent, A., 1975. Threshold fracture energies for elastomers. *J. Polym. Sci., Part B: Polym. Phys.* 13, 1903–1911.
- Akagi, Y., Sakurai, H., Gong, J.P., Chung, U.-i., Sakai, T., 2013. Fracture energy of polymer gels with controlled network structures. *J. Chem. Phys.* 139, 144905.
- Atkinson, C., Craster, R.V., 1991. Plane strain fracture in poroelastic media. *Proc. Roy. Soc. Lond. Math. Phys. Sci.* 434, 605.
- Augst, A.D., Kong, H.J., Mooney, D.J., 2006. Alginate hydrogels as biomaterials. *Macromol. Biosci.* 6, 623–633.
- Bai, R., Chen, B., Yang, J., Suo, Z., 2018a. Tearing a Hydrogel of Complex Rheology. (submitted for publication).
- Bai, R., Morelle, X.P., Yang, J., Suo, Z., 2018b. Rupture and Debonding of Soft Layered Materials. (In preparation).
- Bai, R., Yang, J., Morelle, X.P., Suo, Z., 2019. Flaw-insensitive Hydrogels under Static and Cyclic Loads. (submitted for publication).
- Bai, R., Yang, J., Morelle, X.P., Yang, C., Suo, Z., 2018c. Fatigue fracture of self-recovery hydrogels. *ACS Macro Lett.* 312–317.
- Bai, R., Yang, Q., Tang, J., Morelle, X.P., Vlassak, J., Suo, Z., 2017. Fatigue fracture of tough hydrogels. *Extreme Mech. Lett.* 15, 91–96.
- Bai, T., Zhang, P., Han, Y., Liu, Y., Liu, W., Zhao, X., Lu, W., 2011. Construction of an ultrahigh strength hydrogel with excellent fatigue resistance based on strong dipole–dipole interaction. *Soft Matter* 7, 2825–2831.
- Bai, Y., Chen, B., Xiang, F., Zhou, J., Wang, H., Suo, Z., 2014. Transparent hydrogel with enhanced water retention capacity by introducing highly hydratable salt. *Appl. Phys. Lett.* 105, 151903.
- Bajpai, S., Sharma, S., 2004. Investigation of swelling/degradation behaviour of alginate beads crosslinked with Ca²⁺ and Ba²⁺ ions. *React. Funct. Polym.* 59, 129–140.
- Balmforth, N.J., Frigaard, I.A., Ovarlez, G., 2014. Yielding to stress: recent developments in viscoplastic fluid mechanics. *Annu. Rev. Fluid Mech.* 46, 121–146.
- Bao, G., Suo, Z., 1992. Remarks on crack-bridging concepts. *Appl. Mech. Rev.* 45, 355–366.
- Barnes, H.A., 1999. The yield stress—a review or ‘*παντα ρει*’—everything flows? *J. Non-Newtonian Fluid Mech.* 81, 133–178.
- Basinski, Z., Korbel, A., Basinski, S., 1980. The temperature dependence of the saturation stress and dislocation substructure in fatigued copper single crystals. *Acta Metall.* 28, 191–207.
- Baumard, T.L.M., Thomas, A.G., Busfield, J.J.C., 2012. Fatigue peeling at rubber interfaces. *Plast. Rubber Compos.* 41, 296–300.
- Baumberger, T., Caroli, C., Martina, D., 2006a. Fracture of a biopolymer gel as a viscoplastic disentanglement process. *Eur. Phys. J. E* 21, 81–89.
- Baumberger, T., Caroli, C., Martina, D., 2006b. Solvent control of crack dynamics in a reversible hydrogel. *Nat. Mater.* 5, 552–555.
- Baumberger, T., Ronsin, O., 2009. From thermally activated to viscosity controlled fracture of biopolymer hydrogels. *J. Chem. Phys.* 130, 061102.
- Baumberger, T., Ronsin, O., 2010. A convective instability mechanism for quasistatic crack branching in a hydrogel. *Eur. Phys. J. E* 31, 51–58.
- Begley, J., Landes, J., 1972. The J Integral as a Fracture Criterion, Fracture Toughness: Part II. ASTM International.
- Bernardi, L., Mazza, E., Ehret, A.E., 2018. The effect of clamping conditions on tearing energy estimation for highly stretchable materials. *Eng. Fract. Mech.* 188, 300–308.
- Bhowmick, A.K., 1988. Threshold fracture of elastomers. *J. Macromol. Sci., Part C* 28, 339–370.
- Bigi, A., Panzavolta, S., Rubini, K., 2004. Relationship between triple-helix content and mechanical properties of gelatin films. *Biomaterials* 25, 5675–5680.
- Biot, M.A., 1941. General theory of three-dimensional consolidation. *J. Appl. Phys.* 12, 155–164.
- Böger, L., Keip, M.-A., Miehe, C., 2017. Minimization and saddle-point principles for the phase-field modeling of fracture in hydrogels. *Comput. Mater. Sci.* 138, 474–485.
- Bonn, D., Kellay, H., Prochnow, M., Ben-Djemaa, K., Meunier, J., 1998. Delayed fracture of an inhomogeneous soft solid. *Science* 280, 265–267.
- Bouklas, N., Landis, C.M., Huang, R., 2015. Effect of solvent diffusion on crack-tip fields and driving force for fracture of hydrogels. *J. Appl. Mech.* 82, 081007.
- Braccini, I., Pérez, S., 2001. Molecular basis of Ca²⁺-induced gelation in alginates and pectins: the egg-box model revisited. *Biomacromolecules* 2, 1089–1096.
- Brown, H.R., 2007. A model of the fracture of double network gels. *Macromolecules* 40, 3815–3818.
- Buwalda, S.J., Boere, K.W.M., Dijkstra, P.J., Feijen, J., Vermonden, T., Hennink, W.E., 2014. Hydrogels in a historical perspective: from simple networks to smart materials. *J. Contr. Release* 190, 254–273.
- Cai, S., Suo, Z., 2012. Equations of state for ideal elastomeric gels. *EPL (Europhysics Letters)* 97, 34009.
- Caló, E., Khutoryanskiy, V.V., 2015. Biomedical applications of hydrogels: a review of patents and commercial products. *Eur. Polym. J.* 65, 252–267.
- Calvert, P., 2009. Hydrogels for soft machines. *Adv. Mater.* 21, 743–756.
- Candau, F., Leong, Y.S., Fitch, R.M., 1985. Kinetic study of the polymerization of acrylamide in inverse microemulsion. *J. Polym. Sci. Polym. Chem. Ed.* 23, 193–214.
- Caulfield, M.J., Qiao, G.G., Solomon, D.H., 2002. Some aspects of the properties and degradation of polyacrylamides. *Chem. Rev.* 102, 3067–3084.
- Chavasit, V., Torres, J.A., 1990. Chitosan-Poly(acrylic acid): mechanism of complex

- formation and potential industrial applications. *Biotechnol. Prog.* 6, 2–6.
- Chen, B., Yang, J., Bai, R., Suo, Z., 2018. Adhesion of Molecular Staples. (Unpublished).
- Chen, C., Wang, Z., Suo, Z., 2017. Flaw sensitivity of highly stretchable materials. *Extreme Mech. Lett.* 10, 50–57.
- Chen, Q., Chen, H., Zhu, L., Zheng, J., 2016a. Engineering of tough double network hydrogels. *Macromol. Chem. Phys.* 217, 1022–1036.
- Chen, Q., Yan, X., Zhu, L., Chen, H., Jiang, B., Wei, D., Huang, L., Yang, J., Liu, B., Zheng, J., 2016b. Improvement of mechanical strength and fatigue resistance of double network hydrogels by ionic coordination interactions. *Chem. Mater.* 28, 5710–5720.
- Cheng, P., 2004. Chemical and Photolytic Degradation of Polyacrylamides Used in Potable Water Treatment.
- Choi, M., Humar, M., Kim, S., Yun, S.H., 2015. Step-index optical fiber made of bio-compatible hydrogels. *Adv. Mater.* 27, 4081–4086.
- Coyle, S., Majidi, C., LeDuc, P., Hsia, K.J., 2018. Bio-inspired soft robotics: Material selection, actuation, and design. *Extreme Mech. Lett.* 22, 51–59.
- Creton, C., 2017. 50th anniversary perspective: networks and gels: soft but dynamic and tough. *Macromolecules* 50, 8297–8316.
- Creton, C., Ciccotti, M., 2016. Fracture and adhesion of soft materials: a review. *Rep. Prog. Phys.* 79, 046601.
- Cui, K., Sun, T.L., Liang, X., Nakajima, K., Ye, Y.N., Chen, L., Kurokawa, T., Gong, J.P., 2018. Multiscale energy dissipation mechanism in tough and self-healing hydrogels. *Phys. Rev. Lett.* 121, 185501.
- Day, J.C., Robb, I.D., 1981. Thermodynamic parameters of polyacrylamides in water. *Polymer* 22, 1530–1533.
- de Gennes, P.G., 1996. Soft adhesives. *Langmuir* 12, 4497–4500.
- Deng, G., Li, F., Yu, H., Liu, F., Liu, C., Sun, W., Jiang, H., Chen, Y., 2012. Dynamic hydrogels with an environmental adaptive self-healing ability and dual responsive sol-gel transitions. *ACS Macro Lett.* 1, 275–279.
- Deng, G., Tang, C., Li, F., Jiang, H., Chen, Y., 2010. Covalent cross-linked polymer gels with reversible Sol–Gel transition and self-healing properties. *Macromolecules* 43, 1191–1194.
- Dorgan, K.M., Jumars, P.A., Johnson, B., Boudreau, B.P., Landis, E., 2005. Burrow extension by crack propagation. *Nature* 433, 475.
- Draget, K.I., 2009. Alginates, *Handbook of Hydrocolloids*, second ed. Elsevier, pp. 807–828.
- Du, G., Gao, G., Hou, R., Cheng, Y., Chen, T., Fu, J., Fei, B., 2014. Tough and fatigue resistant biomimetic hydrogels of interlaced self-assembled conjugated polymer belts with a polyelectrolyte network. *Chem. Mater.* 26, 3522–3529.
- Du, J., Thouless, M.D., Yee, A.F., 2000. Effects of rate on crack growth in a rubber-modified epoxy. *Acta Mater.* 48, 3581–3592.
- Evans, A., Wiederhorn, S., 1974. Proof testing of ceramic materials—an analytical basis for failure prediction. *Int. J. Fract.* 10, 379–392.
- Evans, A.G., 1990. Perspective on the development of high-toughness ceramics. *J. Am. Ceram. Soc.* 73, 187–206.
- Fang, Y., Al-Assaf, S., Phillips, G.O., Nishinari, K., Funami, T., Williams, P.A., Li, L., 2007. Multiple steps and critical behaviors of the binding of calcium to alginate. *J. Phys. Chem. B* 111, 2456–2462.
- Fleck, N.A., Kang, K.J., Ashby, M.F., 1994. Overview no. 112: the cyclic properties of engineering materials. *Acta Metall. Mater.* 42, 365–381.
- Foegeding, E.A., Gonzalez, C., Hamann, D.D., Case, S., 1994. Polyacrylamide gels as elastic models for food gels. *Food Hydrocolloids* 8, 125–134.
- Gao, Y., Wu, K., Suo, Z., 2018. Photodetachable adhesion. *Adv. Mater.*, 1806948.
- García Cerdá, D., Ballester, A.M., Aliena-Valero, A., Carabén-Redaño, A., Lloris, J.M., 2015. Use of cyanoacrylate adhesives in general surgery. *Surg. Today* 45, 939–956.
- Gelfi, C., Righetti, P.G., 1981a. Polymerization kinetics of polyacrylamide gels I. Effect of different cross-linkers. *Electrophoresis* 2, 213–219.
- Gelfi, C., Righetti, P.G., 1981b. Polymerization kinetics of polyacrylamide gels II. Effect of temperature. *Electrophoresis* 2, 220–228.
- Gent, A., 1996. Adhesion and strength of viscoelastic solids. Is there a relationship between adhesion and bulk properties? *Langmuir* 12, 4492–4496.
- Gent, A.N., Hamed, G.R., 1977. Peel mechanics of adhesive joints. *Polym. Eng. Sci.* 17, 462–466.
- Gent, A., Lai, S.M., 1994. Interfacial bonding, energy dissipation, and adhesion. *J. Polym. Sci., Part B: Polym. Phys.* 32, 1543–1555.
- Gent, A.N., 2012. Engineering with Rubber: How to Design Rubber Components. Carl Hanser Verlag GmbH Co KG.
- Gent, A.N., Pulford, C.T.R., 1984. Micromechanics of fracture in elastomers. *J. Mater. Sci.* 19, 3612–3619.
- Gent, A.N., Razzaghi-Kashani, M., Hamed, G.R., 2003. Why do cracks turn sideways? *Rubber Chem. Technol.* 76, 122–131.
- Gent, A.N., Schultz, J., 1972. Effect of wetting liquids on the strength of adhesion of viscoelastic material. *J. Adhes.* 3, 281–294.
- Gladman, A.S., Matsumoto, E.A., Nuzzo, R.G., Mahadevan, L., Lewis, J.A., 2016. Biomimetic 4D printing. *Nat. Mater.* 15, 413.
- Gong, J.P., 2010. Why are double network hydrogels so tough? *Soft Matter* 6, 2583–2590.
- Gong, J.P., Katsuyama, Y., Kurokawa, T., Osada, Y., 2003. Double-network hydrogels with extremely high mechanical strength. *Adv. Mater.* 15, 1155–1158.
- Gösele, U., Tong, Q.Y., 1998. SEMICONDUCTOR WAFER BONDING. *Annu. Rev. Mater. Sci.* 28, 215–241.
- Griffith, A.A., 1921. VI. The phenomena of rupture and flow in solids. *Phil. Trans. R. Soc. Lond. A* 221, 163–198.
- Guo, J., Liu, X., Jiang, N., Yetisen, A.K., Yuk, H., Yang, C., Khademhosseini, A., Zhao, X., Yun, S.H., 2016. Highly stretchable, strain sensing hydrogel optical fibers. *Adv. Mater.* 28, 10244–10249.
- Guo, J., Shroff, T., Yoon, C., Liu, J., Breger, J.C., Gracias, D.H., Nguyen, T.D., 2017. Bidirectional and biaxial curving of thermoresponsive bilayer plates with soft and stiff segments. *Extreme Mech. Lett.* 16, 6–12.
- Haghiashiani, G., Habtour, E., Park, S.-H., Gardea, F., McAlpine, M.C., 2018. 3D printed electrically-driven soft actuators. *Extreme Mech. Lett.* 21, 1–8.
- Haque, M.A., Kurokawa, T., Gong, J.P., 2012a. Anisotropic hydrogel based on bilayers: color, strength, toughness, and fatigue resistance. *Soft Matter* 8, 8008–8016.
- Haque, M.A., Kurokawa, T., Gong, J.P., 2012b. Super tough double network hydrogels and their application as biomaterials. *Polymer* 53, 1805–1822.
- Haque, M.A., Kurokawa, T., Kamita, G., Gong, J.P., 2011. Lamellar bilayers as reversible sacrificial bonds to toughen hydrogel: hysteresis, self-recovery, fatigue resistance, and crack blunting. *Macromolecules* 44, 8916–8924.
- Hashimoto, W., Mishima, Y., Miyake, O., Nankai, H., Momma, K., Murata, K., Matsumura, S., Steinbüchel, A., 2005. Biodegradation of alginate, Xanthan, and Gellan. *A. Steinbüchel*.
- He, Q., Wang, Z., Yan, Y., Zheng, J., Cai, S., 2016. Polymer nanofiber reinforced double network gel composite: strong, tough and transparent. *Extreme Mech. Lett.* 9, 165–170.
- Heemskerck, J., Rosmalen, R., Janssen-Van, R., Holtslag, R., Teeuw, D., 1984. Quantification of viscoelastic effects of polyacrylamide solutions. In: *SPE Enhanced Oil Recovery Symposium*. Society of Petroleum Engineers.
- Higgs, P.G., Ross-Murphy, S.B., 1990. Creep measurements on gelatin gels. *Int. J. Biol. Macromol.* 12, 233–240.
- Hoare, T.R., Kohane, D.S., 2008. Hydrogels in drug delivery: progress and challenges. *Polymer* 49, 1993–2007.
- Hochberg, A., Tanaka, T., Nicoli, D., 1979. Spinodal line and critical point of an acrylamide gel. *Phys. Rev. Lett.* 43, 217.
- Hoffman, A.S., 2012. Hydrogels for biomedical applications. *Adv. Drug Del. Rev.* 64, 18–23.
- Hong, S., Sycks, D., Chan, H.F., Lin, S., Lopez, G.P., Guilak, F., Leong, K.W., Zhao, X., 2015. 3D printing of highly stretchable and tough hydrogels into complex, cellularized structures. *Adv. Mater.* 27, 4035–4040.
- Hong, W., Zhao, X., Zhou, J., Suo, Z., 2008. A theory of coupled diffusion and large deformation in polymeric gels. *J. Mech. Phys. Solid.* 56, 1779–1793.
- Hu, Y., Kim, P., Aizenberg, J., 2017. Harnessing structural instability and material instability in the hydrogel-actuated integrated responsive structures (HAIRS). *Extreme Mech. Lett.* 13, 84–90.
- Hu, J., Kurokawa, T., Hiwataishi, K., Nakajima, T., Wu, Z.L., Liang, S.M., Gong, J.P., 2012a. Structure optimization and mechanical model for microgel-reinforced hydrogels with high strength and toughness. *Macromolecules* 45, 5218–5228.
- Hu, J., Kurokawa, T., Nakajima, T., Sun, T.L., Suekama, T., Wu, Z.L., Liang, S.M., Gong, J.P., 2012b. High fracture efficiency and stress concentration phenomenon for microgel-reinforced hydrogels based on double-network principle. *Macromolecules* 45, 9445–9451.
- Hu, X., Vatankhah-Varnoosfaderani, M., Zhou, J., Li, Q., Sheiko, S.S., 2015. Weak hydrogen bonding enables hard, strong, tough, and elastic hydrogels. *Adv. Mater.* 27, 6899–6905.
- Hu, Y., Suo, Z., 2012. Viscoelasticity and poroelasticity in elastomeric gels. *Acta Mech. Solida Sin.* 25, 441–458.
- Hu, Y., Zhao, X., Vlassak, J.J., Suo, Z., 2010. Using indentation to characterize the poroelasticity of gels. *Appl. Phys. Lett.* 96, 121904.
- Huang, J., Yang, J., Jin, L., Clarke, D.R., Suo, Z., 2016. Pattern formation in plastic liquid films on elastomers by ratcheting. *Soft Matter* 12, 3820–3827.
- Huang, Y., King, D.R., Sun, T.L., Nonoyama, T., Kurokawa, T., Nakajima, T., Gong, J.P., 2017. Energy-dissipative matrices enable synergistic toughening in fiber reinforced soft composites. *Adv. Funct. Mater.* 27.
- Hui, C.-Y., Long, R., Ning, J., 2013. Stress relaxation near the tip of a stationary mode I crack in a poroelastic solid. *J. Appl. Mech.* 80, 021014.
- Hui, C.Y., Bennisson, S.J., Londono, J.D., 2003. Crack blunting and the strength of soft elastic solids. *Proc. R. Soc. London, Ser. A: Math. Phys. Eng. Sci.* 459, 1489.
- Hutchinson, J.W., 1983. Fundamentals of the phenomenological theory of nonlinear fracture mechanics. *J. Appl. Mech.* 50, 1042–1051.
- Ihsan, A.B., Sun, T.L., Kurokawa, T., Karobi, S.N., Nakajima, T., Nonoyama, T., Roy, C.K., Luo, F., Gong, J.P., 2016. Self-healing behaviors of tough polyampholyte hydrogels. *Macromolecules* 49, 4245–4252.
- Illeperuma, W.R., Rothmund, P., Suo, Z., Vlassak, J.J., 2016. Fire-resistant hydrogel-fabric laminates: a simple concept that may save lives. *ACS Appl. Mater. Inter.* 8, 2071–2077.
- Illeperuma, W.R., Sun, J.-Y., Suo, Z., Vlassak, J.J., 2014. Fiber-reinforced tough hydrogels. *Extreme Mech. Lett.* 1, 90–96.
- Illeperuma, W.R.K., Sun, J.-Y., Suo, Z., Vlassak, J.J., 2013. Force and stroke of a hydrogel actuator. *Soft Matter* 9, 8504–8511.
- Jeon, I., Cui, J., Illeperuma, W.R., Aizenberg, J., Vlassak, J.J., 2016. Extremely stretchable and fast self-healing hydrogels. *Adv. Mater.* 28, 4678–4683.
- Jia, H., Huang, Z., Fei, Z., Dyson, P.J., Zheng, Z., Wang, X., 2017. Bilayered polyurethane/dipole-dipole and H-bonding interaction reinforced hydrogels as thermo-responsive soft manipulators. *J. Mater. Chem. B* 5, 8193–8199.
- Kakuta, T., Takashima, Y., Harada, A., 2013. Highly elastic supramolecular hydrogels using host-guest inclusion complexes with cyclodextrins. *Macromolecules* 46, 4575–4579.
- Kalcioglu, Z.L., Mahmoodian, R., Hu, Y., Suo, Z., Van Vliet, K.J., 2012. From macro-to microscale poroelastic characterization of polymeric hydrogels via indentation. *Soft Matter* 8, 3393–3398.
- Karobi, S.N., Sun, T.L., Kurokawa, T., Luo, F., Nakajima, T., Nonoyama, T., Gong, J.P., 2016. Creep behavior and delayed fracture of tough polyampholyte hydrogels by tensile test. *Macromolecules* 49, 5630–5636.
- Katagiri, K., Omura, A., Koyanagi, K., Awatani, J., Shiraiishi, T., Kaneshiro, H., 1977. Early stage crack tip dislocation morphology in fatigued copper. *Metall. Trans. A* 8,

- 1769–1773.
- Kellaris, N., Venkata, V.G., Smith, G.M., Mitchell, S.K., Keplinger, C., 2018. Peano-HASEL actuators: muscle-mimetic, electrohydraulic transducers that linearly contract on activation. *Sci. Robot.* 3, eaar3276.
- Keplinger, C., Sun, J.Y., Foo, C.C., Rothemund, P., Whitesides, G.M., Suo, Z., 2013. Stretchable, transparent, ionic conductors. *Science* 341, 984–987.
- Kim, K.S., Aravas, N., 1988. Elastoplastic analysis of the peel test. *Int. J. Solids Struct.* 24, 417–435.
- Kim, C.C., Lee, H.H., Oh, K.H., Sun, J.Y., 2016. Highly stretchable, transparent ionic touch panel. *Science* 353, 682–687.
- Kim, J.Y., Liu, Z., Weon, B.M., Hui, C.-Y., Dufresne, E.R., Style, R.W., 2018. Scale-free Fracture in Soft Solids. arXiv preprint arXiv:1811.00841.
- Knauss, W.G., 2015. A review of fracture in viscoelastic materials. *Int. J. Fract.* 196, 99–146.
- Kolvin, I., Cohen, G., Fineberg, J., 2017. Topological defects govern crack front motion and facet formation on broken surfaces. *Nat. Mater.* 17, 140.
- Kuhn, W., Grün, F., 1942. Beziehungen zwischen elastischen Konstanten und Dehnungsdoppelbrechung hochelastischer Stoffe. *Kolloid Z.* 101, 248–271.
- Lake, G., Thomas, A., 1967. The strength of highly elastic materials. *Proc. R. Soc. London, Ser. A* 300, 108–119.
- Lake, G.J., 2003. Fracture mechanics and its application to failure in rubber articles. *Rubber Chem. Technol.* 76, 567–591.
- Landes, D., Begley, J., 1972. The Effect of Specimen Geometry on J IC, Fracture Toughness: Part II. ASTM International.
- Larson, C., Peele, B., Li, S., Robinson, S., Totaro, M., Beccai, L., Mazzolai, B., Shepherd, R., 2016. Highly stretchable electroluminescent skin for optical signaling and tactile sensing. *Science* 351, 1071–1074.
- Law, B., Wilshaw, T.R., 1993. Fracture of Brittle Solids. Cambridge university press.
- Le Floch, P., Yao, X., Liu, Q., Wang, Z., Nian, G., Sun, Y., Jia, L., Suo, Z., 2017. Wearable and washable conductors for active textiles. *ACS Appl. Mater. Inter.* 9, 25542–25552.
- Lee, H.-R., Kim, C.-C., Sun, J.-Y., 2018. Stretchable ionics – a promising candidate for upcoming wearable devices. *Adv. Mater.* 30, 1704403.
- Lee, K.Y., Mooney, D.J., 2001. Hydrogels for tissue engineering. *Chem. Rev.* 101, 1869–1880.
- Lee, K.Y., Mooney, D.J., 2012. Alginate: properties and biomedical applications. *Prog. Polym. Sci.* 37, 106–126.
- Lefranc, M., Bouchaud, E., 2014. Mode I fracture of a biopolymer gel: rate-dependent dissipation and large deformations disentangled. *Extreme Mech. Lett.* 1, 97–103.
- Lei, Z., Wang, Q., Sun, S., Zhu, W., Wu, P., 2017. A bioinspired mineral hydrogel as a self-healable, mechanically adaptable ionic skin for highly sensitive pressure sensing. *Adv. Mater.* 29.
- Leomach, M., Perge, C., Divoux, T., Manneville, S., 2014. Creep and fracture of a protein gel under stress. *Phys. Rev. Lett.* 113, 038303.
- Li, C., Rowland, M.J., Shao, Y., Cao, T., Chen, C., Jia, H., Zhou, X., Yang, Z., Scherman, O.A., Liu, D., 2015. Responsive double network hydrogels of interpenetrating DNA and CB[8] host–guest supramolecular systems. *Adv. Mater.* 27, 3298–3304.
- Li, J., Celiz, A.D., Yang, J., Yang, Q., Wamala, L., Whyte, W., Seo, B.R., Vasilyev, N.V., Vlassak, J.J., Suo, Z., Mooney, D.J., 2017a. Tough adhesives for diverse wet surfaces. *Science* 357, 378–381.
- Li, J., Hu, Y., Vlassak, J.J., Suo, Z., 2012. Experimental determination of equations of state for ideal elastomeric gels. *Soft Matter* 8, 8121–8128.
- Li, J., Illeperuma, W.R.K., Suo, Z., Vlassak, J.J., 2014a. Hybrid hydrogels with extremely high stiffness and toughness. *ACS Macro Lett.* 3, 520–523.
- Li, J., Mooney, D.J., 2016. Designing hydrogels for controlled drug delivery. *Nat. Rev. Mater.* 1, 16071.
- Li, J., Suo, Z., Vlassak, J.J., 2014b. Stiff, strong, and tough hydrogels with good chemical stability. *J. Mater. Chem. B* 2, 6708–6713.
- Li, T., Li, G., Liang, Y., Cheng, T., Dai, J., Yang, X., Liu, B., Zeng, Z., Huang, Z., Luo, Y., 2017b. Fast-moving soft electronic fish. *Sci. Adv.* 3, e1602045.
- Liao, I., Moutos, F.T., Estes, B.T., Zhao, X., Guilak, F., 2013. Composite three-dimensional woven scaffolds with interpenetrating network hydrogels to create functional synthetic articular cartilage. *Adv. Funct. Mater.* 23, 5833–5839.
- Liao, M., Wan, P., Wen, J., Gong, M., Wu, X., Wang, Y., Shi, R., Zhang, L., 2017. Wearable, healable, and adhesive epidermal sensors assembled from mussel-inspired conductive hybrid hydrogel framework. *Adv. Funct. Mater.* 27, 1703852.
- Lin, P., Ma, S., Wang, X., Zhou, F., 2015. Molecularly engineered dual-crosslinked hydrogel with ultrahigh mechanical strength, toughness, and good self-recovery. *Adv. Mater.* 27, 2054–2059.
- Lin, S., Cao, C., Wang, Q., Gonzalez, M., Dolbow, J.E., Zhao, X., 2014a. Design of stiff, tough and stretchy hydrogel composites via nanoscale hybrid crosslinking and macroscale fiber reinforcement. *Soft Matter* 10, 7519–7527.
- Lin, S., Zhou, Y., Zhao, X., 2014b. Designing extremely resilient and tough hydrogels via delayed dissipation. *Extreme Mech. Lett.* 1, 70–75.
- Liu, J., Pang, Y., Zhang, S., Cleveland, C., Yin, X., Booth, L., Lin, J., Lee, Y.-A.L., Mazdiyasn, H., Saxton, S., 2017a. Triggerable tough hydrogels for gastric resident dosage forms. *Nat. Commun.* 8, 124.
- Liu, Q., 2018. Bonding hydrophilic and hydrophobic soft materials for functional soft devices. <http://imechanica.org/node/22900>.
- Liu, S., Boatti, E., Bertoldi, K., Kramer-Bottiglio, R., 2018a. Stimuli-induced bi-directional hydrogel unimorph actuators. *Extreme Mech. Lett.* 21, 35–43.
- Liu, Q., Nian, G., Yang, C., Qu, S., Suo, Z., 2018b. Bonding dissimilar polymer networks in various manufacturing processes. *Nat. Commun.* 9, 846.
- Liu, S., Li, L., 2016. Recoverable and self-healing double network hydrogel based on κ-carrageenan. *ACS Appl. Mater. Inter.* 8, 29749–29758.
- Liu, X., Tang, T.-C., Tham, E., Yuk, H., Lin, S., Lu, T.K., Zhao, X., 2017b. Stretchable living materials and devices with hydrogel–elastomer hybrids hosting programmed cells. *Proc. Natl. Acad. Sci. U.S.A.* 114, 2200–2205.
- Liu, X., Yuk, H., Lin, S., Parada, G.A., Tang, T.-C., Tham, E., de la Fuente-Nunez, C., Lu, T.K., Zhao, X., 2017c. 3D printing of living responsive materials and devices. *Adv. Mater.* 30, 1704821.
- Livne, A., Bouchbinder, E., Svetlizky, I., Fineberg, J., 2010. The near-tip fields of fast cracks. *Science* 327, 1359–1363.
- Livne, A., Cohen, G., Fineberg, J., 2005. Universality and hysteretic dynamics in rapid fracture. *Phys. Rev. Lett.* 94, 224301.
- Long, R., Hui, C.-Y., 2015. Crack tip fields in soft elastic solids subjected to large quasi-static deformation—a review. *Extreme Mech. Lett.* 4, 131–155.
- Long, R., Hui, C.-Y., 2016. Fracture toughness of hydrogels: measurement and interpretation. *Soft Matter* 12, 8069–8086.
- Lu, T., Wang, J., Yang, R., Wang, T., 2016. A constitutive model for soft materials incorporating viscoelasticity and Mullins effect. *J. Appl. Mech.* 84 021010-021010-021019.
- Luo, F., Sun, T.L., Nakajima, T., King, D.R., Kurokawa, T., Zhao, Y., Ihsan, A.B., Li, X., Guo, H., Gong, J.P., 2016. Strong and tough polyion-complex hydrogels from oppositely charged polyelectrolytes: a comparative study with polyampholyte hydrogels. *Macromolecules* 49, 2750–2760.
- Luo, F., Sun, T.L., Nakajima, T., Kurokawa, T., Zhao, Y., Sato, K., Ihsan, A.B., Li, X., Guo, H., Gong, J.P., 2015. Oppositely charged polyelectrolytes form tough, self-healing, and rebuildable hydrogels. *Adv. Mater.* 27, 2722–2727.
- Mao, Y., Anand, L., 2018. A theory for fracture of polymeric gels. *J. Mech. Phys. Solid.* 115, 30–53.
- Mao, Y., Lin, S., Zhao, X., Anand, L., 2017. A large deformation viscoelastic model for double-network hydrogels. *J. Mech. Phys. Solid.* 100, 103–130.
- Mars, W., Fatemi, A., 2002. A literature survey on fatigue analysis approaches for rubber. *Int. J. Fatig.* 24, 949–961.
- Mars, W., Fatemi, A., 2004. Factors that affect the fatigue life of rubber: a literature survey. *Rubber Chem. Technol.* 77, 391–412.
- Marshall, D.B., Cox, B.N., Evans, A.G., 1985. The mechanics of matrix cracking in brittle-matrix fiber composites. *Acta Metall.* 33, 2013–2021.
- Masuda, F., 1994. Trends in the Development of Superabsorbent Polymers for Diapers, Superabsorbent Polymers. American Chemical Society, pp. 88–98.
- McMeeking, R.M., Evans, A.G., 1982. Mechanics of transformation-toughening in brittle materials. *J. Am. Ceram. Soc.* 65, 242–246.
- Morelle, X.P., Bai, R., Suo, Z., 2017. Localized deformation in plastic liquids on elastomers. *J. Appl. Mech.* 84, 101002.
- Morelle, X.P., Illeperuma, W.R., Tian, K., Bai, R., Suo, Z., Vlassak, J.J., 2018. Highly stretchable and tough hydrogels below water freezing temperature. *Adv. Mater.* 30, 1801541.
- Mueller, H., Knauss, W., 1971. The fracture energy and some mechanical properties of a polyurethane elastomer. *Trans. Soc. Rheol.* 15, 217–233.
- Mullins, L., 1948. Effect of stretching on the properties of rubber. *Rubber Chem. Technol.* 21, 281–300.
- Mullins, L., 1959. Rupture of rubber. IX. Role of hysteresis in the tearing of rubber. *Trans. Inst. Rubber Ind.* 35, 213–222.
- Mullins, L., 1969. Softening of rubber by deformation. *Rubber Chem. Technol.* 42, 339–362.
- Murosaki, T., Noguchi, T., Kakugo, A., Putra, A., Kurokawa, T., Furukawa, H., Osada, Y., Gong, J.P., Nogata, Y., Matsumura, K., Yoshimura, E., Fusetani, N., 2009. Antifouling activity of synthetic polymer gels against cyprids of the barnacle (*Balanus amphitrite*) in vitro. *Biofouling* 25, 313–320.
- Na, Y.-H., Tanaka, Y., Kawauchi, Y., Furukawa, H., Sumiyoshi, T., Gong, J.P., Osada, Y., 2006. Necking phenomenon of double-network gels. *Macromolecules* 39, 4641–4645.
- Naassaoui, I., Ronsin, O., Baumberger, T., 2018. A poroelastic signature of the dry/wet state of a crack tip propagating steadily in a physical hydrogel. *Extreme Mech. Lett.* 22, 8–12.
- Nakahata, M., Takashima, Y., Yamaguchi, H., Harada, A., 2011. Redox-responsive self-healing materials formed from host–guest polymers. *Nat. Commun.* 2, 511.
- Nakajima, T., Furukawa, H., Tanaka, Y., Kurokawa, T., Osada, Y., Gong, J.P., 2009. True chemical structure of double network hydrogels. *Macromolecules* 42, 2184–2189.
- Nakajima, T., Kurokawa, T., Ahmed, S., Wu, W.-L., Gong, J.P., 2013. Characterization of internal fracture process of double network hydrogels under uniaxial elongation. *Soft Matter* 9, 1955–1966.
- Needleman, A., 1987. A continuum model for void nucleation by inclusion debonding. *J. Appl. Mech.* 54, 525–531.
- Nonoyama, T., Wada, S., Kiyama, R., Kitamura, N., Mredha, M., Islam, T., Zhang, X., Kurokawa, T., Nakajima, T., Takagi, Y., 2016. Double-network hydrogels strongly bondable to bones by spontaneous osteogenesis penetration. *Adv. Mater.* 28, 6740–6745.
- Noselli, G., Lucantonio, A., McMeeking, R.M., DeSimone, A., 2016. Poroelastic toughening in polymer gels: a theoretical and numerical study. *J. Mech. Phys. Solid.* 94, 33–46.
- Obreimoff, J.W., 1930. The splitting strength of mica. *Proc. R. Soc. Lond. - Ser. A Contain. Pap. a Math. Phys. Character* 127, 290–297.
- Orowan, E., 1944. The fatigue of glass under stress. *Nature* 154, 341.
- Papadopoulos, I.C., Thomas, A.G., Busfield, J.J.C., 2008. Rate transitions in the fatigue crack growth of elastomers. *J. Appl. Polym. Sci.* 109, 1900–1910.
- Parada, G.A., Yuk, H., Liu, X., Hsieh, A.J., Zhao, X., 2017. Impermeable robust hydrogels via hybrid lamination. *Adv. Healthc. Mater.* 6, 1700520.
- Parida, K., Kumar, V., Jiangxin, W., Bhavanasi, V., Bendi, R., Lee, P.S., 2017. Highly transparent, stretchable, and self-healing ionic-skin triboelectric nanogenerators for energy harvesting and touch applications. *Adv. Mater.* 29.
- Pavesi, L., Rigamonti, A., 1995. Diffusion constants in polyacrylamide gels. *Phys. Rev.* 51, 3318.

- Peak, C.W., Wilker, J.J., Schmidt, G., 2013. A review on tough and sticky hydrogels. *Colloid. Polym. Sci.* 291, 2031–2047.
- Peppas, N.A., Hilt, J.Z., Khademhosseini, A., Langer, R., 2006. Hydrogels in biology and medicine: from molecular principles to bionanotechnology. *Adv. Mater.* 18, 1345–1360.
- Persson, B.N.J., Albohr, O., Heinrich, G., Ueba, H., 2005. Crack propagation in rubber-like materials. *J. Phys. Condens. Matter* 17, R1071.
- Persson, B.N.J., Brener, E.A., 2005. Crack propagation in viscoelastic solids. *Phys. Rev.* 71, 036123.
- Pharr, M., Sun, J.-Y., Suo, Z., 2012. Rupture of a highly stretchable acrylic dielectric elastomer. *J. Appl. Phys.* 111, 104114.
- Picchioni, F., Muljana, H., 2018. Hydrogels based on dynamic covalent and non covalent bonds: a chemistry perspective. *Gels* 4.
- Pu, X., Liu, M., Chen, X., Sun, J., Du, C., Zhang, Y., Zhai, J., Hu, W., Wang, Z.L., 2017. Ulstretchable, transparent triboelectric nanogenerator as electronic skin for bio-mechanical energy harvesting and tactile sensing. *Sci. Adv.* 3, e1700015.
- Qi, Y., Caillard, J., Long, R., 2018. Fracture toughness of soft materials with rate-independent hysteresis. *J. Mech. Phys. Solid.* 118, 341–364.
- Qin, M., Sun, M., Bai, R., Mao, Y., Qian, X., Sikka, D., Zhao, Y., Qi, H.J., Suo, Z., He, X., 2018. Bioinspired hydrogel interferometer for adaptive coloration and chemical sensing. *Adv. Mater.* 1800468.
- Radi, E., Bigoni, D., Lorent, B., 2002. Steady crack growth in elastic-plastic fluid-saturated porous media. *Int. J. Plast.* 18, 345–358.
- Rice, J.R., 1968. Mathematical analysis in the mechanics of fracture. *Fract.: Adv. Treatise* 2, 191–311.
- Rice, J.R., Cleary, M.P., 1976. Some basic stress diffusion solutions for fluid-saturated elastic porous media with compressible constituents. *Rev. Geophys.* 14, 227–241.
- Ritchie, R., 1988. Mechanisms of fatigue crack propagation in metals, ceramics and composites: role of crack tip shielding. *Mater. Sci. Eng., A* 103, 15–28.
- Rivlin, R., Thomas, A.G., 1953. Rupture of rubber. I. Characteristic energy for tearing. *J. Polym. Sci., Part A: Polym. Chem.* 10, 291–318.
- Roberts, M.C., Hanson, M.C., Massey, A.P., Karren, E.A., Kiser, P.F., 2007. Dynamically restructuring hydrogel networks formed with reversible covalent crosslinks. *Adv. Mater.* 19, 2503–2507.
- Robinson, S.S., O'Brien, K.W., Zhao, H., Peele, B.N., Larson, C.M., Mac Murray, B.C., Van Meerbeek, I.M., Dunham, S.N., Shepherd, R.F., 2015. Integrated soft sensors and elastomeric actuators for tactile machines with kinesthetic sense. *Extreme Mech. Lett.* 5, 47–53.
- Rose, S., PrevotEAU, A., Elzière, P., Hourdet, D., Marcellan, A., Leibler, L., 2013. Nanoparticle solutions as adhesives for gels and biological tissues. *Nature* 505, 382.
- Rothmund, P., Morelle, X.P., Jia, K., Whitesides, G.M., Suo, Z., 2018. A transparent membrane for active noise cancellation. *Adv. Funct. Mater.* 28, 1800653.
- Rowley, J.A., Madlambayan, G., Mooney, D.J., 1999. Alginate hydrogels as synthetic extracellular matrix materials. *Biomaterials* 20, 45–53.
- Rubinstein, M., Colby, R.H., 2003. *Polymer Physics*. Oxford University Press.
- Sarwar, M.S., Dobashi, Y., Preston, C., Wyss, J.K., Mirabbasi, S., Madden, J.D.W., 2017. Bend, stretch, and touch: locating a finger on an actively deformed transparent sensor array. *Sci. Adv.* 3, e1602200.
- Sato, K., Nakajima, T., Hisamatsu, T., Nonoyama, T., Kurokawa, T., Gong, J.P., 2015. Phase-separation-induced anomalous stiffening, toughening, and self-healing of polyacrylamide gels. *Adv. Mater.* 27, 6990–6998.
- Schapery, R.A., 1975. A theory of crack initiation and growth in viscoelastic media. *Int. J. Fract.* 11, 141–159.
- Schroeder, T.B., Guha, A., Lamoureux, A., VanRenterghem, G., Sept, D., Shtein, M., Yang, J., Mayer, M., 2017. An electric-eel-inspired soft power source from stacked hydrogels. *Nature* 552, 214.
- Sheng, H., Wang, X., Kong, N., Xi, W., Yang, H., Wu, X., Wu, K., Li, C., Hu, J., Tang, J., Zhou, J., Duan, S., Wang, H., Suo, Z., 2019. Neural Interfaces by Hydrogels. (submitted for publication).
- Shull, K.R., Flanagan, C.M., Crosby, A.J., 2000. Fingering instabilities of confined elastic layers in tension. *Phys. Rev. Lett.* 84, 3057–3060.
- Sikorski, P., Mo, F., Skjåk-Braek, G., Stokke, B.T., 2007. Evidence for egg-box-compatible interactions in calcium-alginate gels from fiber X-ray diffraction. *Biomacromolecules* 8, 2098–2103.
- Slaughter, B.V., Khurshid, S.S., Fisher, O.Z., Khademhosseini, A., Peppas, N.A., 2009. Hydrogels in regenerative medicine. *Adv. Mater.* 21, 3307–3329.
- Smith, E.A., Prues, S.L., Oehme, F.W., 1997. Environmental degradation of polyacrylamides. *Ecotoxicol. Environ. Saf.* 37, 76–91.
- Sørensen, B.F., Jacobsen, T.K., 2003. Determination of cohesive laws by the J integral approach. *Eng. Fract. Mech.* 70, 1841–1858.
- Sun, J.Y., Keping, C., Whitesides, G.M., Suo, Z., 2014. Ionic skin. *Adv. Mater.* 26, 7608–7614.
- Sun, J.Y., Zhao, X., Illeperuma, W.R., Chaudhuri, O., Oh, K.H., Mooney, D.J., Vlassak, J.J., Suo, Z., 2012. Highly stretchable and tough hydrogels. *Nature* 489, 133–136.
- Sun, M., Bai, R., Yang, X., Song, J., Qin, M., Suo, Z., He, X., 2018. Hydrogel interferometry for ultrasensitive and highly selective chemical detection. *Adv. Mater.* 0, 1804916.
- Sun, T.L., Cui, K., Gong, J.P., 2017a. Tough, self-recovery and self-healing polyampholyte hydrogels. *Polym. Sci. C* 59, 11–17.
- Sun, T.L., Kurokawa, T., Kuroda, S., Ihsan, A.B., Akasaki, T., Sato, K., Haque, M.A., Nakajima, T., Gong, J.P., 2013. Physical hydrogels composed of polyampholytes demonstrate high toughness and viscoelasticity. *Nat. Mater.* 12, 932–937.
- Sun, T.L., Luo, F., Hong, W., Cui, K., Huang, Y., Zhang, H.J., King, D.R., Kurokawa, T., Nakajima, T., Gong, J.P., 2017b. Bulk energy dissipation mechanism for the fracture of tough and self-healing hydrogels. *Macromolecules* 50, 2923–2931.
- Suresh, S., 1998. *Fatigue of Materials*. Cambridge university press.
- Tanaka, Y., 2007. A local damage model for anomalous high toughness of double-network gels. *EPL (Europhysics Letters)* 78, 56005.
- Tanaka, Y., Fukao, K., Miyamoto, Y., 2000. Fracture energy of gels. *Eur. Phys. J. E* 3, 395–401.
- Tanaka, Y., Kuwabara, R., Na, Y.-H., Kurokawa, T., Gong, J.P., Osada, Y., 2005. Determination of fracture energy of high strength double network hydrogels. *J. Phys. Chem. B* 109, 11559–11562.
- Tanaka, Y., Shimazaki, R., Yano, S., Yoshida, G., Yamaguchi, T., 2016. Solvent effects on the fracture of chemically crosslinked gels. *Soft Matter* 12, 8135–8142.
- Tang, J., Li, J., Vlassak, J.J., Suo, Z., 2016. Adhesion between highly stretchable materials. *Soft Matter* 12, 1093–1099.
- Tang, J., Li, J., Vlassak, J.J., Suo, Z., 2017. Fatigue fracture of hydrogels. *Extreme Mech. Lett.* 10, 24–31.
- Tang, L., Liu, W., Liu, G., 2010. High-strength hydrogels with integrated functions of H-bonding and thermoresponsive surface-mediated reverse transfection and cell detachment. *Adv. Mater.* 22, 2652–2656.
- Tankasala, H.C., Deshpande, V.S., Fleck, N.A., 2015. 2013 Koiter medal paper: crack-tip fields and toughness of two-dimensional elastoplastic lattices. *J. Appl. Mech.* 82, 091004-091004-091010.
- Taylor, D.L., in het Panhuis, M., 2016. Self-healing hydrogels. *Adv. Mater.* 28, 9060–9093.
- Thomas, A., 1958. Rupture of rubber. V. Cut growth in natural rubber vulcanizates. *J. Polym. Sci.* 31, 467–480.
- Thompson, N., Wadsworth, N., Louat, N., 1956. Xi. The origin of fatigue fracture in copper. *Philos. Mag. A* 1, 113–126.
- Tian, K., Bae, J., Bakarich, S.E., Yang, C., Gately, R.D., Spinks, G.M., Suo, Z., Vlassak, J.J., 2017. 3D printing of transparent and conductive heterogeneous hydrogel-elastomer systems. *Adv. Mater.* 29.
- Tian, K., Bae, J., Suo, Z., Vlassak, J.J., 2018. Adhesion between hydrophobic elastomer and hydrogel through hydrophilic modification and interfacial segregation. *ACS Appl. Mater. Inter.* 10, 43252–43261.
- Tobita, H., Hamielec, A., 1990. Crosslinking kinetics in polyacrylamide networks. *Polymer* 31, 1546–1552.
- Tobolsky, A.V., Prettyman, I.B., Dillon, J.H., 1944. Stress relaxation of natural and synthetic rubber stocks. *Rubber Chem. Technol.* 17, 551–575.
- Tuncaboylu, D.C., Argun, A., Algi, M.P., Okay, O., 2013. Autonomic self-healing in covalently crosslinked hydrogels containing hydrophobic domains. *Polymer* 54, 6381–6388.
- Tvergaard, V., Hutchinson, J.W., 1992. The relation between crack growth resistance and fracture process parameters in elastic-plastic solids. *J. Mech. Phys. Solid.* 40, 1377–1397.
- Visser, J., Melchels, F.P.W., Jeon, J.E., van Bussel, E.M., Kimpton, L.S., Byrne, H.M., Dhert, W.J.A., Dalton, P.D., Huttmacher, D.W., Malda, J., 2015. Reinforcement of hydrogels using three-dimensionally printed microfibrils. *Nat. Commun.* 6, 6933.
- Wang, W., Zhang, Y., Liu, W., 2017a. Bioinspired fabrication of high strength hydrogels from non-covalent interactions. *Prog. Polym. Sci.* 71, 1–25.
- Wang, X., Hong, W., 2012. Delayed fracture in gels. *Soft Matter* 8, 8171–8178.
- Wang, Y., Wang, Z., Wu, K., Wu, J., Meng, G., Liu, Z., Guo, X., 2017b. Synthesis of cellulose-based double-network hydrogels demonstrating high strength, self-healing, and antibacterial properties. *Carbohydr. Polym.* 168, 112–120.
- Wang, Z., Tang, J., Bai, R., Zhang, W., Lian, T., Lu, T., Wang, T., 2018a. A phenomenological model for shakedown of tough hydrogels under cyclic loads. *J. Appl. Mech.* 85, 091005-091005-091008.
- Wang, Z., Xiang, C., Yao, X., Le Floch, P., Mendez, J., Suo, Z., 2018b. Stretchable Materials of High Toughness and Low Hysteresis. (submitted for publication).
- Webber, R.E., Creton, C., Brown, H.R., Gong, J.P., 2007. Large strain hysteresis and Mullins effect of tough double-network hydrogels. *Macromolecules* 40, 2919–2927.
- Wei, R.P., 2010. *Fracture Mechanics: Integration of Mechanics, Materials Science and Chemistry*. Cambridge University Press.
- Wei, Y., Hutchinson, J.W., 1998. Interface strength, work of adhesion and plasticity in the peel test. In: Knauss, W.G., Schapery, R.A. (Eds.), *Recent Advances in Fracture Mechanics: Honoring Mel and Max Williams*. Springer Netherlands, Dordrecht, pp. 315–333.
- Wei, Z., Yang, J.H., Du, X.J., Xu, F., Zrinyi, M., Osada, Y., Li, F., Chen, Y.M., 2013. Dextran-based self-healing hydrogels formed by reversible diels-alder reaction under physiological conditions. *Macromol. Rapid Commun.* 34, 1464–1470.
- Wei, Z., Yang, J.H., Zhou, J., Xu, F., Zrinyi, M., Dussault, P.H., Osada, Y., Chen, Y.M., 2014. Self-healing gels based on constitutional dynamic chemistry and their potential applications. *Chem. Soc. Rev.* 43, 8114–8131.
- Weiss, N., Silberberg, A., 1977. Inhomogeneity of polyacrylamide gel structure from permeability and viscoelasticity. *Br. Polym. J.* 9, 144–150.
- Wichterle, O., Lim, D., 1960. Hydrophilic gels for biological use. *Nature* 185, 117.
- Wichterle, O., Lim, D., 1961. Process for producing shaped articles from three-dimensional hydrophilic high polymers. *US Patent 2,976,576*.
- Wiederhorn, S., Bolz, L., 1970. Stress corrosion and static fatigue of glass. *J. Am. Ceram. Soc.* 53, 543–548.
- Wirhli, D., Pichler, R., Drack, M., Kettlhuber, G., Moser, R., Gerstmayr, R., Hartmann, F., Bradt, E., Kaltseis, R., Siket, C.M., Schausberger, S.E., Hild, S., Bauer, S., Kaltenbrunner, M., 2017. Instant tough bonding of hydrogels for soft machines and electronics. *Sci. Adv.* 3, e1700053.
- Wu, Y., Shah, D.U., Liu, C., Yu, Z., Liu, J., Ren, X., Rowland, M.J., Abell, C., Ramage, M.H., Scherman, O.A., 2017. Bioinspired supramolecular fibers drawn from a multiphase self-assembled hydrogel. *Proc. Natl. Acad. Sci. U.S.A.* 114, 8163–8168.
- Xiang, C., Wang, Z., Yang, C.H., Yao, X., Suo, Z., 2019. Water-matrix Composites with High Elasticity, Toughness and Stability. (Unpublished).
- Xin, H., Brown, H.R., Naficy, S., Spinks, G.M., 2015. Time-dependent mechanical properties of tough ionic-covalent hybrid hydrogels. *Polymer* 65, 253–261.

- Xu, L., Zhao, X., Xu, C., Kotov, N.A., 2018. Water-rich biomimetic composites with abiotic self-organizing nanofiber network. *Adv. Mater.* 30.
- Xu, W., Huang, L.B., Wong, M.C., Chen, L., Bai, G., Hao, J., 2017. Environmentally friendly hydrogel-based triboelectric nanogenerators for versatile energy harvesting and self-powered sensors. *Adv. Energy Mater.* 7.
- Yang, C., Suo, Z., 2018. Hydrogel ionotronics. *Nat. Rev. Mater.* 1.
- Yang, C., Zhou, S., Shian, S., Clarke, D.R., Suo, Z., 2017. Organic liquid-crystal devices based on ionic conductors. *Mater. Horiz.* 4, 1102–1109.
- Yang, C.H., Chen, B., Lu, J.J., Yang, J.H., Zhou, J., Chen, Y.M., Suo, Z., 2015. Ionic cable. *Extreme Mech. Lett.* 3, 59–65.
- Yang, C.H., Chen, B., Zhou, J., Chen, Y.M., Suo, Z., 2016a. Electroluminescence of giant stretchability. *Adv. Mater.* 28, 4480–4484.
- Yang, C.H., Wang, M.X., Haider, H., Yang, J.H., Sun, J.-Y., Chen, Y.M., Zhou, J., Suo, Z., 2013. Strengthening alginate/polyacrylamide hydrogels using various multivalent cations. *ACS Appl. Mater. Inter.* 5, 10418–10422.
- Yang, J., Bai, R., Li, J., Yang, C.H., Yao, X., Liu, Q., Vlassak, J., Mooney, D.J., Suo, Z., 2018a. Topologies of Hydrogel Adhesion. (submitted for publication).
- Yang, J., Bai, R., Suo, Z., 2018b. Topological adhesion of wet materials. *Adv. Mater.* 30, 1800671.
- Yang, Y., Wang, X., Yang, F., Shen, H., Wu, D., 2016b. A universal soaking strategy to convert composite hydrogels into extremely tough and rapidly recoverable double-network hydrogels. *Adv. Mater.* 28, 7178–7184.
- You, J., Xie, S., Cao, J., Ge, H., Xu, M., Zhang, L., Zhou, J., 2016. Quaternized chitosan/poly(acrylic acid) polyelectrolyte complex hydrogels with tough, self-recovery, and tunable mechanical properties. *Macromolecules* 49, 1049–1059.
- Yu, A.C., Chen, H., Chan, D., Agmon, G., Stapleton, L.M., Sevit, A.M., Tibbitt, M.W., Acosta, J.D., Zhang, T., Franzia, P.W., Langer, R., Appel, E.A., 2016. Scalable manufacturing of biomimetic moldable hydrogels for industrial applications. *Proc. Natl. Acad. Sci. U.S.A.* 113, 14255–14260.
- Yu, Q.M., Tanaka, Y., Furukawa, H., Kurokawa, T., Gong, J.P., 2009. Direct observation of damage zone around crack tips in double-network gels. *Macromolecules* 42, 3852–3855.
- Yu, Y., Landis, C.M., Huang, R., 2018. Steady-state crack growth in polymer gels: a linear poroelastic analysis. *J. Mech. Phys. Solid.* 118, 15–39.
- Yuk, H., Lin, S., Ma, C., Takaffoli, M., Fang, N.X., Zhao, X., 2017. Hydraulic hydrogel actuators and robots optically and sonically camouflaged in water. *Nat. Commun.* 8, 14230.
- Yuk, H., Lu, B., Zhao, X., 2019. Hydrogel bioelectronics. *Chem. Soc. Rev.*
- Yuk, H., Zhang, T., Lin, S., Parada, G.A., Zhao, X., 2016a. Tough bonding of hydrogels to diverse non-porous surfaces. *Nat. Mater.* 15, 190–196.
- Yuk, H., Zhang, T., Parada, G.A., Liu, X., Zhao, X., 2016b. Skin-inspired hydrogel-elastomer hybrids with robust interfaces and functional microstructures. *Nat. Commun.* 7, 12028.
- Zhang, E., Bai, R., Morelle, X.P., Suo, Z., 2018a. Fatigue fracture of nearly elastic hydrogels. *Soft Matter* 14, 3563–3571.
- Zhang, J., Daubert, C.R., Foegeeding, E.A., 2005. Characterization of polyacrylamide gels as an elastic model for food gels. *Rheol. Acta* 44, 622–630.
- Zhang, T., Lin, S., Yuk, H., Zhao, X., 2015. Predicting fracture energies and crack-tip fields of soft tough materials. *Extreme Mech. Lett.* 4, 1–8.
- Zhang, W., Liu, X., Wang, J., Tang, J., Hu, J., Lu, T., Suo, Z., 2018b. Fatigue of double-network hydrogels. *Eng. Fract. Mech.* 187, 74–93.
- Zhang, W., Tang, J., Hu, J., Wang, Z., Wang, J., Lu, T., Suo, Z., 2019. Fracture toughness and fatigue threshold of tough hydrogels. *ACS Macro. Lett.* (submitted).
- Zhang, Y., Tao, L., Li, S., Wei, Y., 2011. Synthesis of multiresponsive and dynamic chitosan-based hydrogels for controlled release of bioactive molecules. *Biomacromolecules* 12, 2894–2901.
- Zhang, Y.S., Khademhosseini, A., 2017. Advances in engineering hydrogels. *Science* 356.
- Zhao, X., 2014. Multi-scale multi-mechanism design of tough hydrogels: building dissipation into stretchy networks. *Soft Matter* 10, 672–687.
- Zhao, X., Huebsch, N., Mooney, D.J., Suo, Z., 2010. Stress-relaxation behavior in gels with ionic and covalent crosslinks. *J. Appl. Phys.* 107, 63509.
- Zurick, K.M., Bernards, M., 2013. Recent biomedical advances with polyampholyte polymers. *J. Appl. Polym. Sci.* 131.